

Copyright  
by  
Zelalem Alebel Arega  
2014

**The Dissertation Committee for Zelalem Alebel Arega Certifies that this is the  
approved version of the following dissertation:**

**Characteristics of Foamed Asphalt Binders for Warm Mix Asphalt  
Applications**

**Committee:**

---

Amit Bhasin, Supervisor

---

Wei Li, Co-Supervisor

---

Jorge A Prozzi

---

Zhanmin Zhang

---

Maria G Juenger

**Characteristics of Foamed Asphalt Binders for Warm Mix Asphalt  
Applications**

**by**

**Zelalem Alebel Arega, B.S.; M.S.**

**Dissertation**

Presented to the Faculty of the Graduate School of

The University of Texas at Austin

in Partial Fulfillment

of the Requirements

for the Degree of

**Doctor of Philosophy**

**The University of Texas at Austin**

**August 2014**

*To my parents*

*Ayehu Mekuriaw and Alebel Arega*

## **Acknowledgements**

I would like to express my deepest gratitude to my advisor and supervisor, Dr. Amit Bhasin, for his support and guidance in completing this study. Dr. Bhasin has both inspired and challenged me throughout the course of this study. I would also like to extend my gratitude to my co-supervisor, Dr. Wei Li, for his invaluable insight and feedback.

I would like to thank Dr. Jorge A Prozzi, Dr. Zhanmin Zhang, and Dr. Maria G Juenger for their willingness to serve as committee members. Their contribution is greatly appreciated.

I wish to thank Patricia Osmari for her help in running some of the surface tension tests, and Texas A & M Transportation Institute (TTI) for providing me the mixture data that I used in this study.

I would also like to thank my family for their incredible patience and support for which I am always grateful.

Finally, the support of the National Cooperative Highway Research Program (NCHRP) is highly appreciated.

# **Characteristics of Foamed Asphalt Binders for Warm Mix Asphalt Applications**

Zelalem Alebel Arega, PhD

The University of Texas at Austin, 2014

Supervisor: Amit Bhasin

Co-supervisor: Wei Li

An increase in environmental awareness and energy concerns had recently prompted efforts to make pavement construction cheaper and more environmentally friendly. Warm mix asphalt (WMA) is an asphalt mixture production technology that promises to reduce production costs and greenhouse gas emissions. Foamed asphalt binder is increasingly being used to produce WMA. This dissertation addresses several issues related to the use of foamed asphalt binder for WMA applications. The first objective of the research presented in this dissertation is to develop a method and metrics to precisely quantify the characteristics of asphalt binder foams. Laboratory measurements were obtained using the newly developed method to evaluate the extent and stability of foams produced using different asphalt binders at different water contents and laboratory foaming devices. Results demonstrate that the method developed is promising in terms of its ability to provide a detailed history of the behavior of foamed asphalt binder as the foam collapses. In addition, results indicate that the method is sensitive to distinguish between foaming characteristics of different asphalt binders as well as different water contents and foaming devices. The second objective of this study was to relate intrinsic properties of the asphalt binder to its foaming characteristics. A

physical model was developed for expansion of asphalt binder foam based on foam physics and fluid mechanics of micro-droplets. The model relates foamant water and asphalt binder mixing efficiency with the surface tension of the asphalt binder. The model can be used to predict which binder can be effectively foamed and used, and whether any chemical modification to the binder is necessary to achieve the same. Results indicate that only a small percentage of water is effective in foaming the asphalt binder. The last objective of this research was to evaluate the influence of foaming on asphalt binder residues and mixture workability and coatability. The influence of foaming process on the rheological properties of asphalt binder residue was investigated. In addition, the significance of foamed asphalt binder characteristics on mixture workability and coatability was evaluated. Results from this last part of the study can be used to optimize binder foaming such that the resulting mixture is coated and compacted without compromising performance.

## Table of Contents

List of Tables .....	xi
List of Figures .....	xii
Chapter 1: Introduction .....	1
1.1. Background .....	1
1.2. Problem Statement .....	3
1.3. Objectives and Research Methodology .....	4
1.3.1. Objectives .....	4
1.3.2. Research Methodology .....	5
1.4. Thesis Organization .....	6
Chapter 2: Characteristics of Asphalt Binders Foamed in the Laboratory to Produce Warm Mix Asphalt .....	8
2.1. Overview .....	8
2.2. Introduction .....	9
2.3. Test Methods and Metrics to Characterize Asphalt Foam .....	10
2.3.1. Test Methods .....	10
2.3.1.1. Non-Contact Measurement of Foam Expansion and Decay .....	10
2.3.1.2. Image Based Method to Obtain Bubble Size .....	14
2.3.1.3. Measurement of Foam Density .....	16
2.3.1.4. Dipstick .....	17
2.3.2. Metrics to Characterize Foam .....	18
2.4. Materials and Experimental Plan for Laboratory Study of Foam Characteristics .....	28
2.5. Laboratory Study Of Foam Characteristics .....	30
2.5.1. Influence of Water Content and Foaming Device on Foam Characteristics .....	30
2.5.2. Influence of Asphalt Source and Grade on Foam Characteristics .....	39



2.5.3.	Influence of Foaming Nozzle Pressure on Foam Characteristics .....	40
2.5.4.	Influence of Temperature on Foam Characteristics .....	43
2.5.5.	Influence of Liquid Additives on Foam Characteristics ....	45
2.5.6.	Foaming Using Water Bearing Additives .....	49
2.6.	Conclusion and Discussion .....	54
Chapter 3: Parametric Analysis of Factors that Affect Asphalt Binder Foam Characteristics .....		
3.1.	Overview .....	56
3.2.	Background .....	56
3.3.	Objectives .....	60
3.4.	Materials .....	61
3.5.	Test Methods .....	62
3.6.	Analytical Background .....	66
3.7.	Results from the Parametric Analysis .....	67
3.7.1.	Influence of Surface Tension on Bubble Size .....	67
3.7.2.	Influence of bubble size distribution on maximum expansion ratio .....	69
3.7.3.	Effective Water Content and Foaming Efficiency .....	75
3.8.	Foam Stability .....	79
3.9.	Conclusion .....	83
Chapter 4: Influence of Foaming on Asphalt Binder and Mixture Properties .....		
4.1.	Introduction .....	85
4.2.	Materials and Experimental Plan .....	86
4.3.	Tests and Results .....	88
4.3.1.	Residual Moisture in Asphalt Binder .....	88
4.3.2.	Rheological Properties of Foamed Binder Residue .....	89
4.4.	Evaluating Properties Relevant to Mixture Workability and Coatability .....	97
4.4.1.	Viscosity of Asphalt Binder Foam .....	97
4.4.2.	Viscosity of Foamed Binder Residue .....	99

4.4.3. Comparison of Asphalt Binder Foam Characteristics to Mixture Workability and Coatability .....	101
4.5. Conclusion .....	107
Chapter 5: Summary of Findings and Recommendations .....	109
Appendix 1: Determining Asphalt Binder Expansion and Collapse by Using the Laser Distance Measurement (LDM) test.....	112
A1.1.Scope.....	112
A1.2.Significance and Use.....	112
A1.3.Apparatus .....	113
A1.4.Procedure .....	114
A1.5.Report.....	117
References .....	119

## **List of Tables**

Table 3.1:	Surface Tension of Binders and Final Temperature of Asphalt Foams at Different Water Contents. ....	77
Table 3.2:	Solubility of Asphalt Foams. ....	77
Table 3.3:	Effective Water Content of Asphalt Foams. ....	77
Table 4.1:	Influence of Foaming on the High-Temperature Grade of Binders. ....	91
Table 4.2:	Influence of Foaming and Liquid Additive on the High-Temperature Grade of Binders. ....	92

## List of Figures

Figure 2.1: Ultrasonic and Laser Sensors Test Setup.....	13
Figure 2.2: Expansion Ratio Measurements Using the Two Types of Sensors. .	13
Figure 2.3: Images Showing Change of Bubble Sizes on Foamed Asphalt Surface with Time. ....	15
Figure 2.4: Ultrasonic Density Test Setup. ....	17
Figure 2.5: Two Replicates of Expansion Ratio Measurements using Laser Sensor. .....	18
Figure 2.6: Stability and Shape of Asphalt Foams as a Function of Time. ....	23
Figure 2.7: Binder N6 with 3% Water Content.....	26
Figure 2.8: Change of Bubble Size Distribution of N6 Binder with 3% Water Content with Time. ....	26
Figure 2.9: Binder N6 with 1% Water Content.....	27
Figure 2.10: Change of Bubble Size Distribution of N6 Binder with 1% Water Content with Time. ....	27
Figure 2.11: InstroTek Accufoamer Foaming Device.....	31
Figure 2.12: Wirtgen WLB 10S Foaming Device ( <a href="http://www.wirtgen.de/en/products/cold-recyclers/wlb-10-s/">http://www.wirtgen.de/en/products/cold-recyclers/wlb-10-s/</a> ).....	32
Figure 2.13: Influence of Water Content and Binder Type on the Maximum Expansion Ratio of Asphalt Foams.....	34
Figure 2.14: Influence of Water Content and Binder Type on the Rate of Collapse of the Semi-stable Foam.....	36

Figure 2.15: Surface of Foamed Asphalt Binder at Approximately 30 Seconds after Foaming in the Wirtgen for the Same Binder at 3% Water Content (left) and 1% Water Content (right).....	37
Figure 2.16: Bubble Size Distribution of N6 Binder at 1% and 3% Water Content.....	37
Figure 2.17: Foam Decay in O7 Binder. ....	38
Figure 2.18: Foam Decay in O7 – Magnified View of Expansion from 1 to 3 Minutes. .....	39
Figure 2.19: Maximum Expansion ratio and k-value of Asphalt Foams at 2% Water Content using the Accufoamer.....	40
Figure 2.20: Effect of Water Content and Nozzle Pressure on the Maximum Expansion Ratio of Asphalt Foams.....	42
Figure 2.21: Effect of Water Content and Nozzle Pressure on Stability of Asphalt Foams.....	42
Figure 2.22: Expansion Ratio versus Time for O6 at 1% with/without Heating Mantle from the Accufoamer. ....	44
Figure 2.23: Expansion Ratio versus time for O6 at 3% with/without Heating Mantle from the Accufoamer. ....	45
Figure 2.24: Influence of Additives on N7 Binder Foam Expansion.....	47
Figure 2.25: Influence of Additives on N7 Binder Foam Decay. ....	47
Figure 2.26: Influence of Additive 1 on Foam Expansion. ....	48
Figure 2.27: Influence of Additive 1 on Foam Decay at 3% Water Content. ....	48
Figure 2.28: Influence of Water Content on Foam Decay of N6 Binder Modified with 0.5% Additive 1. ....	49
Figure 2.29: Bubble Size of Foams Produced using Zeolite.....	52
Figure 2.30: A Schematic for Zeolite Modified Asphalt Foam Test Setup.....	52

Figure 2.31: Normalized Change in Height of the Binder with Zeolite.....	53
Figure 2.32: Weight Loss for the Control and Zeolite Blended Binders during RTFO Aging.....	53
Figure 3.1: Camera Setup for Image Acquisition of the Surface of the Foam as it Collapses over Time and Resulting Bubble Size Distribution.....	63
Figure 3.2: Surface Tension Test Setup. ....	65
Figure 3.3: Surface Tension of Binders as a Function of Temperature.....	68
Figure 3.4: Influence of Surface Tension on Asphalt Foam Internal Pressure. ..	69
Figure 3.5: Influence of Bubble Size on Maximum Expansion Ratio. ....	75
Figure 3.6: Relationship between Solubility and Surface Tension of the Asphalt Binder.....	78
Figure 3.7: Relationship between Effective Water Content and Surface Tension of the Asphalt Binder. ....	79
Figure 3.8: Influence of Water Content and Liquid Additive on Stability of Foams. ....	81
Figure 3.9: Relationship between Surface Tension of Binders and Stability of Foams.....	81
Figure 3.10: Viscosity of Binders at 135°C. ....	83
Figure 4.1: Weight Loss in Foamed and Control Binder During RTFO Aging. .	89
Figure 4.2: Influence of Foaming on Resistance to permanent deformation (the Red Lines Indicate the Lower and Upper Single Operator Precision Limits of the Test Method). ....	92
Figure 4.3: Influence of Foaming and Liquid Additive on Resistance to Permanent Deformation (the Red Lines Indicate the Lower and Upper Single Operator Precision Limits of the Test Method). ....	93

Figure 4.4: Influence of Foaming on Resistance to Fatigue Cracking (the Red Lines Indicate the Lower and Upper Single Operator Precision Limits of the Test Method).	94
Figure 4.5: Influence of Foaming and Liquid Additive on Resistance to Fatigue Cracking (the Red Lines Indicate the Lower and Upper Single Operator Precision Limits of the Test Method).	95
Figure 4.6: Influence of Foaming on Creep Stiffness of Binders at -12°C (the Red Lines Indicate the Lower and Upper Single Operator Precision Limits of the Test Method).	96
Figure 4.7: Influence of Foaming on the m-value of Binders at -12°C (the Red Lines Indicate the Lower and Upper Single Operator Precision Limits of the Test Method).	96
Figure 4.8: Asphalt Foam Viscosity Test Setup.	98
Figure 4.9: Viscosity of N6 foam as it collapse over time at 160°C.	99
Figure 4.10: Viscosity of Foamed Asphalt Binder Residue.	101
Figure 4.11: Influence of Water Content on Workability of WMA Mixtures (Values Equal to or Lesser than 1.0 Indicate Workability Similar to or Better Than a Similar HMA).	103
Figure 4.12: Influence of water content on coatability of WMA mixtures (values equal to or greater than 1.0 indicate coatability similar to or better than a similar HMA).	104
Figure 4.13: Comparison of Asphalt Binder Foam Expansion to Mixture Coatability; the Green Arrow Indicates Desirable Range of Coatability Compared to HMA as a Control.	105

Figure 4.14: Comparison of Asphalt Binder Foam Expansion to Mixture Coatability; the Green Arrow Indicates Desirable Range of Coatability Compared to HMA as a Control. ....	105
Figure 4.15: Comparison of Asphalt Binder Foam Expansion to Mixture Workability; the Green Arrow Indicates Desirable Range of Shear Stress Compared to HMA as a Control. ....	106
Figure 4.16: Comparison of Asphalt Binder Foam Stability to Mixture Workability; the Green Arrow Indicates Desirable Range of Shear Stress Compared to HMA as a Control. ....	106
Figure A1.1: Illustration of the bottom of the one-gallon; the grooves can accommodate a significant mass fraction of the binder especially when the mass dispend is small. ....	115
Figure A1.2: Illustration of the LDM pointing into an empty can for calibration. ....	115



## **Chapter 1: Introduction**

### **1.1. BACKGROUND**

In the United States, there are more than 4 million miles of roads of which about 2.6 million miles are paved. About 93% of the paved roads are surfaced using asphalt, mainly using hot mix asphalt (HMA) (NAPA 2011). HMA is a precisely engineered product and has a proven track record as a paving material. Over the past few decades research on HMA material selection and design has matured into well-established design procedures. However, HMA requires heating aggregates and binder to very high temperatures (143°C to 163°C) in order to achieve proper mixing and compaction.

An increase in environmental awareness and energy concerns has recently prompted efforts to make pavement construction cheaper and more environmentally friendly. WMA is an asphalt mixture production technology that promises to reduce production costs and greenhouse gas emissions. WMA was introduced in Europe in the late 1990s and in the United States in early 2004 (D'Angelo et al. 2008). Since then, there have been a number of products and processes introduced to produce WMA. These products and processes help achieve proper mixing and compaction at temperatures that are lower (15°C to 65°C) than those required to mix and compact HMA. Using WMA instead of HMA has several advantages (FHWA 2013):

- lower energy consumption during asphalt mixture production,
- lower greenhouse gas emissions,
- extended construction season,
- ability to haul mix over longer distances before placing, and
- improved working conditions for workers by reducing exposure to fuel emissions, and fumes.

Since the asphalt mixture produced using WMA is relatively less oxidized (due to relatively lower production temperatures) and less stiff compared to HMA, reclaimed asphalt pavement (RAP) or reclaimed asphalt shingles (RAS) is typically used to compensate for this short-coming. As a result, the increase in use of WMA has also resulted in an increase in use of RAP and RAS. For example, from 2009 to 2011, the use of RAP and RAS increased by 19 and 70 percent respectively (Hansen and Copeland 2013).

A survey conducted by the National Asphalt Pavement Association (Hansen and Copeland 2013) showed that the use of WMA increased by 67% from 2010 to 2011, and by over 300% since 2009. The technologies used to produce WMA can be broadly classified into four groups based on the technology used to lower the mixing and compaction temperatures. These groups are: (1) chemical additives (surfactant based products), (2) organic additives (wax based products), (3) foaming additives (zeolite based products), and (4) foaming processes (mechanical injection of a small quantity of water into the asphalt binder). In 2011, 19% of pavements in the US were constructed using WMA. According to Hansen and Copeland 2013, plant foaming was responsible for 83% of the total WMA production in 2009, 92% in 2010, and 95% in 2011 (Hansen and Copeland 2013).

Foamed asphalt binder is produced through the injection of small droplets of water into hot asphalt binder (typically above 150°C). When a droplet of water comes in contact with the hot binder, it turns into steam and expands until a film of binder holds the bubble by balancing the internal pressure with its surface tension. This process occurs for each droplet, resulting in a foamed binder with improved workability, and allowing production and compaction of mixtures at lower than conventional mixing temperatures.

As the use of plant foaming for WMA becomes more prevalent, it is imperative to develop test methods and metrics to characterize asphalt binder foams. It is also important to develop a better understanding of the relationship between the intrinsic properties of asphalt binder and its ability to foam and consequently of the quality and performance of the WMA mixtures produced.

## **1.2. PROBLEM STATEMENT**

In order to effectively use foamed binder to produce WMA, it is important to understand the characteristics of the foamed asphalt binder that influence mixture workability and performance. Three impediments to achieve this are: (1) the ability to precisely quantify the characteristics of the foamed binder in a laboratory environment prior to mixture production, (2) the ability to understand why certain binders can produce better quality foam than others and use this information to employ remedial measures if needed, and (3) the relationship between binder foaming characteristics and mixture workability, coatability and performance. The first two aspects are the primary focus of this research, although all these aspects are further described below.

A review of the literature shows that a graduated dipstick is commonly used to characterize foamed asphalt binders for WMA and base stabilization applications (He and Wong 2006; Namutebi 2011). Most investigators have also regarded the maximum expansion ratio ( $ER_{max}$ ) and half-life (HL) of the foam as meaningful indicators for the quality of the foam (Abel 1978; Brennen et al. 1983; Jenkins 2000; Namutebi 2011). However, using the dipstick method to measure HL and  $ER_{max}$  has the following limitations:

- The method is highly dependent on the operator as it is based on manual observation of foam height and time.

- The approach is limited to only two points in time that describe the rate at which the foamed asphalt binder collapses.
- The idea of using HL to describe foaming characteristics of the binder implicitly assumes that the foam collapses following an exponential decay.

Despite a steady increase in the use of foamed binder by the construction industry, there is also a lack of understanding of the physical and chemical properties of asphalt binders that affect their foaming characteristics and subsequently impact on mixture workability, coatability and performance. So far, there is very little to no understanding of the relationships between the physical properties of asphalt binders and its foaming characteristics. Given the diversity and continually changing nature of the chemical and physical properties of asphalt binders, such relationships are extremely important to predict which binder can be effectively foamed and used, and whether any chemical modification to the binder is necessary to achieve the same.

The last major impediment in the application of foamed binders for WMA is that, to date, there are no established relationships between asphalt binder foam characteristics to mixture workability, coatability, or performance. The sensitivity of foamed asphalt binder characteristics on mixture workability and coatability is not well known. This is important to ensure that binder foaming is optimized such that resulting mixture can be coated and compacted without compromising performance.

### **1.3. OBJECTIVES AND RESEARCH METHODOLOGY**

#### **1.3.1. Objectives**

The objectives of this research are:

1. develop a method and metrics to quantify the characteristics of asphalt binder foams,

2. use the method and metrics developed to evaluate the effect of water content, binder type, liquid additive, foaming device, temperature, and foaming nozzle pressure on the characteristics of asphalt binder foams,
3. quantify the residual moisture in foamed binders, and investigate the effect of foaming process on the short-term and long-term rheological properties of foamed asphalt binder residues,
4. develop a physical model that can be used to relate the impact of fundamental asphalt binder properties on asphalt binder foam characteristics, and
5. relate the foaming characteristics of asphalt binders to mixture coatability and workability

### **1.3.2. Research Methodology**

The objectives of this research were accomplished through execution of the following tasks.

#### **Task 1: Development of a method to characterize foaming in asphalt binders**

The development of an appropriate method to accurately and precisely characterize foam growth and collapse is an important component of this research. Three different approaches were considered and evaluated:

1. Non-contact methods to measure foam expansion and decay over time. Two different methods were evaluated under this category.
  - 1.1. Laser based volume expansion and collapse measurement
  - 1.2. Ultrasonic based volume expansion and collapse measurement
2. Image based method to characterize foam based on bubble size distribution, and
3. An in-situ density measurement method to characterize foam density over time.

#### **Task 2: Metrics to Characterize Foam**

Results from the methods developed in Task 2 were used to develop metrics to characterize asphalt foam

#### Task 3: Laboratory Study of Foam Characteristics

The method and metrics developed in Tasks 2 and 3 were used to evaluate the influence of factors such as binder source, water content, foaming device, liquid additive, and temperature on the characteristics of asphalt foams.

#### Task 4: Influence of Binder Properties on Foam Expansion and decay

In this task, a physical model that relates asphalt binder foam characteristics to asphalt binder fundamental properties was developed.

#### Task 5: Effect of Foaming on the Properties of Asphalt Binder

This task investigates the possible presence of residual water in foamed binder residues and effect of foaming on the rheological properties of asphalt binders.

#### Task 6: Comparison of asphalt binder foam characteristics to mixture workability and coatability

The significance of asphalt foam characteristics to mixture workability and coatability was investigated in this task.

### **1.4. THESIS ORGANIZATION**

This dissertation includes five chapters including this chapter. The remaining four chapters are organized as follows:

Chapter 2 presents the approach used to quantify asphalt binder foam. In this chapter, a method and metrics to characterize the quality of asphalt binder foam were developed. The method and metrics developed were then used to evaluate the influence of various factors (e.g. water content, binder type, foaming device, liquid additive, temperature) on asphalt foam characteristics.

Chapter 3 discusses the development of a framework to analyze asphalt binder foam expansion based on foam physics and fluid mechanics of micro droplets. The model was used to link intrinsic asphalt binder properties, temperature, and water content to asphalt binder foam expansion. The model was also used to quantify the influence of asphalt binder properties and liquid additive on expansion of asphalt binder foam.

In Chapter 4, the influence of the foaming process on asphalt binder and mixture properties is discussed. The residual moisture in foamed asphalt binder is quantified. In addition, the impact of foaming on the viscosity, and on the high, intermediate and low temperature rheological properties of foamed binder residue is presented. Chapter 4 also details the relationship between asphalt binder foam properties and mixture workability and coatability. Asphalt binder foam quality indicators such as expansion ratio and stability were measured using the laser distance measuring device. Workability and coatability of asphalt mixtures prepared using same binders were linked to asphalt binder foam parameters.

Finally, Chapter 5 summarizes the major findings and contributions from the work. Additionally, recommendations for future work are presented.

## **Chapter 2: Characteristics of Asphalt Binders Foamed in the Laboratory to Produce Warm Mix Asphalt**

### **2.1. OVERVIEW**

In order to effectively use foamed binder to produce WMA, it is important to understand the characteristics of the foamed asphalt binder that influence mixture workability and performance. This section presents summary of the work done to (i) develop a method to precisely quantify the characteristics of asphalt binder foams and (ii) use this method to evaluate the influence of factors such as water content, binder type, liquid additive, and foaming device on the quality of foamed asphalt binders. Laser and ultrasonic distance-measuring tools were used in combination with digital imaging of the foamed surface to quantify and better understand the expansion and decay of foamed asphalt binders over time. Measurements obtained from these methods were used to evaluate the extent and stability of foams produced using asphalt binders from different sources at water contents that varied from 1% to 5% and two different laboratory foaming devices. Results indicate that both the laser- and ultrasonic-based methods were promising in terms of their ability to provide a repeatable and detailed history of the change in volume of the foamed asphalt binder as the foam collapses. It was also shown that water content and binder type have a significant influence on the maximum expansion ratio and rate of collapse of foams. Higher water contents were associated with higher expansion ratios but also faster rates of collapse. The two foaming devices used in this study produced foams with similar properties. Foam characteristics of binders modified with liquid additive demonstrated that asphalt binder foam characteristics can be significantly improved using carefully selected liquid additives.

---

*(This chapter has been published in the Journal of Materials in Civil Engineering and published in the dissertation with permission from ASCE. This material may be downloaded for personal use only. Any other use requires prior permission of the American Society of Civil Engineers.)*



## 2.2. INTRODUCTION

In order to effectively use foamed binder to produce WMA, it is important to understand the characteristics of the foamed asphalt binder that influence mixture workability and performance. An impediment to achieve this is the ability to precisely quantify the characteristics of the foamed binder in a laboratory environment prior to mixture production. As briefly discussed in Chapter 1, a graduated dipstick is commonly used to characterize foamed asphalt binders for WMA and base stabilization applications (He and Wong 2006; Namutebi 2011). The expansion ratio (ER) and half-life (HL) of the foam measured using the dipstick are the two parameters commonly used to quantify the quality of the foam (Abel 1978; Brennen et al. 1983; Jenkins 2000; Namutebi 2011). In fact, similar metrics (and bubble size distribution, which will be discussed later in this chapter) are typically used to characterize foam in other industries such as food and polymer (Huang et al. 1997; Phillips et al. 1987; Wilde 1996). However, the dipstick method that is typically used to measure both HL and ER, is highly dependent on the operator as it is based on manual observation of foam height and time. This approach is also limited to only two points that describe the rate at which the foamed asphalt binder collapses. Also, the idea of using HL to describe foaming characteristics of the binder implicitly assumes that the foam collapses following an exponential decay form. Due to the limitations discussed above, the parameters  $ER_{max}$  and HL measured using the dipstick method are not suitable to characterize foamed asphalt.

Three different approaches were considered and evaluated in this study: (1) two different non-contact methods to measure foam expansion and decay over time, (2) image based method to characterize foam based on bubble size distribution, and (3) an in-situ density measurement method to characterize foam density over time. Results from these methods were used to develop metrics to characterize asphalt foam. The following

sections describe the development of test methods and metrics used to characterize the properties of asphalt binder foams over time.

### **2.3. TEST METHODS AND METRICS TO CHARACTERIZE ASPHALT FOAM**

The development of an appropriate method and metrics to accurately and precisely characterize foam expansion and collapse is an important component of this research. The objective of this part of the research was to develop a method by which to quantify the foaming characteristics of different asphalt binders. This method was subsequently used to evaluate the effect of factors such as water content, foaming device, binder type and additive on the foaming characteristics.

A method to characterize foaming in asphalt binders comprises of two components: (1) the hardware or technique that captures the foaming expansion, collapse and/or bubble size, and (2) the parameters obtained by analyzing the data collected. The following sections detail the different techniques and parameters explored in this study.

#### **2.3.1. Test Methods**

In terms of the hardware or technique, four different methods were explored to measure the foaming characteristics. A brief summary of the techniques and summary of findings related to each one of these techniques is presented below.

##### ***2.3.1.1. Non-Contact Measurement of Foam Expansion and Decay***

Two different types of sensors were used to measure the change in height and corresponding change in volume of the foamed asphalt binder: (1) an ultrasonic sensor and (2) a laser-based sensor. The following sections briefly describe the use of the ultrasonic and the laser-based sensor to measure the change in the height and volume of the foamed binder.

The ultrasonic sensor comprises a transmitter and receiver to measure the distance from the sensor to a surface based on time-of-flight measurement. The laser-based sensor comprises an emitter and detector to measure the distance from the sensor to a reflecting surface based on the phase-shift principle. The main difference between the two methods is that the ultrasonic sensor measures the height of the surface by reflecting sound waves over a circular area of about 100 mm in diameter, whereas the laser sensor measures the height of the surface by reflecting light of different wavelengths over a very small circular spot of about 1 mm in diameter. The ultrasonic sensor was able to collect data more frequently (about 10 points per second) but was susceptible to secondary sound reflections from the sidewalls of the container if not properly centered. The laser sensor collects data less frequently (about 1 point per second) but was more robust. Note that the limitation in the data collection rate for the laser sensor may be overcome using different hardware operating on the same principle.

The following method was used to measure the height and corresponding change in volume of the foam using the two aforementioned sensors. The two sensors were mounted on a tripod and aligned to point directly into a one-gallon can of asphalt binder. The sensors were at least 1-m away from the surface of the can to avoid damage due to splatter from the hot foaming asphalt binder. A tube was used to enclose the ultrasonic sensor and prevent the sound waves from spreading to a larger area before reaching the container. No such arrangement was necessary for the laser sensor. The sensors were then connected to a computer using their respective data acquisition systems. The distance of each sensor from the bottom of the one-gallon can was measured. Since the bottom of the one-gallon can was not perfectly smooth but corrugated to improve stiffness, measurements were made to calibrate the weight and volume of the binder to the height of the binder in the can. In order to measure the decay in the foaming of an asphalt

binder, a sample of the foamed binder was dispensed into a one-gallon container. The container was immediately removed from underneath the foamer and placed under the sensors to measure the height of the foam as it collapsed over time. The ER was determined as the ratio of the volume of the foamed asphalt to the volume of the same mass of the asphalt binder without foaming. The volume of the foam (as a function of time) was calculated using the diameter of the can and height of the foam, which was measured using the sensors as it collapsed over time. The same weight of binder used for foaming was placed into a similar can, and the height of the binder in the can was measured. The height of the binder and the diameter of the can were used to calculate the volume of the binder without foaming.

Figure 2.1 shows the setup of the sensors and Figure 2.2 illustrates the ER for a typical foamed asphalt binder using both the ultrasonic and laser sensors. In Figure 2.2, the electrical noise resulting from the ultrasonic sensor measurement was filtered. Based on test results collected in this study, both methods were promising in terms of their ability to provide a detailed history of the change in the ER of the foamed asphalt binder. However, the method using the laser sensor was preferred because of two reasons. First, it requires minimal hardware and software for set up and use. Second, the laser can be pointed into the sampling container without interference from other parts of the foaming unit. This allows measurement of foam formation and collapse as it is being dispensed into the sampling container. A detailed procedure to measure the asphalt binder foam expansion and decay using the laser sensor is described in Appendix A.

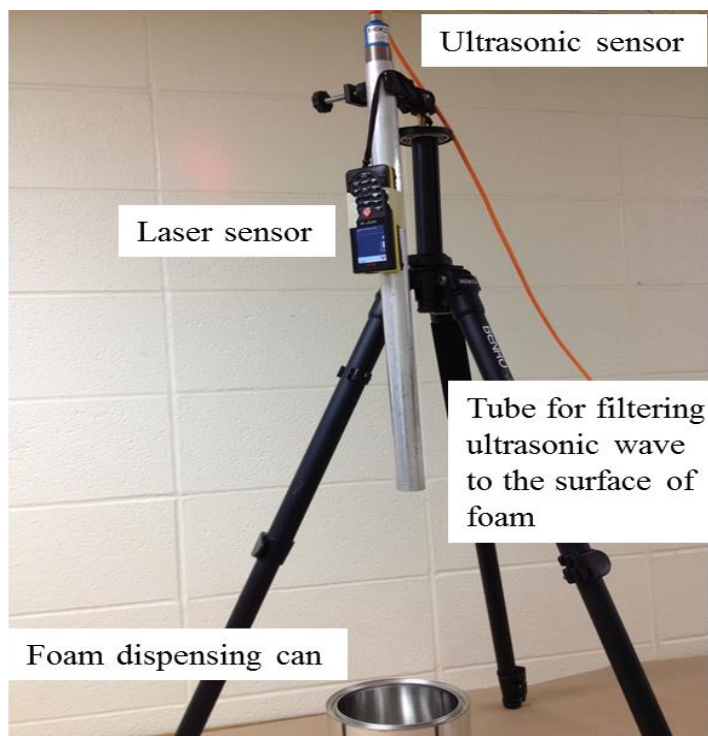


Figure 2.1: Ultrasonic and Laser Sensors Test Setup.

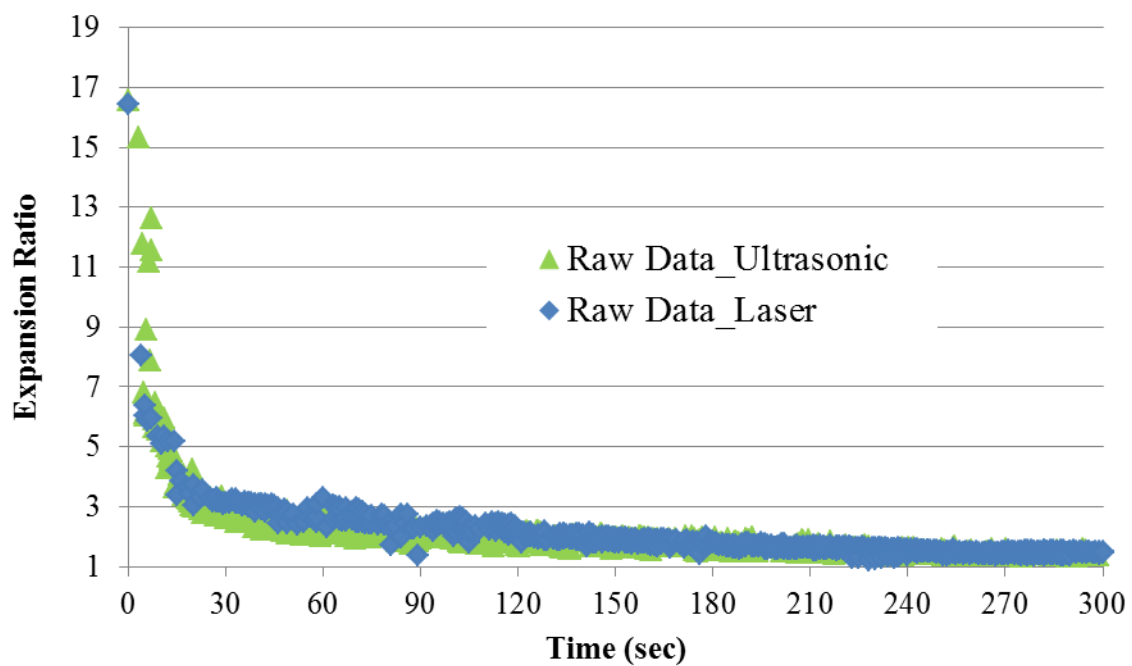


Figure 2.2: Expansion Ratio Measurements Using the Two Types of Sensors.

### ***2.3.1.2. Image Based Method to Obtain Bubble Size***

This approach entails acquiring the digital image of the foamed surface at very short intervals of time. The objective was to obtain the surface bubble size distribution to characterize the foam. Images of the foamed surface at different points in time were analyzed using an image processing and analysis program, ImageJ, to obtain the size and distribution of the bubble diameter on the surface. The following is a brief description of the methodology used to obtain this distribution.

A digital camera with a flash pointing directly into the foamed container was used to periodically photograph the surface of the foamed binder. Due to the spherical nature of the bubbles, light from the flash is reflected strongly at the center of the bubble and along the edges of the bubble. The highlight at the center and edge combined with the low reflection of the curved surface (between the bubble center and edge) creates a distinct high contrast annular ring for each bubble. The outer circumference of this annular ring was used as a measure of the bubble diameter. The image analysis was achieved in three steps. The first step was to convert the acquired image to a black and white image using imageJ; this step demarcates the bubble boundaries from the center of the bubble. The second step was to identify individual bubble boundaries on the image. This was achieved using Hough transformation, which is an algorithm typically used to identify circular boundaries. The boundaries identified using this transformation were overlaid onto the image and manually compared and corrected for any artifacts. The final step was to use the particle analysis feature in ImageJ to obtain the size (and location) of individual bubbles. Each image was calibrated with the known internal diameter of the container to convert the image dimensions from pixels to millimeters. It must be noted that this analysis could only be conducted on images obtained after approximately 15 seconds of foaming when the large unstable bubbles had collapsed and smaller semi-

stable bubbles became clearly discernible. Figure 2.3 shows a typical image of foamed asphalt surface demonstrating the change of bubble size with time.

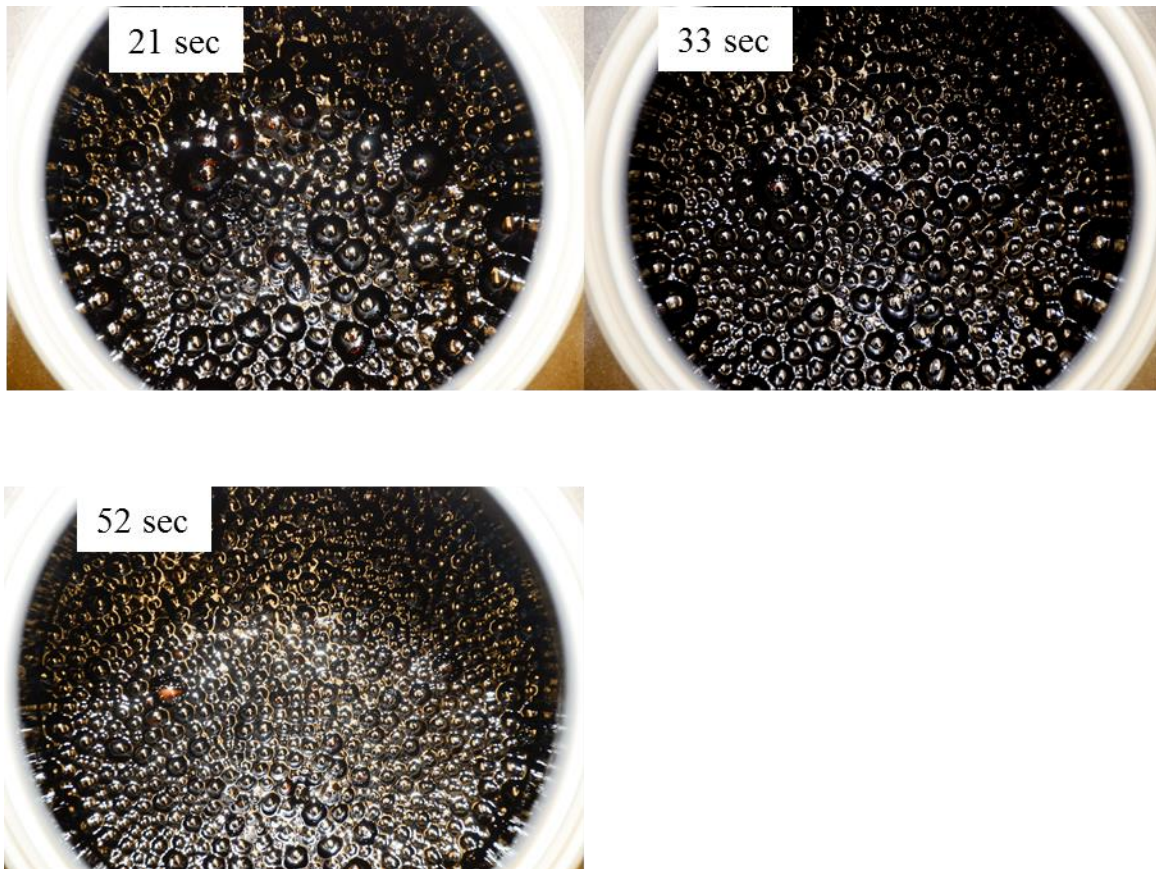


Figure 2.3: Images Showing Change of Bubble Sizes on Foamed Asphalt Surface with Time.

An alternative method to obtain the bubble size distribution is by using a three dimensional X-ray CT scanning. However, unlike taking photographic images, CT scanning is a time intensive technique. In other words, depending on the resolution and specimen dimensions it can take approximately 30 minutes or more to obtain a single 3D image. The previously described photographic method was preferred in lieu of CT scanning for the following reasons. In order to conduct CT scanning the foamed binder

must be cryogenically frozen immediately after foaming by immersing a sample container in a liquid nitrogen bath. However, in order to freeze the foam in the shortest duration of time, the diameter of the container with the foam sample must be minimized. In other words, the foam inside a larger diameter container takes several seconds to freeze to its core even when immersed in liquid nitrogen. In contrast, the foam inside a smaller diameter container freezes to its core more rapidly. However, a container with a smaller diameter also influences the quality of the foam since the average size of the bubbles several seconds after dispensing the foam is still of the order of several millimeters, as will be shown in the results later. Considering these two factors, it was concluded that although CT scanning would provide some insights into the bubble size distribution (albeit at a compromise to the bubble structure itself), similar insights could also be gained by evaluating the bubble size distribution on the surface of the foam.

#### ***2.3.1.3.Measurement of Foam Density***

In addition to the two methods described above, ultrasonic density method was initially considered for asphalt foam characterization. This method relies on the use of ultrasonic waves passing through a cross section of the foamed asphalt binder to characterize the foam in real time. As the ultrasonic waves pass through the foam, the wave amplitude is damped. The magnitude of damping is directly proportional to the overall foam density, i.e. damping increases as the foam collapses over time. However, this approach was found to be very sensitive to changes in the viscosity of the binder due to small changes in temperature. Consequently this approach was deemed appropriate when working with larger volumes of foamed sample under tight temperature controlled conditions that are less susceptible to temperature fluctuations. A picture of the ultrasonic density test setup is shown in Figure 2.4.





Figure 2.4: Ultrasonic Density Test Setup.

#### ***2.3.1.4.Dipstick***

This is the approach stipulated in the literature to measure expansion ratio and half-life. However, based on the foaming characteristics of different asphalt binders, at different water contents, and using two different types of foaming equipment, it was concluded that this approach was incapable of providing accurate, repeatable or meaningful information on the foaming characteristics of different asphalt binders. In addition, this method presented a safety risk to the personnel.

In summary, it was concluded that the method based on the laser distance measurement was more appropriate to characterize asphalt foaming and collapse for this research. Digital imaging and bubble size distribution were used for some cases to validate the hypothesized mechanism of foaming in asphalt binders. The ultrasonic sensor for distance measurement was used on a limited basis for validation. One of the conclusions of this research is that the manual method using the dipstick not be used for

these measurements. Figure 2.5 illustrates the ER for two replicates of a typical foamed asphalt binder using the laser sensor at two different water contents.

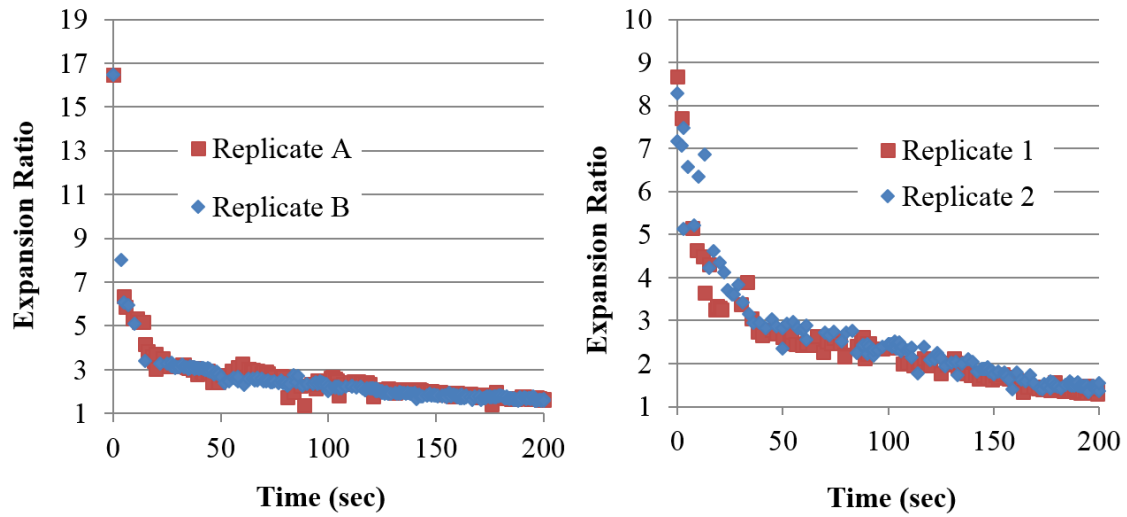


Figure 2.5: Two Replicates of Expansion Ratio Measurements using Laser Sensor.

### 2.3.2. Metrics to Characterize Foam

The aforementioned sections presented different methods by which different characteristics of the foam can be measured in real time. The next step was to use these methods to understand the process of foam expansion and decay and also to extract a metric or metrics from the measurements to quantitatively describe the foamed binder. In order to do so, I first developed a hypothesis for the mechanism of foam expansion and collapse in asphalt binders. The hypothesis was framed based on a review of foaming in other materials in the literature and refined based on observations made during this study.

In the case of asphalt foams produced by water injection, a foaming device homogenously combines very fine droplets of water with the asphalt binder at elevated temperatures. The water droplets turn into steam that expands and takes the form of bubbles within the asphalt binder resulting in the formation of foam. The foamed binder was believed to have increased workability and aggregate coatability at temperatures

lower than conventional HMA temperatures. The overall expanded volume as well as stability of the foam are important for WMA applications. It is hypothesized that foam with a higher expansion has a lower overall viscosity and easily coats aggregate particles. Also, foam with a lower decay rate has a longer effective time to coat the aggregate particles.

Jenkins (2000) developed an exponential decay model (Equation 2.1) for asphalt foam as a function of time, and two other parameters  $ER_{max}$ , and HL. This model was adapted from the isotope decay model.

$$ER(t) = ER_{max} * e^{\frac{-\ln 2}{HL} * t} \quad [2.1]$$

where,

$ER(t)$  – The foam volume at time  $t$  to the volume of the asphalt binder after the foam collapses

$t$  – Time starting from end of foam dispensing

The parameters HL and  $ER_{max}$  were measured using a dipstick. The use of a dipstick to measure these parameters is highly dependent on the operator as it is based on manual observation of foam height and time. This approach is also limited to only two points in time that describe the rate at which the foamed asphalt binder collapses. Furthermore, observations made during this study show that HL is typically in the range of 1 to 4 seconds, consequently manual measurements of HL are prone to high variability. Data collected in this study using the more precise and faster methods (as described in the previous sections) to measure expansion also indicate that the asphalt foam does not necessarily collapse following an exponential decay form.

The following two stages of bubble growth and collapse are proposed based on a review of foaming mechanisms for asphalt and other materials in the literature (Saye and Sethian 2013; Schick 2004; Schramm 1994; Sunarjono 2008) as well as observations made during this study.

1. Unstable and short-life bubbles

Initially, foamed asphalt binder consists of a cluster of bubbles separated by a thin layer of liquid asphalt (as shown in Figure 2.6). The thickness of the liquid asphalt layer is a function of  $ER_{max}$ . As  $ER_{max}$  increases, the ratio of liquid to gas (steam) volume decreases, resulting in a decrease in the initial thickness of the asphalt film layer. Unstable bubbles cause a sharp decrease in the volume of the foam in a few seconds. The following are the possible mechanisms that can explain the collapse of the unstable bubbles:

- Liquid flow: Immediately after the foam is dispensed into a can, the liquid asphalt flows downwards along the interconnected network of channels between the bubbles. At the same time the bubbles also move up due to the buoyant force. As the liquid asphalt moves down and the bubbles move up, the film layer thins out and finally the bubbles collapse. As the bubbles on the surface collapse, the liquid between these bubbles redistributes to the nearby bubbles.
- Excessive Steam Pressure: In the case of larger water droplets (or coalescence of many fine droplets) that turn into steam, the vapor pressure inside the bubble causes the internal pressure of the steam inside the bubble exerting tensile stresses in the binder film surrounding the bubble exceeds the tensile strength of the binder resulting bubble collapse.

- Drop in the temperature of steam: For bubbles that are in direct contact with the atmosphere, the temperature of the steam may drop and cause the foam to collapse (implode).
- Rising velocity: Larger bubbles rise to the surface at much higher speeds (proportional to the square of the diameter) and ultimately collapse. As will be shown later, this phenomenon can be used to explain why foams with higher water contents and higher expansion ratios are typically less stable compared to foams with lower water contents and expansion ratios. While the rising velocity by itself is not a mechanism of failure, it greatly promotes or accelerates the failure of larger bubbles in the foamed binder.

## 2. Semi-stable and long-life bubbles

As the unstable bubbles collapse after the first few seconds of foaming, the volume of liquid asphalt that separates the bubbles from each other increases. The increase in liquid asphalt volume, by itself, increases the relative stability of the bubbles. In the case of smaller water droplets that turn into steam, the vapor pressure inside the bubble causes the bubble diameter to grow rapidly as before. However, the bubble diameter reaches an equilibrium size since the surface forces of the bubble balance the internal pressure of the steam and allow the foam to remain stable for a finite time. The equilibrium bubble diameter or radius is given by Laplace as shown in Equation 2.2 (Pellicer et al. 2000). As before, such bubbles migrate towards the surface of the binder. However, the bubble velocity is much lower due to the smaller size, and the ratio of liquid asphalt to air (steam) volume is higher, resulting in an increase in the shell thickness of the individual bubbles. The relationship between bubble velocity and bubble diameter is given by Stoke's law in Equation 2.3 and clearly shows that the bubble velocity is directly proportional to the square of the bubble diameter and inversely

proportional to the viscosity of the fluid. Finally, when such bubbles reach to the surface of the binder, the shell thickness decreases due to liquid asphalt flow, and the vapor pressure inside the bubbles reduces due to cooling triggering an unstable reduction in the bubble diameter and collapse.

$$P_{bubble} - P_{atm} = \frac{2\gamma}{R} \quad [2.2]$$

where,

$P_{bubble}$  – Pressure inside the bubble (Pa)

$P_{atm}$  – Atmospheric pressure (Pa)

$\gamma$  – Surface tension of the binder (N/m)

$R$  – Bubble radius (m)

$$D = \sqrt{\frac{18\mu V}{(\rho_f - \rho_b)g}} \quad [2.3]$$

where,

$V$  - Rising velocity of the bubble (m/s)

$\rho$  - Density of the binder and the bubble ( $\rho_f, \rho_b$ ) (Kg/m<sup>3</sup>)

$\mu$  - Viscosity of the binder (Pa.s)

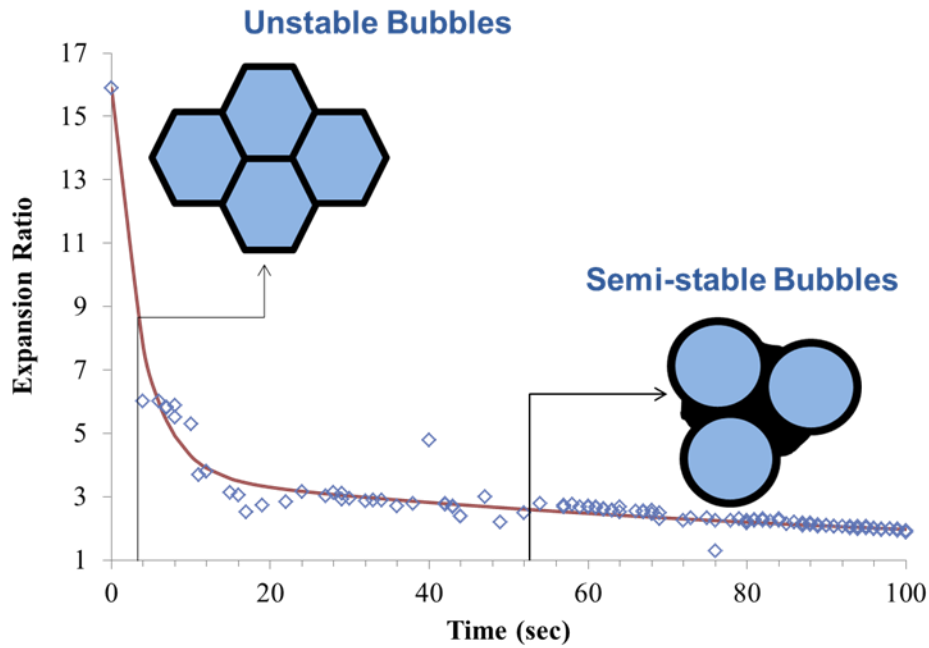


Figure 2.6: Stability and Shape of Asphalt Foams as a Function of Time.

In summary, the largest bubbles that contribute most to the expansion of the binder are also the most unstable and short-lived. This effect was observed during the first few seconds as the foamed binder collapsed and was exaggerated at higher water contents (i.e. higher air to liquid asphalt ratio) that are likely to result in larger water droplets and larger bubbles (see Figure 2.7). The collapse of the larger unstable bubbles was followed by a gradual rise and collapse of relatively less unstable or semi-stable smaller diameter bubbles. This effect was relatively more clear at lower water contents where bubbles continued to rise and collapse with the smaller bubbles taking the longest to rise and collapse (see Figure 2.9).

Based on the aforementioned understanding, the following approach was used to characterize the foamed asphalt binder. The exponential decay model developed by Jenkins (2000) did not reflect the initial sudden collapse of foams in the first few seconds.

Instead on experimental observations, the following function was found to fit the data obtained from testing the different binder, water content, and foaming equipment combinations:

$$ER_t = 1 + ae^{-bt} + (ER_{max} - a - 1)e^{-ct} \quad [2.4]$$

where,

$ER_t$  – The expansion ratio at any time  $t$

$a$ ,  $b$ , and  $c$  – Constants

$ER_{max}$  – The maximum expansion ratio that was directly measured during the foaming process

Based on the form of this equation, it may be tempting to conclude that the overall decay observed in the foam is the sum effect of two different decay processes proceeding at different rates. However, it must be noted that the above equation was used only for data reduction purposes and it is inappropriate to interpret the phenomenon purely based on its mathematical form. In fact, observations of the foam decay process suggest that it may be more appropriate to model the collapse in the semi-stable foam after the first few seconds of foaming when the foam is in the semi-stable stage. This will be discussed in more detail below.

Figure 2.7 and Figure 2.9 illustrate the typical measurements for the ER of the binder versus time for a typical asphalt binder (denoted as N6) at 1% and 3% moisture content. The discrete points illustrate the raw data and the continuous line shows the fit. The expansion at the high water content shown in Figure 2.7 is extremely short-lived and the collapse of foam is faster as compared to the lower water content presented in Figure 2.9, where the foam collapse is slower. The figures also illustrate a digitally inverted



image of the surface of the foamed binder with bubbles at different points in time (bright annular bands indicate locations of bubbles). As discussed before, the foamed binder with 3% water content initially expands much more than the foamed binder with 1% water content does. However, the foamed binder at the lower water content is more stable or semi-stable and clearly shows the migration and collapse of bubbles at the surface with the diameter of the bubbles decreasing with time.

Selected images of the foamed surface at different points in time were analyzed using the image processing and analysis program, ImageJ, to obtain the size and distribution of the bubble diameter on the surface. Figure 2.8 and Figure 2.10 show the size distribution of bubbles at three different points in time on the surface of the N6 asphalt binder foamed with 3% and 1% water contents, respectively. The Figures show that the bubble diameter at the surface becomes smaller as the foam continues to collapse over time. This is consistent with what can be expected from Equation 2.3, in that the larger diameter bubbles rise to the surface faster. In addition, the effect of water content and time on the mean diameter of the bubbles is clearly visible from the two figures.

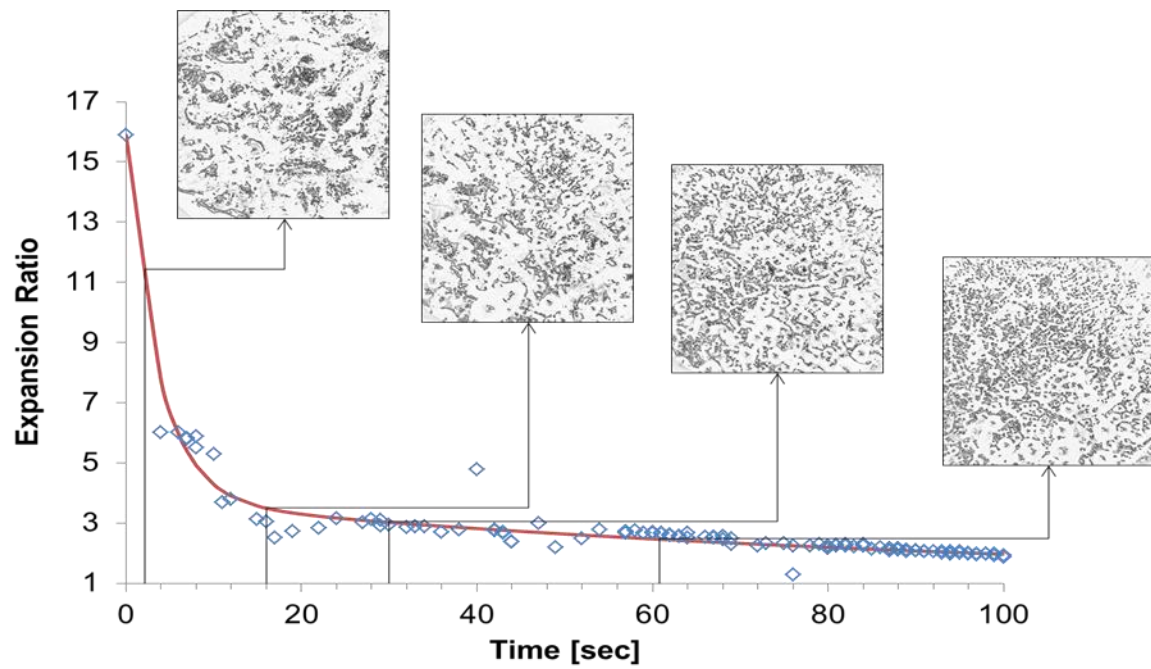


Figure 2.7: Binder N6 with 3% Water Content.

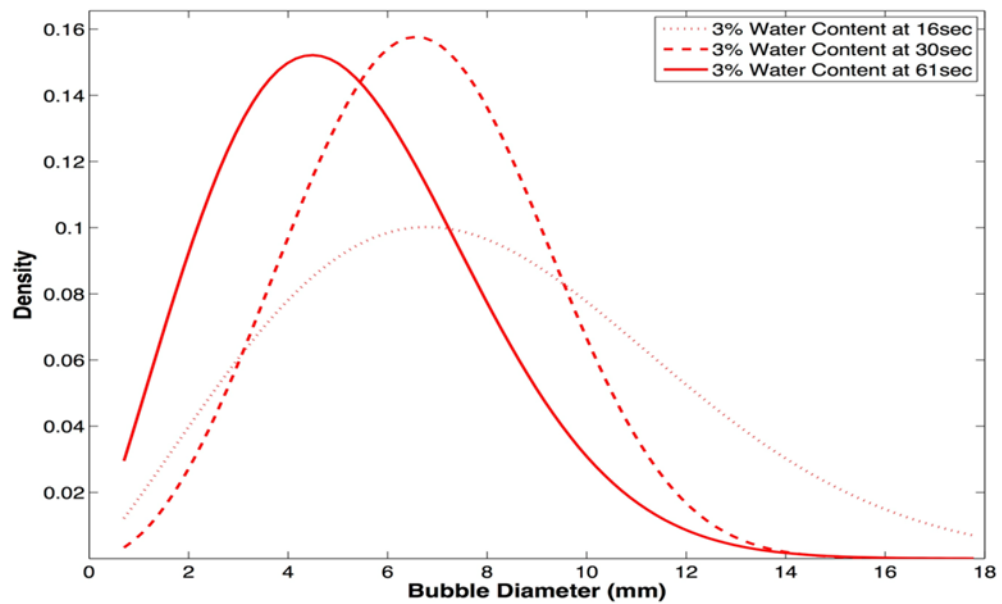


Figure 2.8: Change of Bubble Size Distribution of N6 Binder with 3% Water Content with Time.

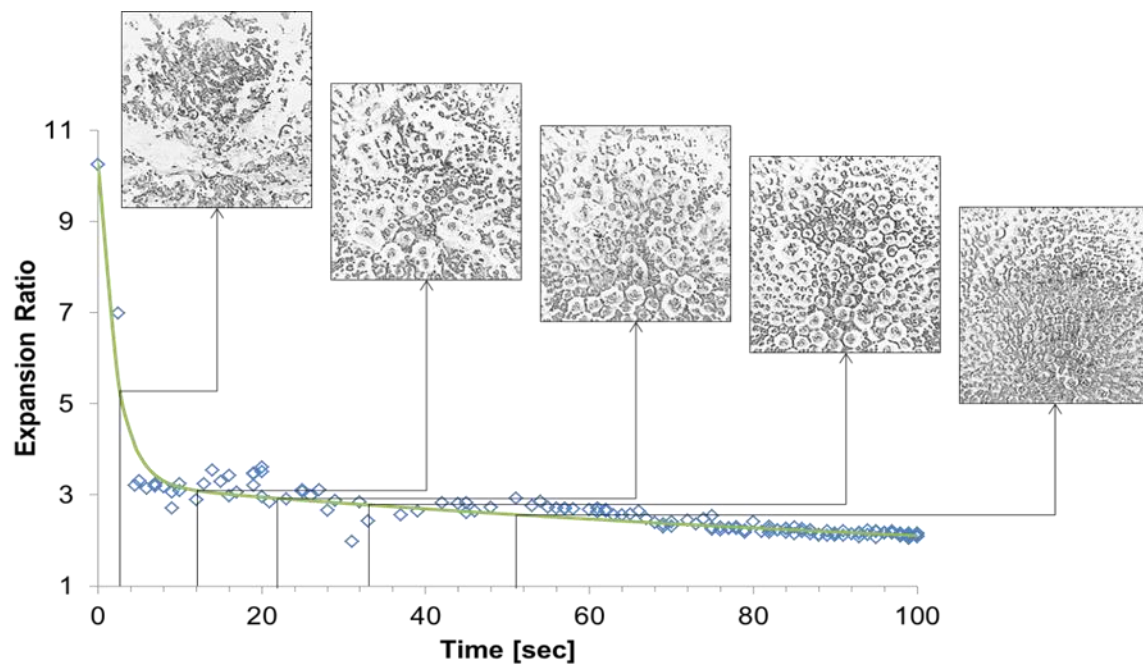


Figure 2.9: Binder N6 with 1% Water Content.

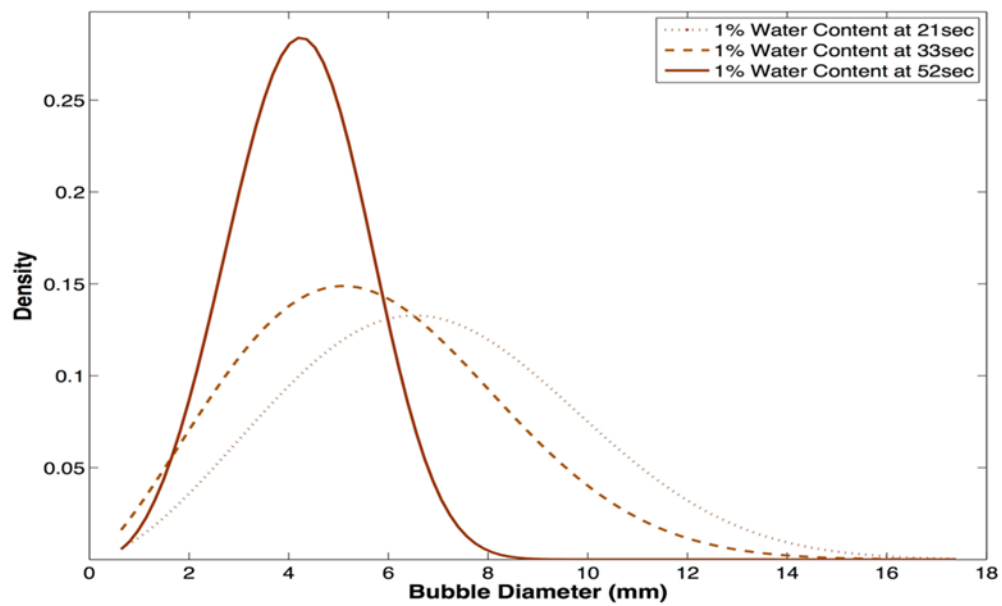


Figure 2.10: Change of Bubble Size Distribution of N6 Binder with 1% Water Content with Time.

The following metrics were considered to characterize foamed asphalt binders.

1. Maximum expansion ratio: This is the ratio of the maximum volume occupied by the foamed asphalt binder to the volume occupied by the same mass of the binder without any water or foam in it.
2. Rate of collapse of semi-stable foam: Based on the results obtained thus far, a significant portion of the unstable bubbles collapsed during the first few seconds after foaming. The rate of collapse of the semi-stable foam was determined as the parameter  $k$  obtained by fitting the ER versus time to an exponential curve:  $ER_t = 1 + ce^{-kt}$ . Note, that the ER after 10 seconds of foaming was used to determine this parameter.
3. Bubble size distribution: Bubble size distribution from image acquisition and analysis was also considered as an important metric to characterize asphalt foams. Bubble size distribution through image acquisition and analysis was also used in some cases to better understand the mechanisms that drive foam expansion and collapse.

Note that the half-life for most combinations of binder, water content and foaming equipment, was in the range of 1 to 4 seconds. This parameter was not very repeatable and was associated with the more turbulent collapse of larger unstable bubbles in the foamed binders. Consequently, this parameter was not used to characterize foamed binders.

#### **2.4. MATERIALS AND EXPERIMENTAL PLAN FOR LABORATORY STUDY OF FOAM CHARACTERISTICS**

Asphalt binders from different producers and refineries were collected and tested. Eight binders from six different sources were foamed in the Accufoamer and their foaming characteristics at 2% water content and at a temperature of 60°C were

determined in terms of  $ER_{max}$  and k-value to investigate the influence of asphalt source and grade on foaming characteristics. The binders tested are designated as PG64-22 (N6, O6, T6, M6, H6, and Y6) and PG70-22 (N7, and O7).

Three binders from two sources were used to evaluate the influence of water content and type of foamer on foaming characteristics. One of the three binders was N6 and the other two binders were N7 and O7. Water content used for foaming was varied from 1 to 5%. The N7 and N6 binders were foamed at 1, 3, and 5% water contents, and the O7 binder was foamed at 1, 2, and 3% water content. All foamed binders were produced at a temperature of 160°C. All three binders were foamed using both Wirtgen and Accufoamer (from D&H and Instrotek) foaming units.

The binder designated as O6 was used to investigate the influence of temperature on foaming characteristics. The binder was foamed at 1% and 3% water content and allowed to collapse at room temperature as well as at 160°C. A heating mantle was used to maintain the temperature of the foam at 160°C.

The binders designated as N6, N7 and O7 were modified with 0.5% by weight of two liquid additives from two different sources (Additive 1 and Additive 2) and foamed in the Accufoamer at 1%, 2%, and 3% water contents to investigate the effect of additives on foaming characteristics. In addition to the liquid additives, zeolite was also added to N7 and O7 binders to evaluate foaming using water bearing additives.

The quality of the foam was evaluated based on the parameters  $ER_{max}$  and k-value derived from the semi-stable foam for all binder-water content combinations produced using the two foaming units.  $ER_{max}$  is an indirect indicator of the workability of the foamed asphalt binder, and affects dispersion of the foamed binder in the mix. Foam with higher  $ER_{max}$  has a lower overall viscosity and easily coats aggregate particles. The parameter 'k' represents the stability of the foam, and affects the time available for

mixing before the semi-stable foam collapses. Foam with a lower k-value decays at a lower rate and has more effective time to coat the aggregate particles.

## **2.5. LABORATORY STUDY OF FOAM CHARACTERISTICS**

This section presents a summary of the work done to achieve the second step discussed in section 2.1, i.e., to use the method and metrics developed in section 2.3 to evaluate the influence of factors such as binder source, water content, and additive on the characteristics of the foam.

### **2.5.1. Influence of Water Content and Foaming Device on Foam Characteristics**

Characteristics of foamed asphalt binders produced using the Accufoamer foaming device (InstroTek Accufoamer) and Wirtgen foaming device (Wirtgen WLB 10S) were compared. The two units produce foamed asphalt binder differently resulting in possibly different foam structure and property. The following is a brief description of the working principles of the two foaming units.

#### **1. InstroTek Accufoamer**

The Accufoamer is designed to deliver asphalt binder and the foaming agent (water) by regulating the overhead pressure that drives the flow of these liquids. The foaming unit is calibrated to determine the time taken to deliver a certain mass of binder at a fixed driving pressure as well as the time taken to deliver a certain mass of water at different pressures. A foam production temperature of 160°C and binder pressure of 30 psi was selected for all tests according to manufacturer recommendation, unless otherwise indicated. The device comes with an excel template programmed with the relationship between water content and pressure for a given asphalt binder flow rate. Once the calibration parameters are set in the template, it can be used to determine the

flow time and water pressure that are required to produce desired mass of foamed binder at any desired water content. Figure 2.11 presents a photo of the unit used in this study.



Figure 2.11: Instron Accufoamer Foaming Device.

## 2. Wirtgen WLB 10S

The Wirtgen foaming unit is designed to regulate the amount of dispensed binder and water by mass flow meters. The asphalt binder is heated to 160°C and circulated inside the unit. Then, the foamed binder is produced by combining specific quantities of water, compressed air, and heated asphalt binder inside an expansion chamber. During this process, the added water vaporizes and causes the asphalt to foam in the expansion chamber. The pressure at which the water and the air are injected in the expansion chamber is about 72 psi. After the asphalt is foamed, it is usually dispensed directly from the nozzle into the mixer, where it is combined with the heated aggregates. The unit can

dispense about 200 grams of asphalt in 2 seconds due to the high pressure at which the water and air are injected. Figure 2.12 illustrates the photo of the unit used in this study. The device used was at Texas A & M Transportation Institute (TTI) and the measurements were taken jointly with a research team at TTI.



Figure 2.12: Wirtgen WLB 10S Foaming Device  
(<http://www.wirtgen.de/en/products/cold-recyclers/wlb-10-s/>).

There are two notable differences between the Accufoamer and the Wirtgen foamer. First, the nozzle types that spray the binder and the water to produce the foamed



mix are different. Second, the Wirtgen foamer produces the foam by directing the two nozzles at each other. The resulting foam is dispensed into a container directly as it is being formed. The Accufoamer also produces the foam by directing the two nozzles at each other but the foam is produced inside a small mixing chamber before being dispensed through a quarter inch tube into a container or mixer. As a result, the Accufoamer dispenses about 200 grams of foamed binder in 10-12 seconds, while the Wirtgen dispenses about 200 grams of binder in 2 seconds. This arrangement also slightly reduces the maximum expansion achieved by the Accufoamer as the foamed binder is being dispensed. Notwithstanding these differences, the goal of this exercise was to determine whether the characteristics of different foamed binders at different water contents were similar for the two foaming units. Figure 2.13 compares  $ER_{max}$  for the different binders at different water contents produced using the Accufoamer and Wirtgen foaming units.

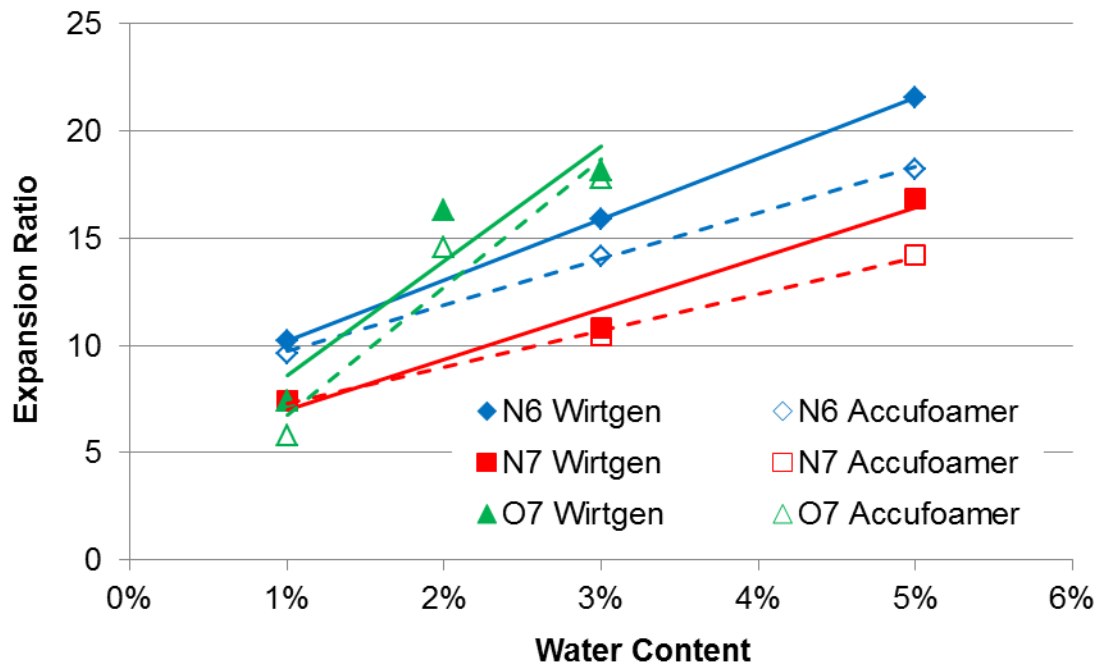


Figure 2.13: Influence of Water Content and Binder Type on the Maximum Expansion Ratio of Asphalt Foams.

The following observations can be made based on data presented in Figure 2.13:

- Different binders clearly have different  $ER_{max}$  values at the same water content. This finding was consistent with foams produced using both foaming units.
- For any given binder,  $ER_{max}$  increases with an increase in the water content and the relationship appears to be linear. This was consistent for data collected using both Wirtgen and Accufoamer units. The trends for the water content versus  $ER_{max}$  were similar for the two foaming units. However, the foams produced using Accufoamer exhibited slightly lower  $ER_{max}$  values. This can be attributed to the differences in the dispensing mechanisms between the two devices. Recall that the Accufoamer creates the foam in a small enclosed chamber and dispenses it through a 0.25 inch diameter tube into the container, whereas the Wirtgen foamer

creates the foam under atmospheric pressure and is dispensed directly into the container.

- The O7 binder was more sensitive to water content compared to the N6 and N7 binders. Also, both N6 and N7 binders had similar sensitivity to water content. The N6 and N7 binders were from the same refinery and possibly produced using the same crude oil whereas the O7 binder was from a different refinery. According to equations (2.2) and (2.3), properties of the binder such as its surface tension and viscosity are related to the maximum expansion and stability of the foamed binders. The surface tension and viscosity of the O7 binder was very different from that of the N6 and N7 binders. It is hypothesized that these differences influence the efficiency with which water mixes with the asphalt binder during the production of the foam, and consequently on the maximum expansion ratio and rate of collapse. This aspect will be presented in detail in the next chapter.

The rates of collapse,  $k$ , of the semi-stable foam using the two different foaming units are presented in Figure 2.14. This rate corresponds to the rate of collapse of foam after the first ten seconds of foaming. As discussed earlier, during the first few seconds, the foam collapses very rapidly in a turbulent manner. The following similarities and differences are observed in the rate of collapse of the foam:

- For both foaming units, an increase in the water content resulted in an increase in  $k$ -value. This is consistent with the hypothesized mechanism described earlier in this dissertation. Higher water content typically results in larger droplet sizes and larger bubbles, which in turn have a higher velocity to move to the surface (at a given temperature/viscosity) and collapse faster. On the other hand lower water contents produce smaller bubbles that take more time to come to the surface and

collapse. This effect is also illustrated through Figure 2.15 and Figure 2.16 that show the bubble size distribution of the surface of the binder at two different water contents after approximately 30 seconds of foaming.

- The rate of collapse from both foaming units was in the similar range or order of magnitude. Although the general trend for the rate of collapse with respect to increasing water content was similar for both foaming units, the rate of collapse of the semi-stable foam was typically higher for the Accufoamer compared to the Wirtgen foaming unit. It is reasonable to attribute this, at least in part, to the differences in the delivery of the foamed binder between the two units (direct vs. through a tube).

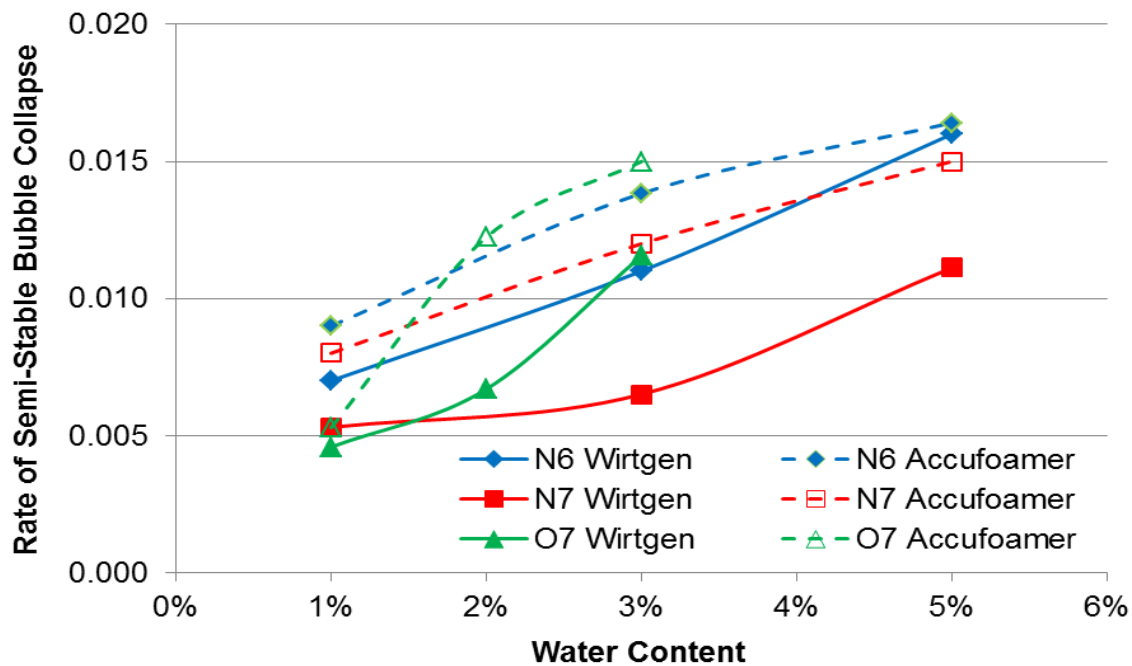


Figure 2.14: Influence of Water Content and Binder Type on the Rate of Collapse of the Semi-stable Foam.

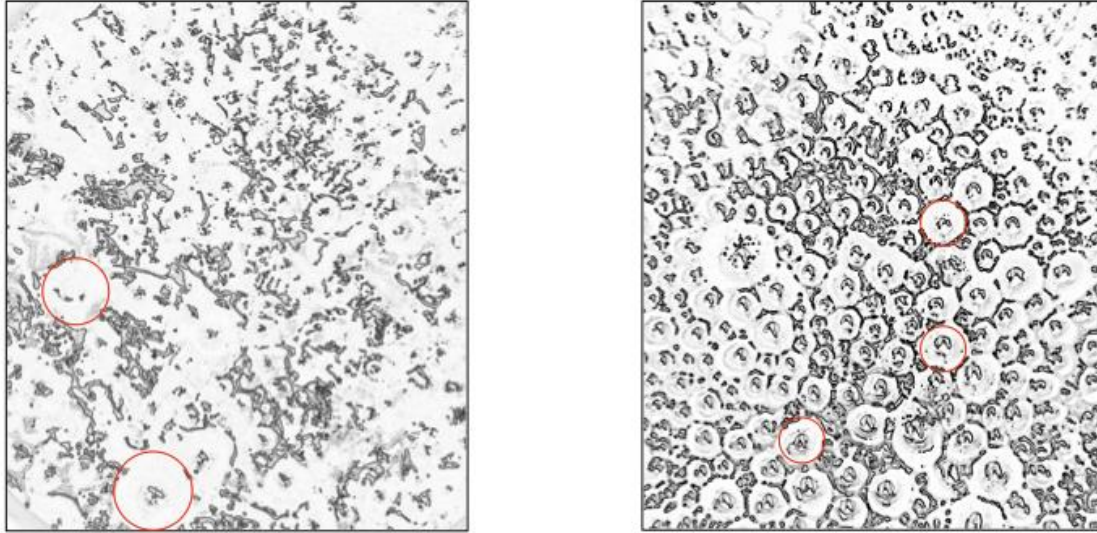


Figure 2.15: Surface of Foamed Asphalt Binder at Approximately 30 Seconds after Foaming in the Wirtgen for the Same Binder at 3% Water Content (left) and 1% Water Content (right).

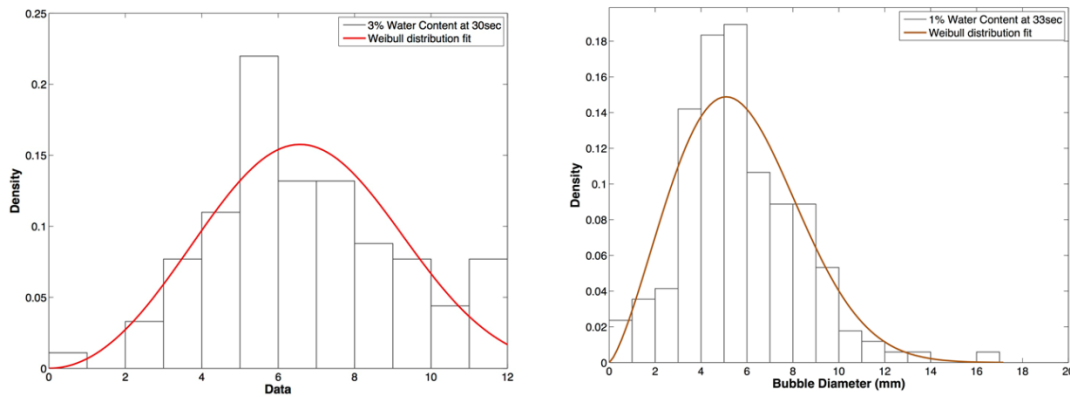


Figure 2.16: Bubble Size Distribution of N6 Binder at 1% and 3% Water Content.

Note that higher water contents result in higher ER but also faster k-value (see Figure 2.17 and Figure 2.18). An interesting consequence of the combination of these two effects is that a binder foamed with higher water content will start out with a higher  $ER_{max}$  compared to binders foamed with lower water contents. However, over time

binders foamed with lower water content will tend to be relatively more stable and retain this expansion longer. This effect is illustrated in Figure 2.17 and Figure 2.18. Also, the almost instantaneous collapse of the foamed binder suggests that the HL of the foamed binder may not be of relevance in a real mixture production scenario at a hot-mix plant. Of greater importance is the state of the foamed asphalt binder after it is exposed to the atmospheric pressure (as in a drum mix plant) for the few minutes during which time the binder is mixed with the aggregates.

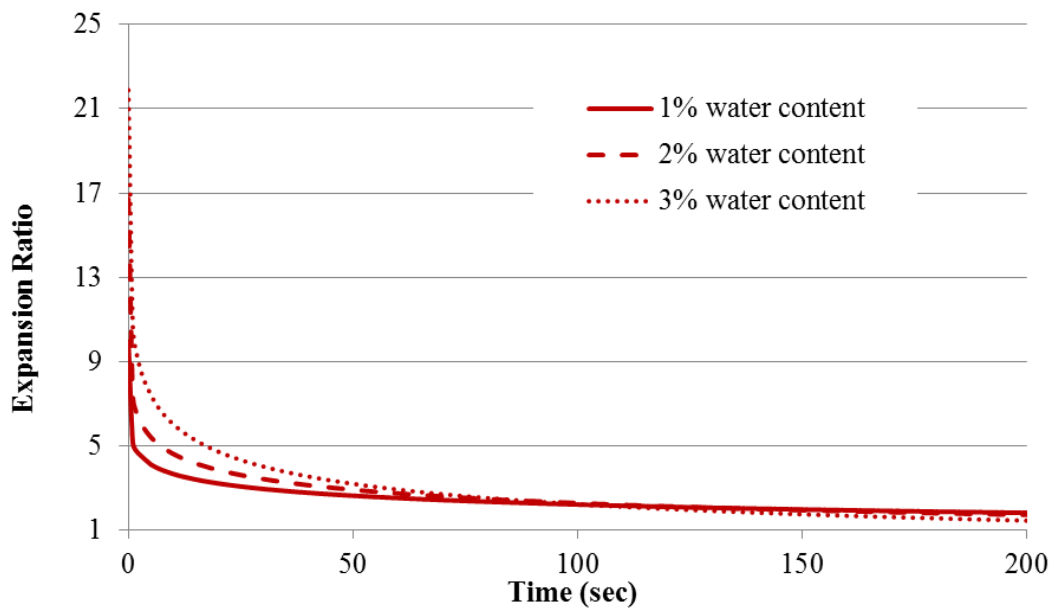


Figure 2.17: Foam Decay in O7 Binder.

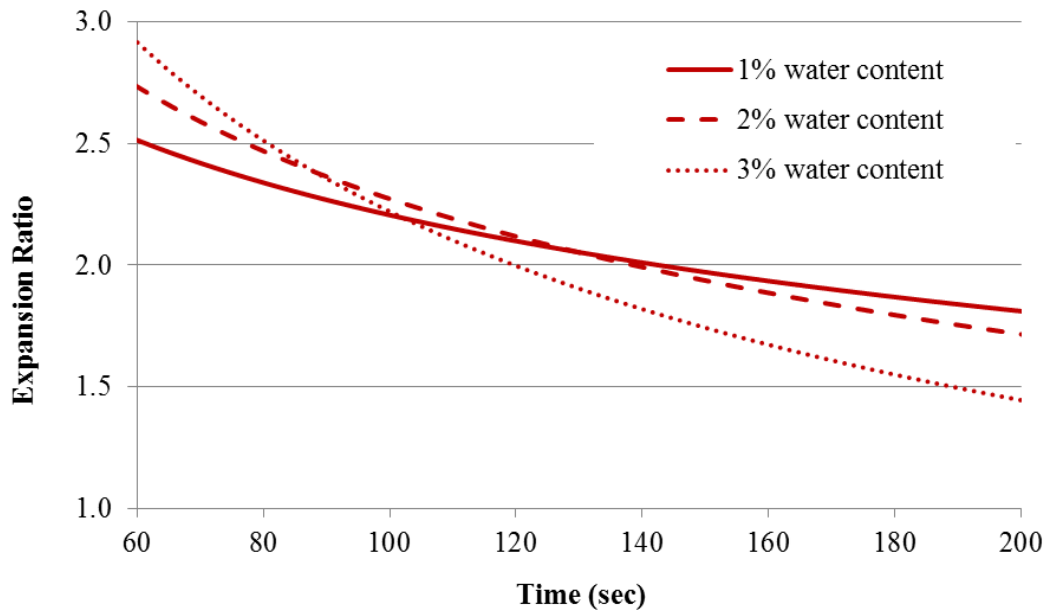


Figure 2.18: Foam Decay in O7 – Magnified View of Expansion from 1 to 3 Minutes.

### 2.5.2. Influence of Asphalt Source and Grade on Foam Characteristics

Asphalt binders from different producers and refineries were collected and tested to investigate the influence of asphalt source and grade on foaming characteristics. Eight binders from six different sources were foamed in the Accufoamer and their foaming characteristics at 2% water content and 160°C were determined in terms of  $ER_{max}$  and k-value. Figure 2.19 presents a summary of results comparing these two parameters for binders of different grades from different sources. Results show that depending on the source and grade of the asphalt binder the  $ER_{max}$  values varied from as low as 3.5 to as high as 13. When comparing different binders, there was no clear relationship between the maximum expansion of a foamed binder and the stability of the foam. In other words,  $ER_{max}$  is not necessarily related to the foam stability (k-values). For example, Y6 has the lowest  $ER_{max}$  and it is also the most un-stable foam (highest k-value). However, for any

given binder an increase in water content resulted in an increase in expansion ratio and a decrease in the stability of the foam or increase in k-value.

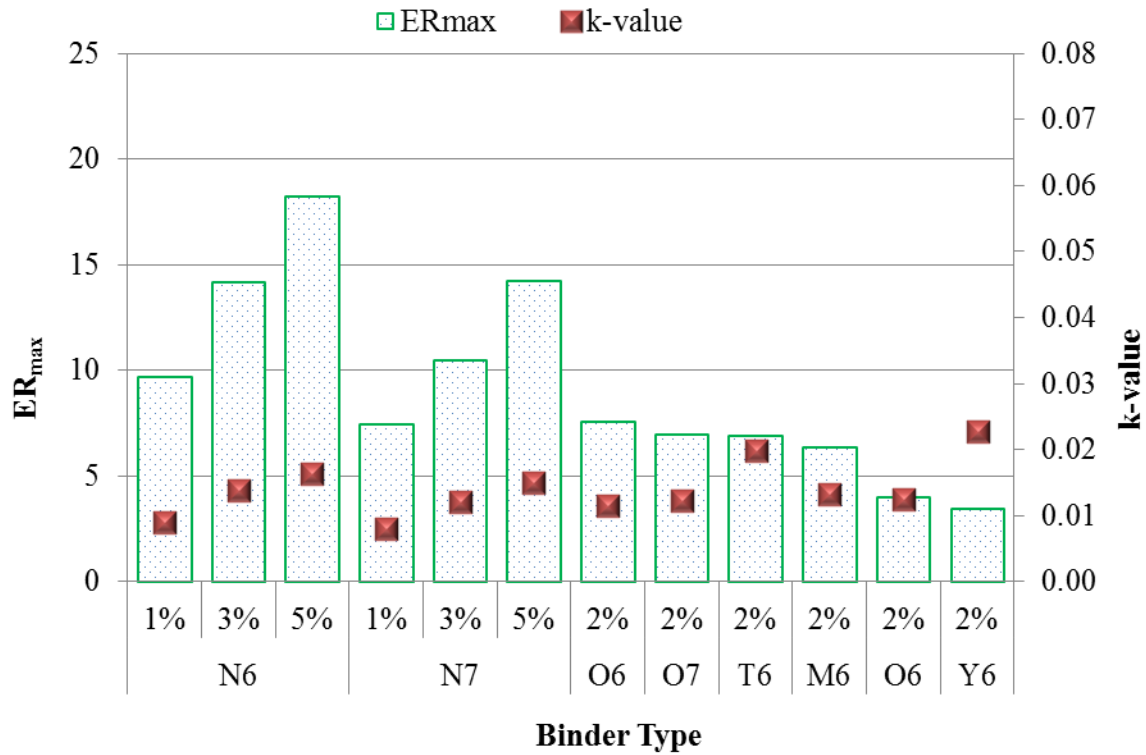


Figure 2.19: Maximum Expansion ratio and k-value of Asphalt Foams at 2% Water Content using the Accufoamer.

### 2.5.3. Influence of Foaming Nozzle Pressure on Foam Characteristics

One of the objectives of this study was to evaluate the influence of foaming pressure on the foaming characteristics of the binder. Henry's law states that at a constant temperature, the amount of a gas that dissolves in a given type and volume of a liquid is directly proportional to the partial pressure of that gas in equilibrium with that liquid. In other words, the solubility of a gas in a liquid is directly proportional to the pressure in the system. It is therefore reasonable to expect that asphalt binders foamed using water will have different foaming characteristics depending on the pressure at



which the two constituents are mixed together. In order to investigate this, three binders (M6, H6, and Y6) from three different sources were foamed at 160°C using Accufoamer at three different water contents (1%, 2%, and 3%) and two different binder nozzle pressures (30 and 40 psi). The binder nozzle pressure is the pressure with which the binder is delivered into the mixing chamber. Although the binder nozzle pressure is not the same as the pressure in the foaming chamber, an increase in the binder nozzle pressure will increase the pressure in the foaming chamber.

Figure 2.20 and Figure 2.21 compare the influence of binder pressure on the maximum expansion ratio,  $ER_{max}$ , and stability parameter, k-value. The results consistently show higher  $ER_{max}$  values for the 40 psi nozzle pressure. However, the magnitude of increase was substantial for only one binder, which was the same binder that had the lowest expansion ratio as shown in Figure 2.20. The influence of nozzle pressure on the k-value was inconsistent for different binders. For the H6 binder, the k-value decreased with an increase in nozzle pressure indicating a slightly more stable foam, whereas for the Y6 binder, the k-value increased with an increase in nozzle pressure indicating a slightly less stable foam. For the M6 binder the k-value increased at 1 and 2% water content, but decreased at 3% water content. These results indicate that parameters related to the foaming device, such as the nozzle pressure influence the foaming characteristics to some extent. It must also be noted that for any given binder and nozzle pressure, the general trend of increasing maximum expansion ratio and k-value (decreasing stability) with increasing water content was preserved. The only exception to this was the k-value for the M6 binder, which needs further evaluation.

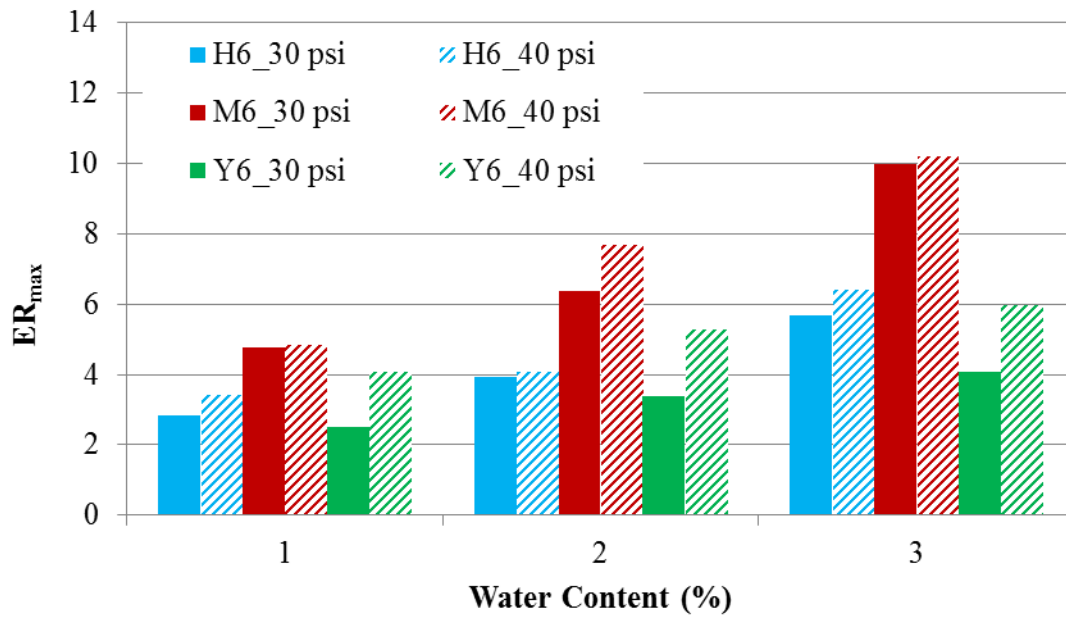


Figure 2.20: Effect of Water Content and Nozzle Pressure on the Maximum Expansion Ratio of Asphalt Foams.

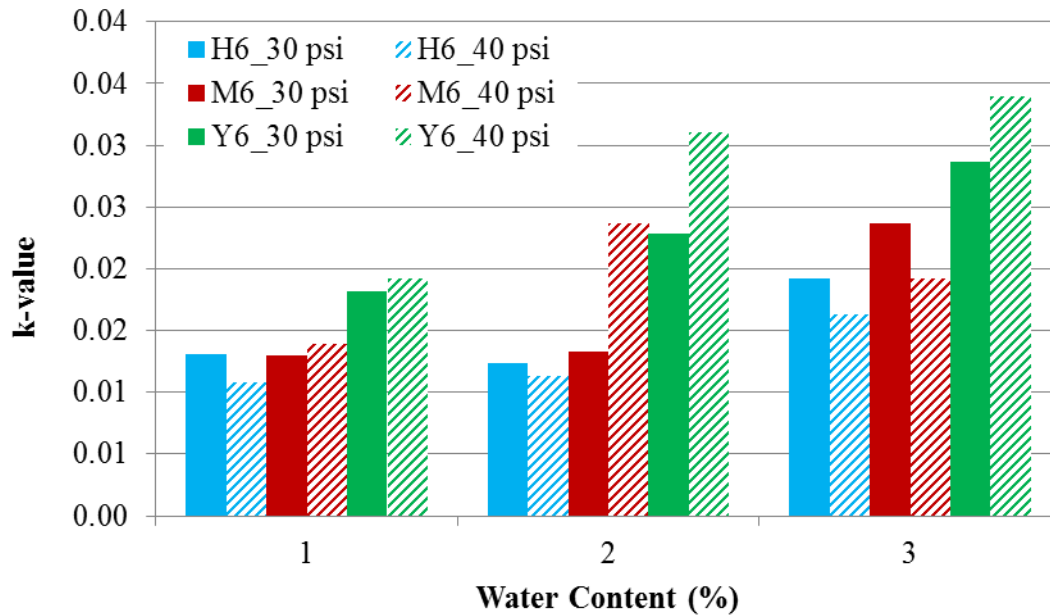


Figure 2.21: Effect of Water Content and Nozzle Pressure on Stability of Asphalt Foams.

#### **2.5.4. Influence of Temperature on Foam Characteristics**

It must be noted that in all the asphalt binder foam tests conducted during this research, the foamed binder was dispensed and the foam collapse was measured at room temperatures. An infrared thermometer was used to estimate the binder temperature after dispensing it in the one-gallon can. Typically the surface temperature of the binder dropped to about 80°C after approximately 45 seconds of being dispensed. This suggests that the water vapor could condense and relieve the pressure causing the foam to collapse (implode). On the other hand, viscosity of the binder increases significantly due to the reduction in temperature. Consequently, the bubble in the binder may not collapse immediately thus retaining its shape for a longer period of time. Also, at higher viscosities the speed with which the bubbles rise to the top reduces slowing down the collapse of the foam. The reverse is true when the foamed binder is maintained at elevated temperatures. In order to investigate the effect of temperature on the rate of collapse of the asphalt foam, the O6 binder was foamed at 1 and 3% water contents in the Accufoamer and allowed to collapse at room temperature as well as at 160°C. The elevated temperature of the foam was maintained by placing the collection can inside the heating mantle. It is important to note that the can was open to air on the top, and that the heating mantle can only maintain the temperature of the wall and bottom of the can. Figure 2.23 and Figure 2.23 compare the results from the foam collapse when the collection can was at room temperature versus foam collapse when the collection can was maintained at 160°C inside a heating mantle. These figures demonstrate that there is no noticeable influence of temperature on the measured foam properties. Similar results were obtained for a couple of other binders. Based on these results temperature of the collecting unit was not considered as a significant factor to characterize asphalt foams.

The temperature of the binder in the foaming unit was not reduced below 160°C because this would result in clogging of the pipes in the foamer.

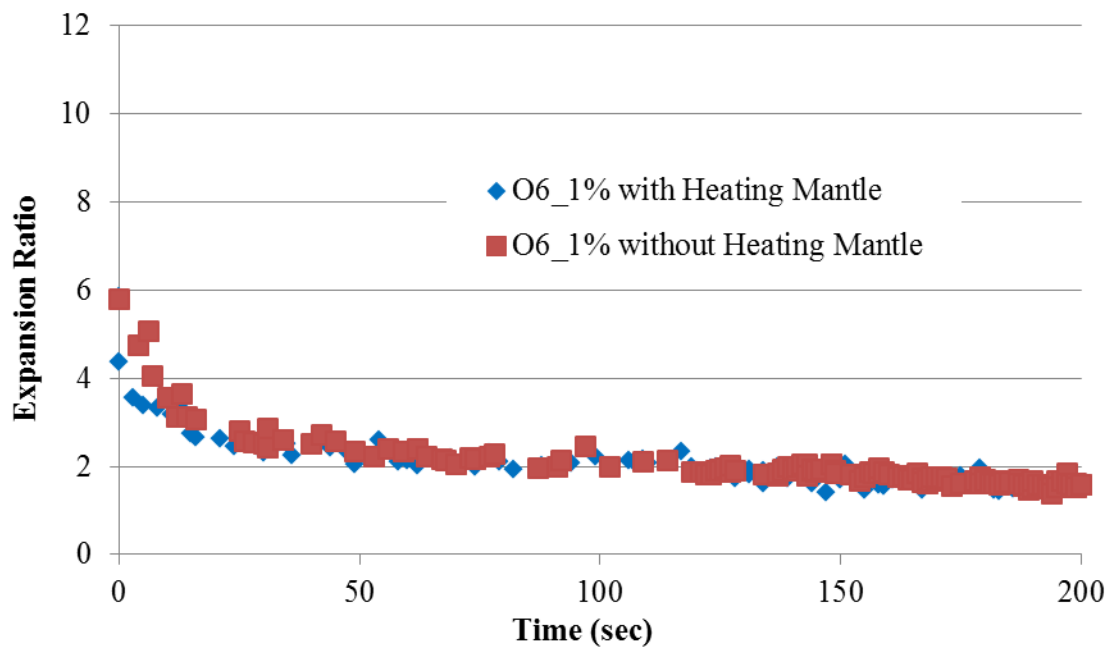


Figure 2.22: Expansion Ratio versus Time for O6 at 1% with/without Heating Mantle from the Accufoamer.

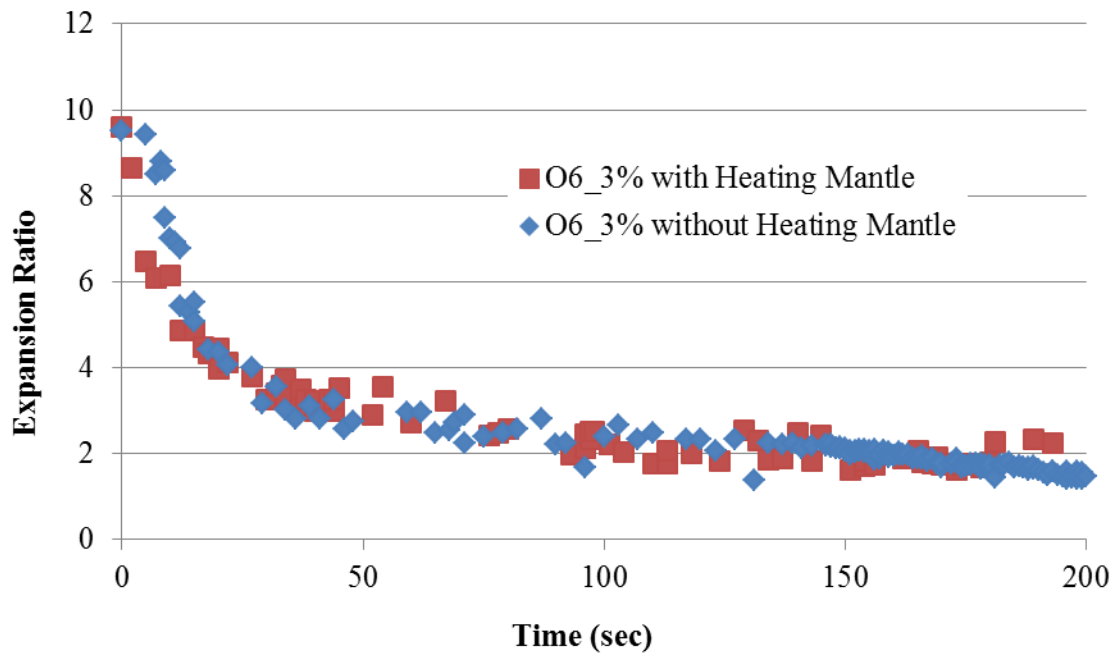


Figure 2.23: Expansion Ratio versus time for O6 at 3% with/without Heating Mantle from the Accufoamer.

### 2.5.5. Influence of Liquid Additives on Foam Characteristics

Liquid additives are used to improve the expansion and decaying characteristics of asphalt binder foams. A liquid additive may be added to the asphalt binder to increase expansion or stability when the asphalt binder does not have the anticipated expansion ratio or stability. Influence of liquid additives on expansion and decaying characteristics of asphalt binders were evaluated using three binders (N6, N7, and O7), two different types of liquid additives (Additive 1 and Additive 2) from different sources, and three water contents. The liquid additives used were emulsion-like alkaline products. The three binders were modified with the additive using 0.5% of the additive by weight of the binder, based on the recommendations of the producer. The additive was blended into the asphalt binder using a RW 20 digital overhead mixer with a four-blade propeller. The binders were pre-heated in an oven using 1-gallon cans at their respective hot mix asphalt

mixing temperatures. The cans were then inserted into a heating mantle and maintained at the asphalt binder's mixing temperature. The additive was added manually and slowly while stirring the binder in the overhead mixer. The binder was stirred for about 20 minutes at a constant speed to allow the additive homogenized completely. Each binder with and without the additive was foamed in the laboratory using the Accufoamer foaming device at three water contents that varied from 1%-3% by weight of the asphalt binder.  $ER_{max}$  and decaying trends of the foams produced using the modified and control binders are presented in Figure 2.24 through Figure 2.28. The following similarities and differences are observed in the expansion and rate of collapse of the foams:

- Additive 1 significantly improved  $ER_{max}$  and rate of collapse of the foams, while Additive 2 from a different producer had a negligible impact on  $ER_{max}$  and stability (Figure 2.24 and Figure 2.25).
- As before, for any given control binder or additive modified binder,  $ER_{max}$  increased with an increase in the water content and the relationship was linear, and the stability decreased with an increase in water content.
- The binder modified using Additive 1 showed markedly different characteristics of foam collapse. In particular, the sudden drop in volume of the foam during the first few seconds was not observed for the binder modified with Additive 1. Instead, the foamed binder showed a gradual collapse over time. It is hypothesised that Additive 1 increased the mixing efficiency of water with binder decreasing the possibility of larger droplets of water being encapsulated in the asphalt binder film. This avoids the sudden collapse of bubbles in the first few seconds resulting in a gradual reduction in volume of the foam over time.

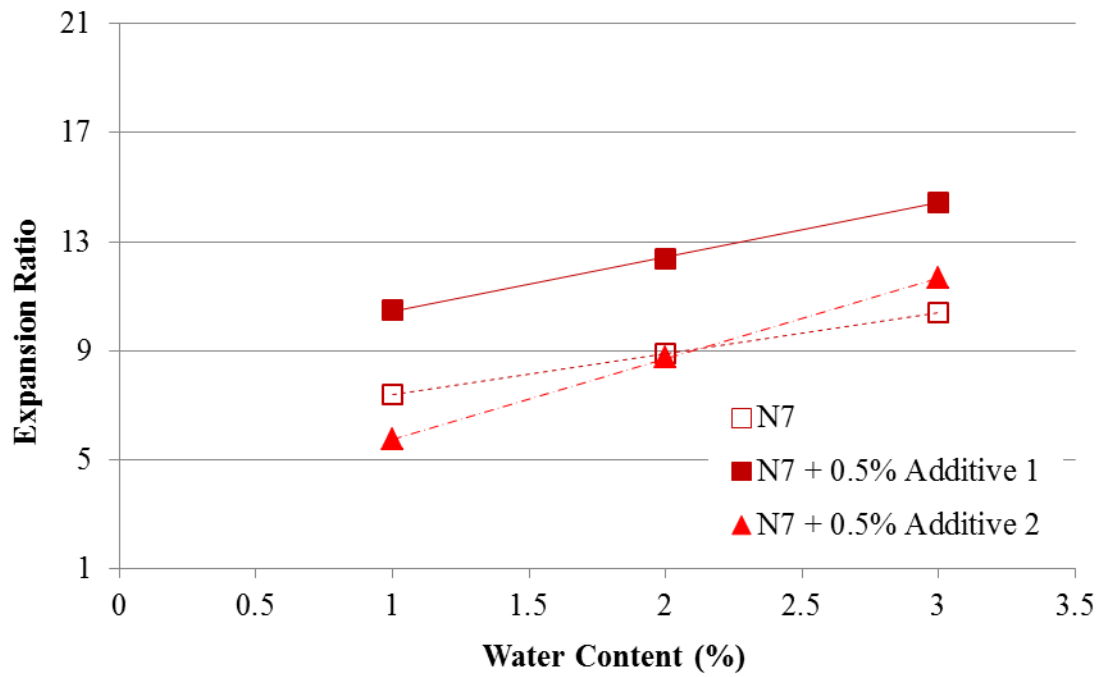


Figure 2.24: Influence of Additives on N7 Binder Foam Expansion.

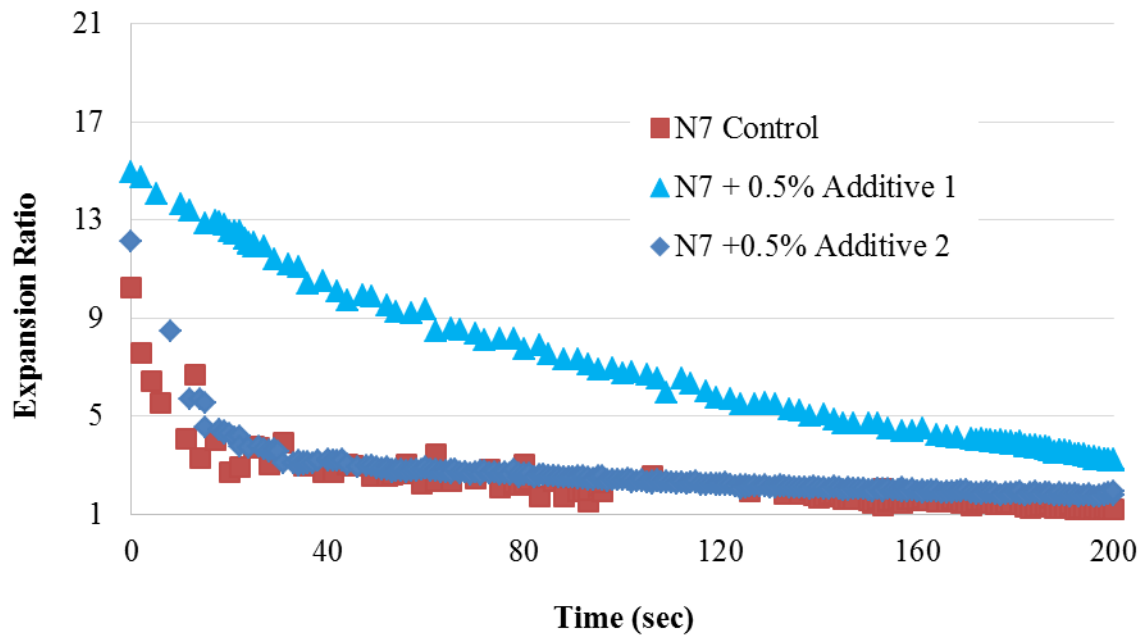


Figure 2.25: Influence of Additives on N7 Binder Foam Decay.

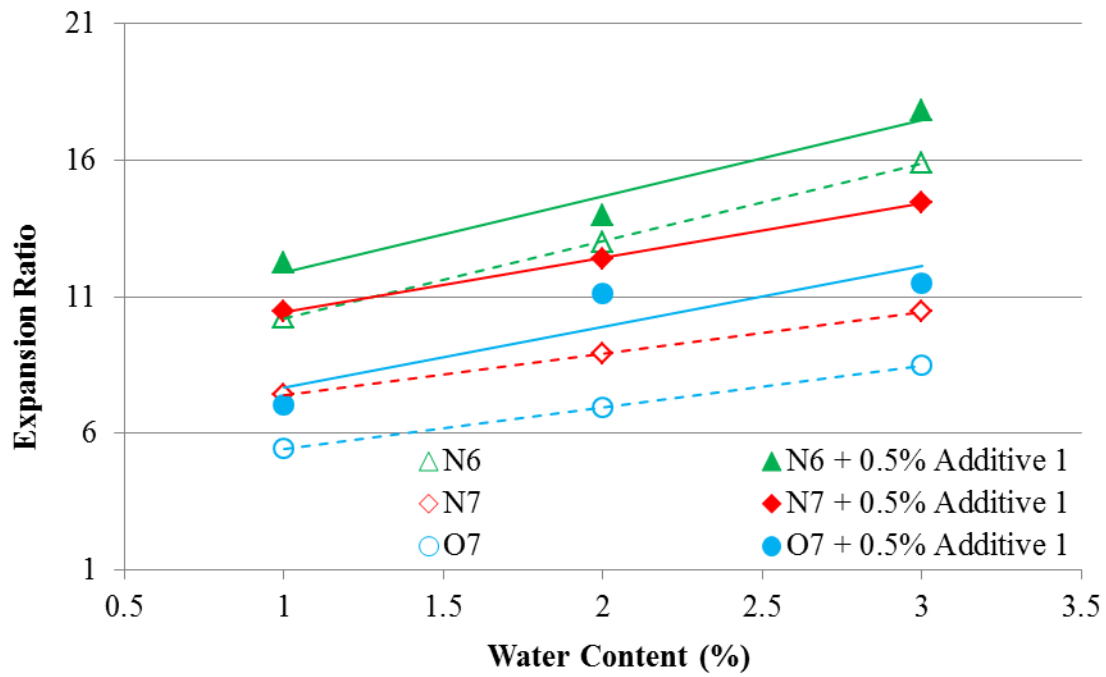


Figure 2.26: Influence of Additive 1 on Foam Expansion.

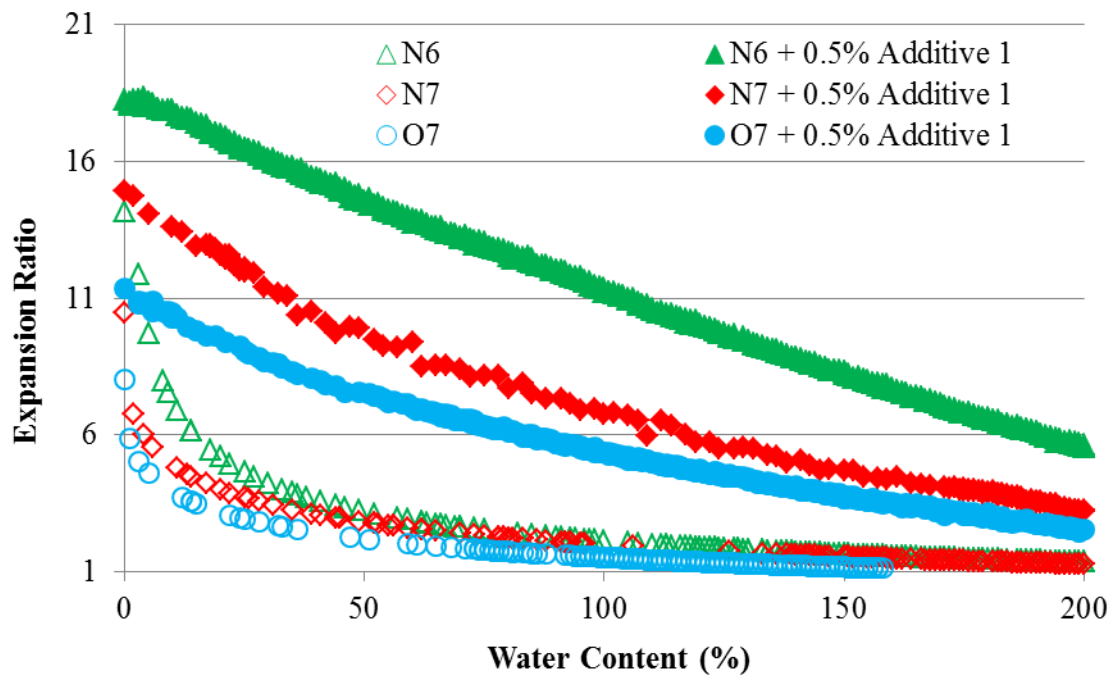


Figure 2.27: Influence of Additive 1 on Foam Decay at 3% Water Content.



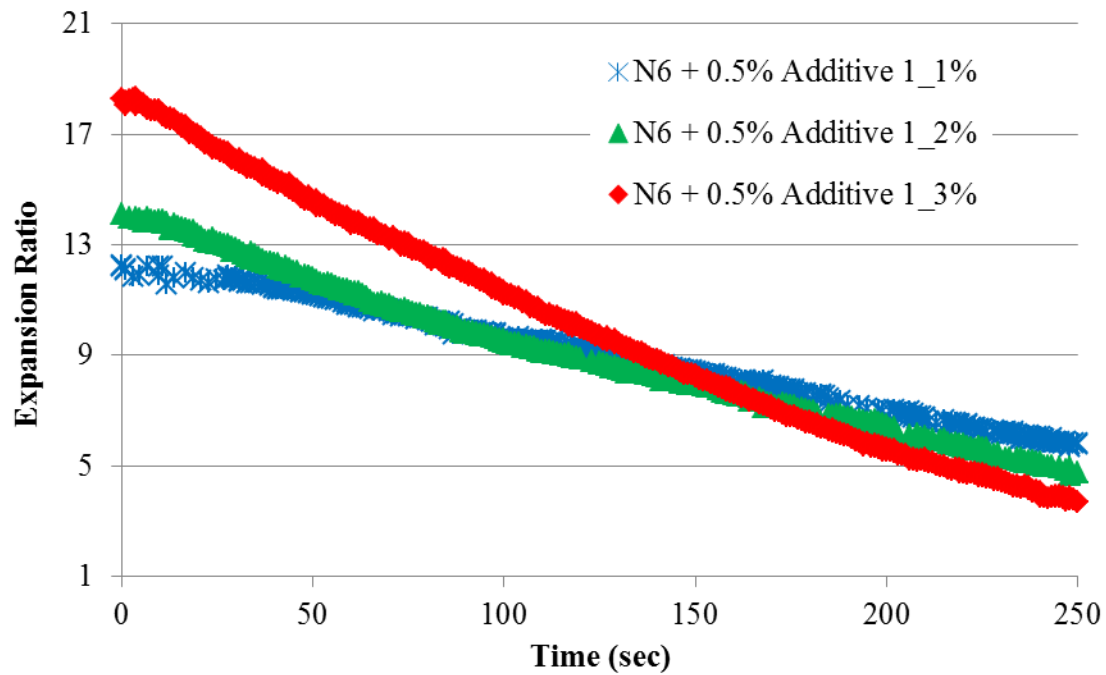


Figure 2.28: Influence of Water Content on Foam Decay of N6 Binder Modified with 0.5% Additive 1.

#### 2.5.6. Foaming Using Water Bearing Additives

In the case of asphalt foams produced using particulate additives such as zeolite, the additive is added to the asphalt binder (or mixture) typically at a rate of 5% by weight of the asphalt binder. These additives are hydro-thermally crystalized silicates with large empty spaces in their structure that allow to store up to 21% of water by weight of the additive (Hurley and Prowell 2005). When zeolites are mixed with hot binder, water is gradually released from their crystal structure to create a micro-foam, which is hypothesized to improve binder workability.

The typical dosage of 5% zeolite will result in approximately 1% water by weight of the binder being released (assuming all the water from the zeolite is released). However, unlike foaming by water injection, the rate of release of water with zeolite is much slower resulting in the expansion and decay of foam to continue over a much

longer duration of time. Consequently,  $ER_{max}$  and the rate of decrease of the overall volume of the binder foamed using zeolite are very low. Due to the small size of bubbles, foams created using zeolite are also more stable (longer life) compared to foams produced using water injection.

Due to major differences in the foaming mechanisms of the two foaming methods, parameters developed to characterize foams by water injection may not be appropriate to characterize zeolite foams. In addition, zeolite particles left after foaming act as particulate fillers that can alter the rheological properties of the foamed binder residue.

Asphalt foams were produced for this study using a synthetic zeolite. The typical recommended dosage for synthetic zeolite as a foaming agent is 0.25% by weight of the mix. Considering typical hot mix asphalt with 5% binder content, this corresponds to approximately 5% zeolite by weight of the binder. Based on this, N7 and O7 binders were blended with 5% zeolite using a RW 20 digital overhead mixer equipped with a four-blade propeller. About 600 grams of the heated binder was poured into a quart can and the can was inserted into a heating mantle to maintain the binder temperature at 160°C. The exact weight of the binder in the can was also determined. Zeolite (5% by weight of the binder) was then slowly added while the binder was stirred using the overhead mixer at a constant speed of 600 rpm. During blending of zeolite with the asphalt binder micro-bubbles approximately 1 mm in diameter (shown in Figure 2.29) were visible on the surface. A laser sensor was used to measure the change in height and corresponding volume of the foam. A schematic for the laser test setup is shown in Figure 2.30. Note that due to the nature of the particulate additive, mixing and expansion had to be measured simultaneously. Since mixing of the binder creates a non-uniform surface profile, the measurement was carried out by pointing the laser to a location approximately

midpoint between the center of the mixing container and its edge. Figure 2.31 illustrates the change in height during mixing for the two blended binders normalized with the constant height that was observed approximately 10 to 15 minutes after starting to mix. This normalization also incorporates the increase in volume due to the addition of the zeolite particles, which was approximately 2%. Note that the normalized change in height is not the factor by which expansion occurs because of the non-uniform surface profile. Rather this change is a qualitative indicator of the foam expansion and decay characteristics.

No noticeable change in the height of the binder occurred after 10 to 15 minutes from the start of blending. At this time, the blended binders were poured into RTFO bottles and aged in the RTFO at 143°C for 120 minutes. A reduced temperature of 143°C was used in lieu of the standard 163°C to simulate a WMA aging condition. The weights of the control binder and the binders blended with zeolite were measured during the RTFO aging processes after 30, 60, 90 and 120 minutes of aging. The average percent mass loss values are presented in Figure 2.32. Two replicate weight measurements were taken for both binders with/without zeolite and the error bars indicate the minimum and maximum values. The results demonstrate that the weight loss in the binders with zeolite was significantly higher than that of the control binder, suggesting the presence and continued release of moisture from the blended binders.



Figure 2.29: Bubble Size of Foams Produced using Zeolite.

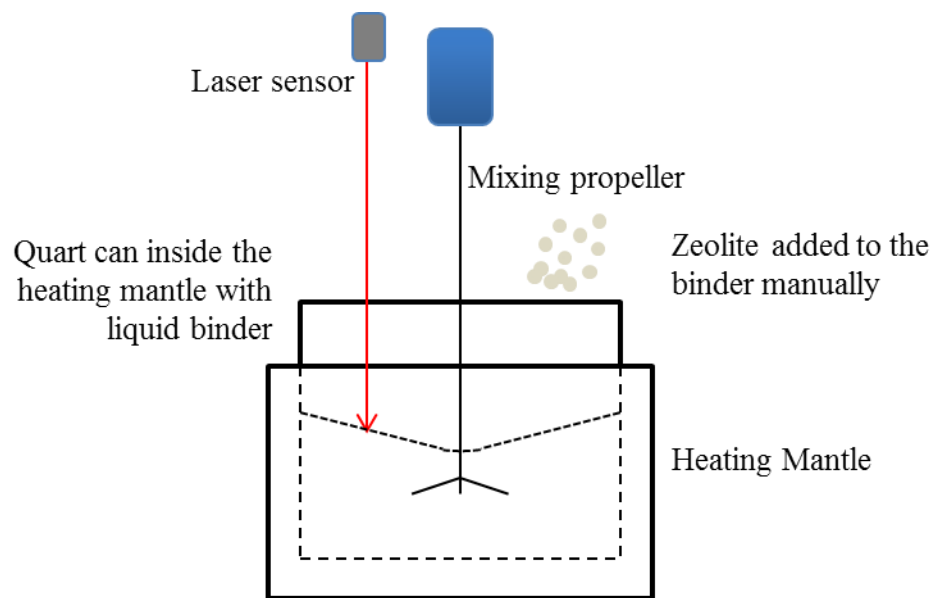


Figure 2.30: A Schematic for Zeolite Modified Asphalt Foam Test Setup.

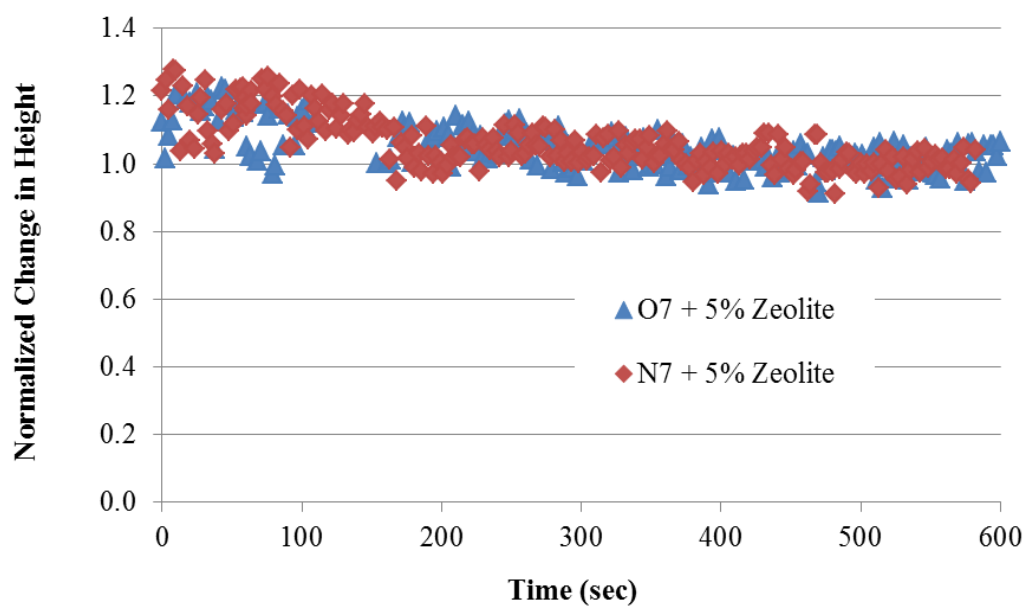


Figure 2.31: Normalized Change in Height of the Binder with Zeolite.

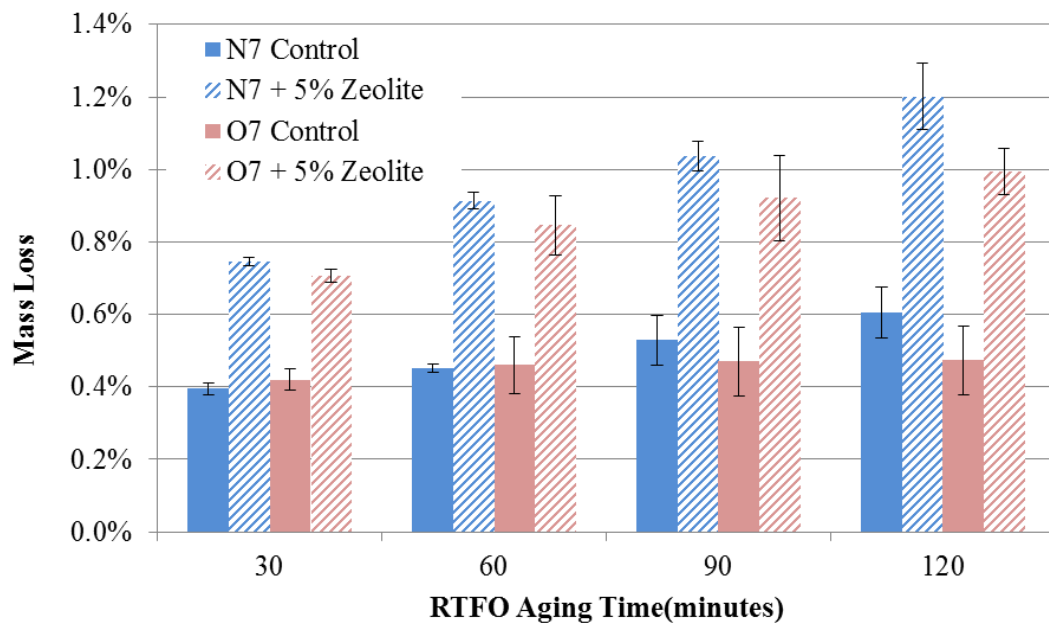


Figure 2.32: Weight Loss for the Control and Zeolite Blended Binders during RTFO Aging.

## **2.6. CONCLUSION AND DISCUSSION**

In order to effectively use foamed binder to produce WMA mixtures, it is important to quantitatively characterize the foaming characteristics of different asphalt binders and to evaluate the impact of foaming on the workability and performance of different WMA mixtures. This chapter focused primarily on the former objective, i.e., to develop a method and concomitant metrics to characterize the quality of foamed binders (i.e., foam expansion and stability). These metrics were used to evaluate the influence of factors such as binder type, water content, additive, foaming device, and temperature on asphalt binder foam characteristics. The next two chapters will focus on physical modeling of asphalt binder foam characteristics as well as on the relationship of the metrics identified in this chapter to the workability, and coatability of asphalt mixtures.

The following conclusions were drawn on the basis of the results presented in this chapter of the dissertation:

1. A laser- or ultrasonic-based distance-measuring sensor can be used to characterize the decay in the foamed binder in an accurate and repeatable manner. The procedure described in this dissertation was sensitive to distinguish between foaming characteristics of different asphalt binders as well as influence of water content on the foaming characteristics of any given asphalt binder. This procedure can be used to relate the foaming characteristics of different asphalt binders to the workability, coatability, and performance properties of full asphalt mixtures.
2. The foaming characteristics of different asphalt binders (expansion and time-stability) varied with the source and type of the asphalt binder in addition to external factors such as water content and liquid additive.

3. For any given asphalt binder, the  $ER_{max}$  increased with an increase in the water content and the relationship appears to be linear. However, an increase in the water content also resulted in an increase in k-value of the foam.
4. The characteristics of foamed asphalt binders produced using two different laboratory foaming devices were evaluated in this study.  $ER_{max}$  and k-value of semi-stable foam were used as the metrics for this comparison. Results show that these two metrics were different for the two foaming units. However, the metrics were in the similar range for the two devices and the relative trends for different combinations of water content and asphalt binders were also similar.
5. There is no noticeable influence of temperature on foam properties when dispensing the foamed binder sample in a container kept at room temperature as compared to a container kept at elevated temperature inside a heating mantle.
6. Foam characteristics of binders modified with two different liquid additives were investigated in this study. One of these two additives produced foams with more expansion and stability, while the other showed negligible effect on both expansion and stability. Results demonstrated that asphalt binder foam characteristics (both expansion and stability) can be significantly improved using carefully selected liquid additives.
7. No noticeable expansion was observed for the binders blended with zeolite. However, the weight loss in the binders with zeolite was significantly higher than that of the control binder, suggesting the presence and continued release of moisture from the blended binders.

## **Chapter 3: Parametric Analysis of Factors that Affect Asphalt Binder Foam Characteristics**

### **3.1. OVERVIEW**

A major impediment in the application of foamed asphalt binder for WMA is that, to date, there is no link that connects asphalt binder properties to its foaming characteristics. The reason why certain binders produce better quality foam than others is unknown. A thorough understanding of the relationship between fundamental asphalt binder properties to its foam characteristics is a vital step to fully characterize asphalt binder foam behavior. In this chapter, the influence of asphalt binder properties on characteristics of asphalt binder foam is quantified. A physical model for expansion of asphalt binder foam is proposed based on foam physics and fluid mechanics of micro-droplets. The developed model quantifies the effect of water content, temperature, surface tension, and liquid additive (through its effect on surface tension) on expansion ratio of asphalt binder foam. Analysis results demonstrate that the water droplet or bubble size distribution does not significantly impact the maximum expansion ratio of asphalt binder foam. The analysis also exhibits that the surface tension of the binder does not significantly influence internal bubble pressure. Comparison of results from the physical model with experimental measurements indicates that only a small percentage of water is effective in foaming the asphalt binder. The effective water content was shown to be strongly correlated with the surface tension of the binder. Foam characteristics of binders modified with additives also demonstrated that stability and expansion of foams can be significantly improved using carefully selected liquid additives.

### **3.2. BACKGROUND**

Foam is a semi-stable two component system consisting of gas bubbles dispersed in a liquid. It has been studied in other industries such as food, pharmaceutical and



healthcare products, and polymers for many years. Foams in other industries are typically classified and studied in two different categories (Adamson and Gast 1997; Pugh 2005):

1. Polyhedral foam (Dry foam): In this type of foam the volume of gas is much larger as compared to the volume of the fluid. The fluid exists in the form of very thin films separating the gas also referred to as lamella. The name is derived from the fact that the gas cells are polyhedral in shape.
2. Spheroidal foam (Wet Foam): In this type of foam the gas volume is relatively low compared to the polyhedral foam. A relatively thicker film of the fluid separates the gas bubbles.

Given the highly dynamic process of foaming, the two types of foam could coexist in the same material. Kutay and Ozturk (2012) showed that asphalt binder foams are spherical, whereas Jenkins (2000) demonstrated that asphalt foams are more close to polyhedral. However, observations made during the course of this study suggested that asphalt foams could start as polyhedral and become spheroidal as the bubbles collapse and the liquid volume increases over time. A schematic that illustrates the two different types of foam in asphalt binders is presented in Figure 3.1.

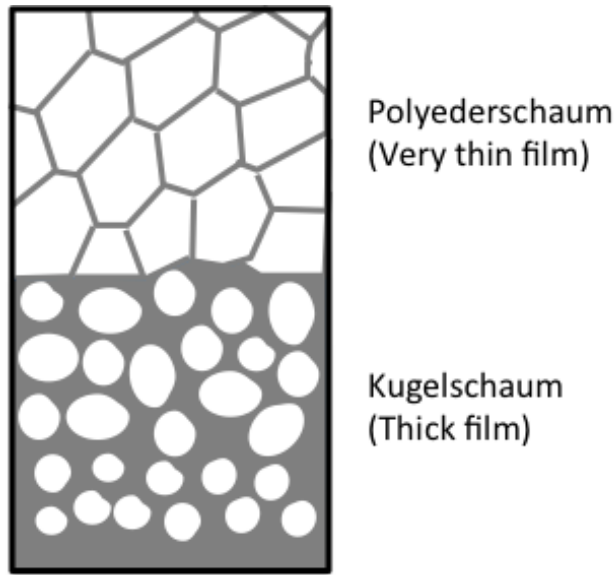


Figure 3.1: Schematic to illustrate the two different types of foam (Adapted from Pugh 2005).

The mechanics of bubble formation in fluids has been studied in literature (Leibson et al. 1956; Xu 2011). There are two mechanisms by which bubbles can be formed in fluids:

1. Gas delivered in the fluid with the use of orifice, nozzles, capillaries, and porous plates.

In this type of bubble formation, the nozzle is submerged in the fluid and the gas is blown into it. Bubble size is a function of orifice diameter, surface tension, fluid density, and gas flow rates. Bubble formation at very slow rates of gas flow is the basis of the drop-volume method for measuring surface tension, which was used later in this study.

2. Gas dissolved in the fluid through diffusion.

One example of a case where gas is delivered in the fluid through diffusion is the microcellular plastics injection molding process (Xu 2011). In the microcellular injection

molding process, a gas-polymer solution is first created in an extruder barrel. The gas at the supercritical fluid state is metered and injected into the barrel and then dissolved into molten polymer. As the gas flows into molten polymer, it forms large gas droplets (bubbles) since it takes time for the gas to be dissolved. The large droplets of gas are sheared, elongated, and broken into smaller bubbles with the rotation of the extruder screw. Then the gas quickly diffuses into the molten polymer due to the increased polymer-gas interfacial area and the reduction of diffusion length. The gas dissolution process obviously depends on many factors, including gas pressure, temperature of the polymer melt, and diffusivity and solubility of the gas. It is possible that the gas is not completely dissolved in polymer and small bubbles still exist during the gas-polymer mixing stage. These small bubbles grow bigger in the next stage when the mixture is released from the exit of the extruder. Nucleation can also happen elsewhere in the mixture, as long as the foaming condition is met. In the microcellular injection process, sudden release of pressure is the cause of bubble nucleation and subsequent bubble growth. In addition to direct gas injection, foaming agents can be mixed with polymer as additives. These additives decompose and give off the gas required for bubble formation inside the extruder barrel. This gas delivery system is typically used in foam extrusion processes that yield larger bubble sizes than the microcellular injection molding process.

Kim and Li (2011) and Wang and Li (2008) studied bubble growth in polymer foaming with carbon dioxide (CO<sub>2</sub>). In these studies, the bubble growth process is modelled as a quasi-static diffusion-driven process in which pressure and momentum in the viscoelastic fluid are balanced. The model relates the bubble growth process with material properties such as surface tension, relaxation time, viscosity, and gas diffusivity, as well as process parameters such as temperature, gas concentration, and the system pressure.

Berthier (2008) studied fluid mechanics of micro-droplets. He demonstrated that on a microscopic scale, surface tension and capillary forces dominate the fluid mechanics of micro-droplets. In another study, Uhlig (1937) investigated the relationship between surface tension and solubility of gases. Uhlig (1937) showed that solubility decreases as the surface tension of the solvent increases. These two studies suggest that mixing characteristics of the asphalt binder and water could be affected by the surface tension of the asphalt binder.

This preliminary understanding of the relationship between material properties and foaming helps explain the findings from other previous studies in the area of foamed asphalt. For example, (Fu et al. 2011) demonstrated that binder grade is not related to its ability to foam. This is expected because the binder grade does not reflect the material properties such as viscosity and surface tension that are related to foaming. Another example is that the addition of liquid anti-strip agents improves the ability of the binder to foam (Abel and Hines 1979; Engelbrecht 1999; Fu et al. 2011). This is also expected because Bhasin et al. (2007) have demonstrated that the addition of liquid anti-strip agents reduces the surface tension of the binder.

### **3.3. OBJECTIVES**

Although the use of plant foaming for WMA application has increased steadily over the years, the factors that affect asphalt binder foam characteristics is not well understood. For example, the influence of fundamental properties of binders (such as surface tension or viscosity) and water droplet size distribution on asphalt foam expansion is not clear. The reason why certain binders can produce better quality foam than others is not well known. This chapter focuses on developing a better understanding of the relationship between the intrinsic properties of an asphalt binder and its ability to

foam and consequently of the quality and performance of the WMA mixtures produced.

The specific objectives are to

- develop a physical model based on foam physics and fluid mechanics of micro-droplets to theoretically determine foam expansion using water content, bubble size distribution, and surface tension of base binders as inputs,
- use the theoretical analysis to explore the impact of temperature, water content, bubble size distribution, surface tension of binders, and liquid additives on expansion ratio, and
- employ the theoretical analysis in conjunction with the experimental data to determine effective water content and foam efficiency.

### **3.4. MATERIALS**

To accomplish the aforementioned objectives, a testing program was designed to measure foam expansion, bubble size distribution on the surface of the foam, and surface tension of the selected binders. Three asphalt binders were used for this study: N6, N7, and O7. Influence of liquid additives on foam expansion characteristics of asphalt binders were also evaluated by modifying the three binders with two liquid additives (Additive 1 and Additive 2) received from two different sources. The liquid additives were alkaline-like emulsion products. The three binders were modified with the additive using 0.5% of the additive by weight of the binder, based on the recommendations of the producer. The additive was blended into the asphalt binders using a RW 20 digital overhead mixer with a four-blade propeller. The binders were pre-heated in an oven in 1-gallon cans at their respective hot mix asphalt mixing temperatures. The cans were then inserted into a heating mantle and maintained at the asphalt binder's mixing temperature. The additive was manually and slowly added while stirring the binder in the overhead mixer. The

binder was stirred for about 20 minutes at a constant speed to allow the additive to be homogenized completely. Each binder with and without the additive was foamed in the laboratory using the Accufoamer foaming device at three water contents that varied from 1%-3% by weight of the asphalt binder. All foaming was carried out at 160°C.

### **3.5. TEST METHODS**

Test methods used include the following: a laser sensor to measure ER as a function of time, a digital camera to measure bubble size distribution on the surface of the foam, a maximum bubble pressure device (manufactured by SensaDyne) to measure surface tension of the binders, and a Brookfield viscometer to measure viscosity of binders.

The laser distance measurement (LDM) test was used to measure the change in height and corresponding volume of the foamed asphalt binder as the foam collapse over time. Foam evaluation parameters,  $ER_{max}$  and k-value, were then obtained by analysing the data collected. More details on the methodology to measure foam expansion and decay, influence of foaming equipment, water content, as well as modelling the time-decay in foamed binders are presented in Chapter 2.

A digital camera was used to periodically photograph the surface of the foamed asphalt binder. Images of the foamed surface at different points in time were analyzed using an image analysis software, ImageJ, to obtain the approximate bubble size and distribution on the surface. Analysis of images taken after 60 seconds of dissipation time (expansion ratio is less than 2 in most cases) shows that bubble sizes typically follow a Weibull distribution with an average diameter of 4 mm. Details of this analysis are presented in Chapter 2. However, an important finding from this analysis is that a significant portion of bubbles contributing to binder expansion have diameters in the

order of 1 mm or higher even after two minutes of foam dissipation and a progressive reduction in average bubble diameter during this time. This information will be used later in this chapter while evaluating the influence bubble size distribution on  $ER_{max}$ . Figure 3.2 shows photograph of a camera taking pictures on asphalt foam surface as it collapses over time and the bubble size distribution for a typical foamed asphalt binder using 1% water content.

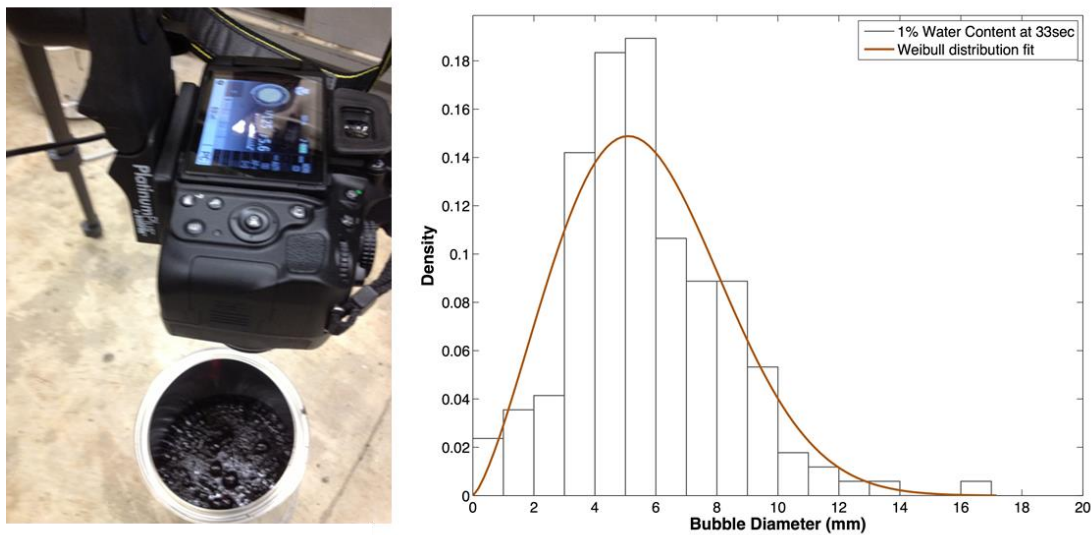


Figure 3.2: Camera Setup for Image Acquisition of the Surface of the Foam as it Collapses over Time and Resulting Bubble Size Distribution.

There are several methods that can be used to measure surface tension of liquids: the capillary rise method, the pendant drop method, the maximum bubble pressure method, and the differential maximum bubble pressure method (Osmari et al. 2013).

The first two are relatively old and simple methods to measure surface tension of liquids. However, they are not the appropriate methods to measure surface tension of asphalt binders because of the following three reasons: (1) surface tension measurements of asphalt binders are conducted at elevated temperatures and keeping the asphalt binder

at higher temperatures has challenges, (2) it takes quite some time for the binder to come to equilibrium due to its high viscosity, and (3) it is difficult to make accurate height measurements due to the dark colour of the binder.

In the maximum bubble pressure method, an inert gas is injected through the liquid via a tube to create a bubble with radius equal to the radius of the tube when its pressure reaches a maximum stage. In this method, the maximum pressure of the tube is experimentally measured and the Young-Laplace equation is used to back-calculate the surface tension of the liquid. Measurement of densities for the gas and the liquid, and depth of immersion of the capillary tube are required in this method.

The last method, the differential maximum bubble pressure method, is similar to the maximum pressure method except that a variation of the bubble pressure method (using small and large tube) is used to avoid measurement of densities for the gas and the liquid, and depth of immersion of the capillary tubes. This method was selected to measure surface tension of the binders.

The surface tension of the three binders with and without liquid additive modification was measured using the differential maximum bubble pressure method using a device manufactured by SensaDyne Instruments. Since LDM results indicated that Additive 2 does not significantly improve foam expansion and decay characteristics of foams, surface tension measurements were not taken for the binders modified with Additive 2. In this study, Argon gas was injected through the binder via two orifices of different diameters (4.0 mm and 0.5 mm). The upstream pressure in the gas was maintained at about 50 psi. This method measures the pressure difference between the large and small orifices as bubbles are produced by injecting a gas through these capillaries when immersed in the liquid binder. The pressure differential between the bubbles from the two tubes was measured using a differential pressure transducer. A



temperature sensor is also attached next to the tubes to measure the temperature of the asphalt binder. First, the temperature sensor was calibrated using ice cold and hot water, and an externally calibrated thermocouple. After completion of the temperature calibration, distilled water and isopropyl alcohol were used to calibrate the surface tension values at a 1 bubble/sec bubble rate. Following the temperature and surface tension calibrations, surface tension of an asphalt binder sample was continually measured and recorded over a range of temperatures. A photograph of the test setup is presented in Figure 3.3.

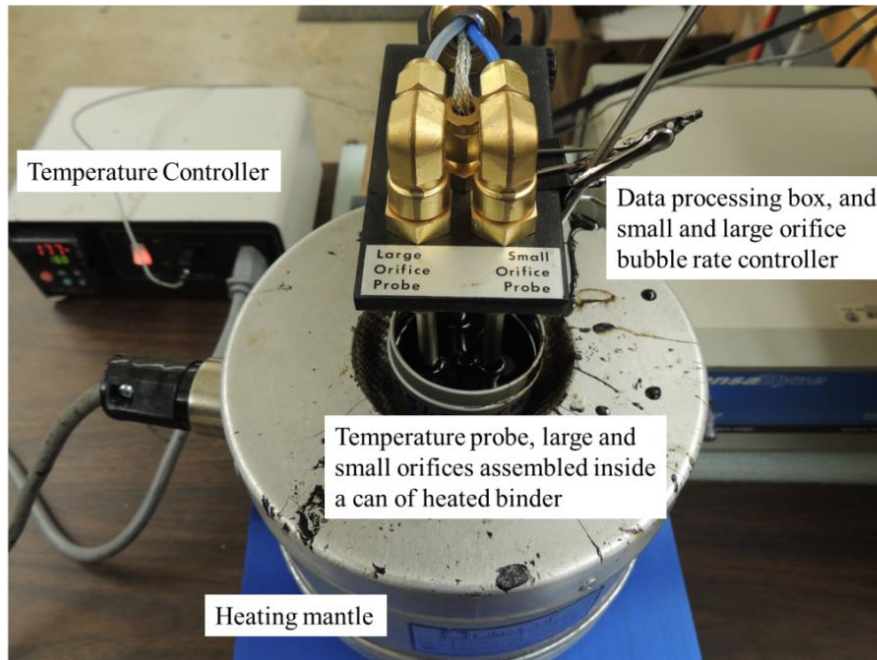


Figure 3.3: Surface Tension Test Setup.

In addition to surface tension, viscosity of binders was measured to evaluate its impact on asphalt foam characteristics. To investigate influence of viscosity on foam expansion and decay characteristics, a Brookfield rotational viscometer was used to measure viscosity of binders. The viscosity of the three binders (N6, N7, and O7) with

and without additive 1 was measured using the Brookfield rotational viscometer with spindle # 27 at 135°C.

### 3.6. ANALYTICAL BACKGROUND

Foamed asphalt binder is produced through the injection of small droplets of cold water into the hot asphalt binder. When a droplet of water comes in contact with the hot binder, it turns into steam and expands to form a bubble. Binder, that forms the skin of the bubble, holds the pressurized steam within it by balancing the difference between the internal and atmospheric pressure with its surface tension. This process occurs for each droplet resulting in a foamed binder. The relationship between external atmospheric pressure, internal pressure due to steam and surface tension is given by the Laplace equation. The internal pressure due to steam can also be calculated using the universal gas law. The two equations (Laplace equation and universal gas law) can be combined to obtain a relationship between the bubble diameter, droplet size, temperature, and surface tension of the binder as shown in Equation 3.1. The main assumptions in these two equations are that the gas (steam) in each of the bubbles is ideal, the bubbles are spherical, and every droplet of water converts into steam, and is effective in forming a bubble. The only unknown parameters to employ these equations are the surface tension of the binder at the foaming temperature, and the size distribution of the water droplets. The size distribution of water droplets diffusing within the binder are in turn dictated by factors such as the water content and design of the foaming nozzle.

$$\frac{P_{atm}\pi D^3}{6} + \frac{2\gamma\pi D^2}{3} - nRT = 0 \quad [3.1]$$

where,

$P_{atm}$  – The atmospheric pressure (Pa),

$\gamma$  – The surface tension of the binder (N/m),  
 $D$  – The diameter of the bubble (m),  
 $n$  – Number of moles (mass/atomic mass of compound),  
 $R$  – The universal gas constant (8.314 J/mole.Kelvin),  
 $T$  – Foaming temperature (Kelvin).

### **3.7. RESULTS FROM THE PARAMETRIC ANALYSIS**

#### **3.7.1. Influence of Surface Tension on Bubble Size**

The impact of surface tension on the internal bubble pressure and bubble size in asphalt foam was evaluated. The surface tension of the binders was measured using the procedure described in section 3.5. A bubble flow rate of 1 bubble/sec was used for the tests. Figure 3.4 shows the surface tension of the three binders with and without the additive as a function of temperature. The test results demonstrate that the surface tension of binders is linearly related to temperature; this is true for most liquids. The test results also indicate that at least one of the additives reduced the surface tension of the binders significantly.

Typical value of surface tension of the asphalt binders was used with the Laplace equation to determine the internal pressure within the foam bubbles. The most important feature of the Laplace equation is that the pressure required to maintain the bubble is inversely proportional to its diameter. This means that smaller bubbles have greater internal steam pressures. The expected internal pressure within the bubbles was calculated for different bubble diameters assuming a typical asphalt binder surface tension value of 45mN/m. Figure 3.5 shows the results from this analysis. These results show that bubble size does not significantly affect the internal bubble pressure for asphalt bubbles that are greater than 100 micro-meters in diameter. In other words, the

contribution of surface tension to internal steam pressure is negligible (for bubbles greater than 100 micro-meters). A corollary to this is that the bubble size distribution of the foamed asphalt binder is not significantly affected by the surface tension of the base binder, and internal steam pressure is approximately equal to atmospheric pressure. Analysis of images of the asphalt foam surface shows that bubbles have sizes that are much higher than 100 micro-meters.

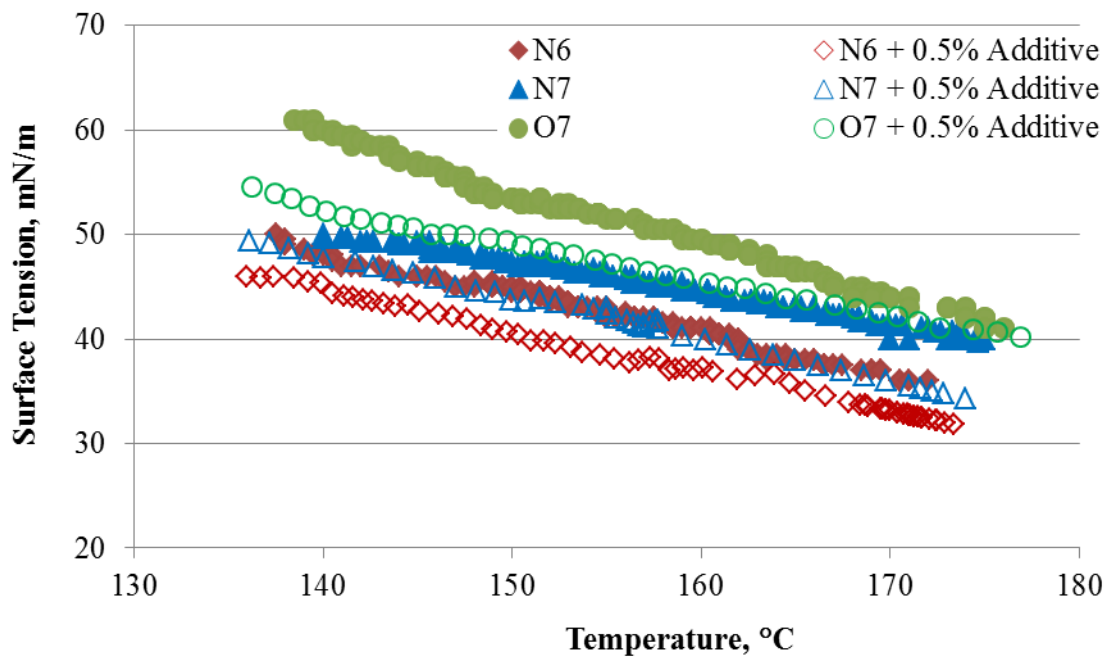


Figure 3.4: Surface Tension of Binders as a Function of Temperature.

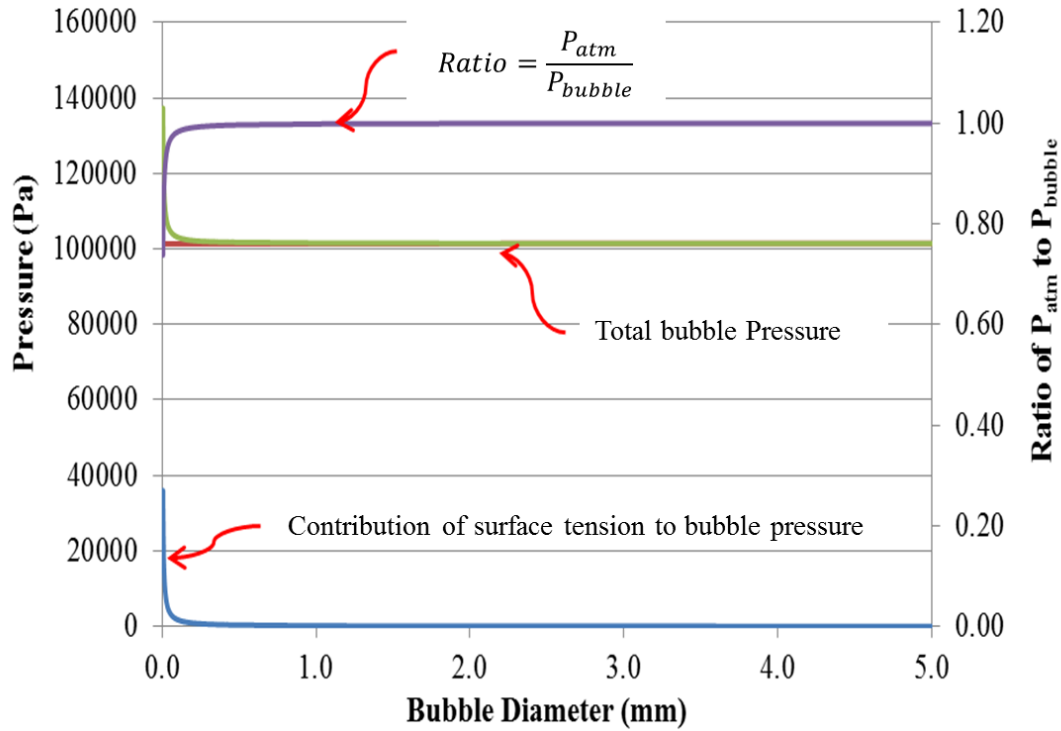


Figure 3.5: Influence of Surface Tension on Asphalt Foam Internal Pressure.

### 3.7.2. Influence of bubble size distribution on maximum expansion ratio

An analysis was conducted to determine whether the initial distribution of water droplets in the mixing unit of the foaming device and the subsequent initial distribution of the bubble diameters had an impact on the maximum expansion ratio ( $ER_{max}$ ).  $ER_{max}$  was calculated for several initial water droplet / bubble size distributions for water contents that varied from 1% to 3% and for a binder surface tension of 45mN/m. The methodology used for this analysis was as follows.

The mass of the binder ( $m_{binder}$ ) used for this analysis was 200 g, which was also the mass used in the experimental measurements. The atmospheric pressure ( $P_{atm}$ ) was taken as 101325 N/m<sup>2</sup>, and it was assumed that  $m_{water}$  grams of water was added by the foaming device by dispensing and mixing it with the binder in the form of  $N$  number of

water droplets. Consequently,  $N$  numbers of asphalt foam bubbles are created. Using the Laplace equation, the following can be obtained for the internal pressure of any bubble  $j$ :

$$P_{bubblej} = P_{atm} + \frac{4\gamma}{D_j} \quad [3.2]$$

The following equation can be derived by solving Equation 3.1 for  $n_j$

$$n_j = \frac{101325\pi D_j^3}{6RT_f} + \frac{2\gamma\pi D_j^2}{3RT_f} \quad [3.3]$$

The number of water droplets,  $N$  can be obtained as,

$$N = \frac{m_{water}}{18n_{avg}} \quad [3.4]$$

Substituting Equation 3.2 and 3.3 into the ideal gas law equation, individual bubble volume ( $V_j$ ) can be calculated as follows:

$$V_j = \frac{n_j RT_f}{P_{bubblej}} = \frac{\frac{P_{atm}\pi D_j^3}{6} + \frac{2\gamma\pi D_j^2}{3}}{P_{atm} + \frac{4\gamma}{D_j}} \quad [3.5]$$

The cumulative volume of foam,  $V_t$ , for  $N$  number of water droplets is the sum of the individual bubble volume and the volume of the binder:

$$V_t = \sum_{j=1}^N V_j + V_{binder} \quad [3.6]$$

$$ER_{max} = \frac{V_t}{V_{binder}} = \frac{\sum_{j=1}^N V_j + V_{binder}}{V_{binder}} \quad [3.7]$$

Volume of the asphalt binder (without foam),  $V_{binder}$ , can be determined using mass ( $m_{binder}$ ) and density of the non-foamed binder, taken as  $1.034\text{g/cm}^3$ .

$$V_{binder} = \frac{m_{binder}}{1.034} = 0.967m_{binder} \quad [3.8]$$

In the above equations,  $T_f$  is the temperature of the foam (not the same as the foaming temperature of the asphalt binder). When the asphalt binder at  $160^\circ\text{C}$  mixes with water at  $25^\circ\text{C}$  (room temperature), the foam will have a temperature lower than the temperature of the asphalt binder. The temperature of the foam can be determined using thermal equilibrium, assuming no heat is lost during the foaming process (Jenkins 2000). If  $T_f$  is the final temperature of the foam, the quantity of excess heat,  $Q$ , available from the asphalt binder to vaporize water can be determined as:

$$Q = m_{binder}C_{binder}(160 - T_f) \quad [3.9]$$

where,  $C_{binder}$  is the specific heat of asphalt binder ( $C_{binder} = 2.093\text{J/g}^\circ\text{C}$ )

The excess heat,  $Q$ , from the asphalt binder is equivalent to the amount of heat needed to vaporize  $m_{water}$  at  $25^\circ\text{C}$ , and raise its temperature to  $T_f$ , which can be determined as:

$$Q = m_{water}C_{water}(T_f - 25) + m_{water}L_v \quad [3.10]$$

where,  $C_{water}$  is the specific heat of water ( $C_{water} = 4.185 \text{ J/g/}^\circ\text{C}$ ),  $L_v$  is latent heat of vaporization ( $L_v = 2256 \text{ J/g}$ )

Combining Equations 3.9 and 3.10, and solving for  $T_f$ :

$$T_f = \frac{160 * m_{binder}C_{binder} + 25 * m_{water}C_{water} - m_{water}L_v}{m_{binder}C_{binder} + m_{water}C_{water}} \quad [3.11]$$

Substituting the above values for the 200g binder foamed at 1% (2 grams) water content, and solving Equation 3.11,  $T_f = 146.8^\circ\text{C}$ .

A typical average bubble size of 4.2 mm diameter was assumed for the analysis. Number of moles,  $n$  for the average bubble size was back-calculated using Equation 3.3.  $N$  was then determined using Equation 3.4. For this example, water is dispensed in the form of 101756 droplets with each weighing 19.65 micrograms to mix with the binder and produce foam. The volume of the bubbles for each of the droplets, and the total volume of the foam was computed. For a mean of 19.65 micrograms, the total volume of the foam was calculated as  $4147 \text{ cm}^3$ . This translates into  $ER_{max}$  of 20.7 for the 200 g of binder used in these calculations.

Similarly,  $ER_{max}$  was computed for several different bubble diameters and number of bubbles. Figure 3.6 presents a summary of results from this analysis. Note that for a given water content only one of the two parameters, initial average bubble diameter or number of bubbles needs to be assumed while the other can be calculated. Results of the analysis demonstrate that  $ER_{max}$  remains the same irrespective of the bubble size and number of bubbles as long as the total water content turning into steam and forming the



bubbles was constant. In other words, for a given volume of binder and water content, bubble size distribution does not significantly affect  $ER_{max}$  of the foam for bubbles that are more than 100 micro-meters in diameter. The theoretical  $ER_{max}$  was also computed by varying the surface tension of the asphalt binder between 40-70 mN/m for fixed water content and an assumed initial bubble/water droplet size distribution. The results from this analysis show that the surface tension of the binders (in the range specified above) does not significantly affect  $ER_{max}$ . This is consistent with the analysis shown in Figure 3.5. It is important to note that the bubble size distribution affects rate of foam decay because of Stoke's law.

Hence, for large bubbles (bubbles that are more than 100 micro-meters in diameter) where the surface tension of the asphalt binder does not affect the bubble volume significantly, the equation for  $ER_{max}$  can be simplified as follows.

From Equation 3.7,  $ER_{max}$  is given by,

$$ER_{max} = \frac{V_t}{V_{binder}} = \frac{V_{bubble} + V_{binder}}{V_{binder}} \quad [3.12]$$

Total volume of the bubble,  $V_{bubble}$ , can be determined using the ideal gas law equation.

$$V_{bubble} = \frac{nRT_f}{P_{atm}} = \frac{\frac{m_{water}}{18}RT_f}{P_{atm}} = \frac{m_{water}RT_f}{18P_{atm}} \quad [3.13]$$

Hence,  $ER_{max}$  can be simplified to:

$$ER_{max} = \frac{V_{bubble} + V_{binder}}{V_{binder}} = \frac{\frac{m_{water}RT_f}{18P_{atm}} + 0.967m_{binder}}{0.967m_{binder}}$$

$$\rightarrow ER_{max} = \frac{m_{water}RT_f + 17.41m_{binder}P_{atm}}{17.41m_{binder}P_{atm}} \quad [3.14]$$

The excess heat available from the asphalt binder can also be used to determine the theoretical maximum amount of water that can be added to the asphalt binder for foaming. If water exceeding this threshold is added, a portion of the foamant water will not be converted to steam due to lack of heat to achieve this.

Combining Equations 3.9 and 3.10, and solving for  $m_{water}$ :

$$m_{water} = \frac{m_{binder}C_{binder}(160 - T_f)}{C_{water}(T_f - 25) + L_v} \quad [3.15]$$

If the minimum foam temperature,  $T_f$ , is set to a typical WMA mixing temperature, for example, to 135°C, the maximum limit will be 3.85 grams. This value translates to 1.93% water content. Also, theoretically a binder at a temperature of 160°C has enough heat to convert a maximum of 4.89% water by weight, resulting in a foam at a temperature of 100°C (boiling point of water). In other words, if we were to mix more than approximately 5% of water at room temperature with the binder at 160°C, the temperature of the resulting foam will fall to 100°C preventing conversion of excess water to steam.

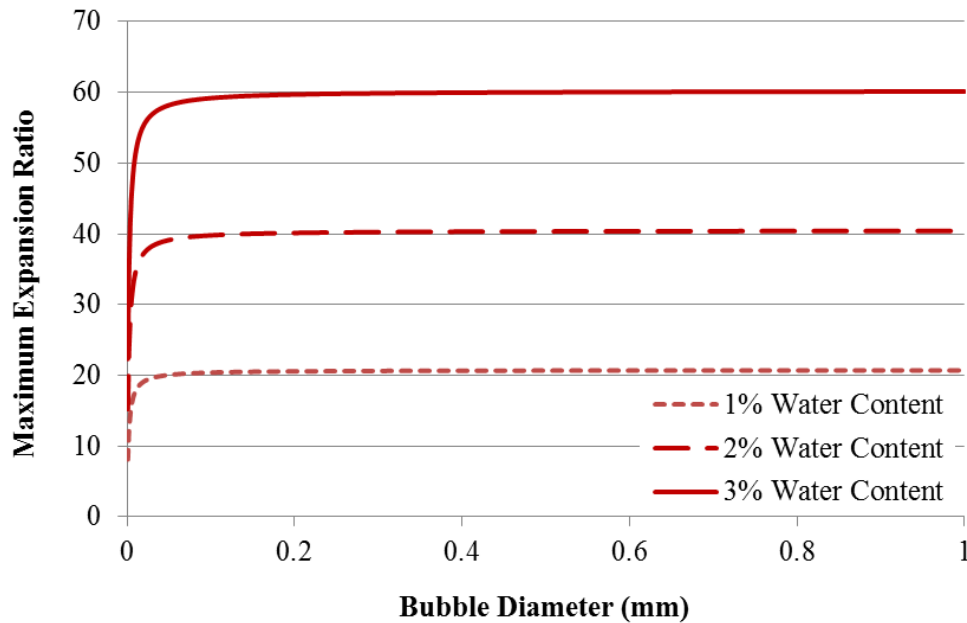


Figure 3.6: Influence of Bubble Size on Maximum Expansion Ratio.

### 3.7.3. Effective Water Content and Foaming Efficiency

By comparing the theoretical  $ER_{max}$  to the measured  $ER_{max}$ , it is possible to determine the percentage of water that is effective in foaming the asphalt binder. This comparison for the three binders at 1, 2, and 3 percent water content reveals that the measured  $ER_{max}$  is consistently much lower than the theoretical  $ER_{max}$ . The ratio between the effective and total water content decreases as the water content increases (Table 3). Despite the ideal conditions assumed for the theoretical  $ER_{max}$ , the results clearly indicate that not all water added to the binder is effective in foaming the binder. It is also clear that as the water content is increased, the percentage of water that is effective in foaming decreases. The reduced foaming may be due to incomplete mixing of the water droplets with the binder during the production of the foam. Other factors such as the dispensing mechanism of the foaming unit can also affect the percentage of water that is effective in foaming.

Although results from Figure 3.6 illustrate that the surface tension of the binder does not influence the size of large foamed bubbles, it must be noted that the surface tension of the binder may still affect the mixing characteristics of water droplets with the asphalt binder, consequently affecting the percentage of water that is effective in foaming. As discussed earlier, Berthier (2008) showed that the surface tension and capillary forces play a key role in determining the behaviour of micro-droplets on different substrates and geometry in micro-systems. Uhlig (1937) also developed a theory to describe the solubility of gases based on energy change in transferring a solute molecule of radius  $r$  to a solvent of surface tension  $\gamma$  as follows:

$$\ln S = \frac{-4\pi r^2 \gamma + E}{kT} \quad [3.16]$$

where,  $E$  is the interaction energy of solute and solvent,  $S$  is solubility (ratio of concentration of solute in the solvent to that in the gas),  $K$  is the Boltzmann's constant,  $T$  is the absolute temperature.

Solubility is defined as the ratio of concentration of solute in the solvent to that in the gas. The equation derived by Uhlig (1937) demonstrates that solubility decreases as the surface tension of the solvent increases. Therefore it is possible that the surface tension of binders at the foaming temperature may affect the efficiency with which the binder and water mix with each other to produce foam. To investigate this, the surface tensions of three binders (N6, N7, and O7) with and without the additive at the foaming temperatures were compared to solubility (ratio of water effective in foaming to that of water wasted). The surface tension of the binders determined using the differential maximum bubble pressure method is presented in Table 3.1. The percent of water

effective in foaming was back-calculated using the lab measured  $ER_{max}$ . The percent effective water content and solubility values for the binders at three water contents are presented in Tables 3.2 and 3.3, respectively.

Water Content, %	Foam Temperature, °C	Surface Tension, mN/m					
		N6	N6 + 0.5% Additive	N7	N7 + 0.5% Additive	O7	O7 + 0.5% Additive
1	146.8	45.8	42.2	48.4	45.0	55.9	50.1
2	134.1	50.9	46.4	52.2	49.8	62.3	55.5
3	121.9	55.8	51.5	55.8	54.3	68.5	60.8

Table 3.1: Surface Tension of Binders and Final Temperature of Asphalt Foams at Different Water Contents.

Water content (%)	Solubility					
	N6	N6 + 0.5% Additive	N7	N7 + 0.5% Additive	O7	O7 + 0.5% Additive
1	0.98	1.45	0.56	1.02	0.36	0.52
2	0.47	0.53	0.28	0.44	0.21	0.38
3	0.36	0.42	0.21	0.32	0.16	0.24

Table 3.2: Solubility of Asphalt Foams.

Water content (%)	Ratio of Effective Water Content to Total Water Content					
	N6	N6 + 0.5% Additive	N7	N7 + 0.5% Additive	O7	O7 + 0.5% Additive
1	0.49	0.59	0.36	0.51	0.26	0.34
2	0.32	0.35	0.22	0.31	0.17	0.28
3	0.26	0.30	0.17	0.24	0.14	0.19

Table 3.3: Effective Water Content of Asphalt Foams.

Figure 3.6 compares the surface tension of the binders to solubility. Figure 3.6 shows a strong correlation between solubility and surface tension of the binders. Figure 3.7 shows a similar trend between percent of water effective in foaming to surface

tension of binders. These empirical results indicate that the surface tension of asphalt binder dictate the efficiency with which water mixes with asphalt binder to produce foam.

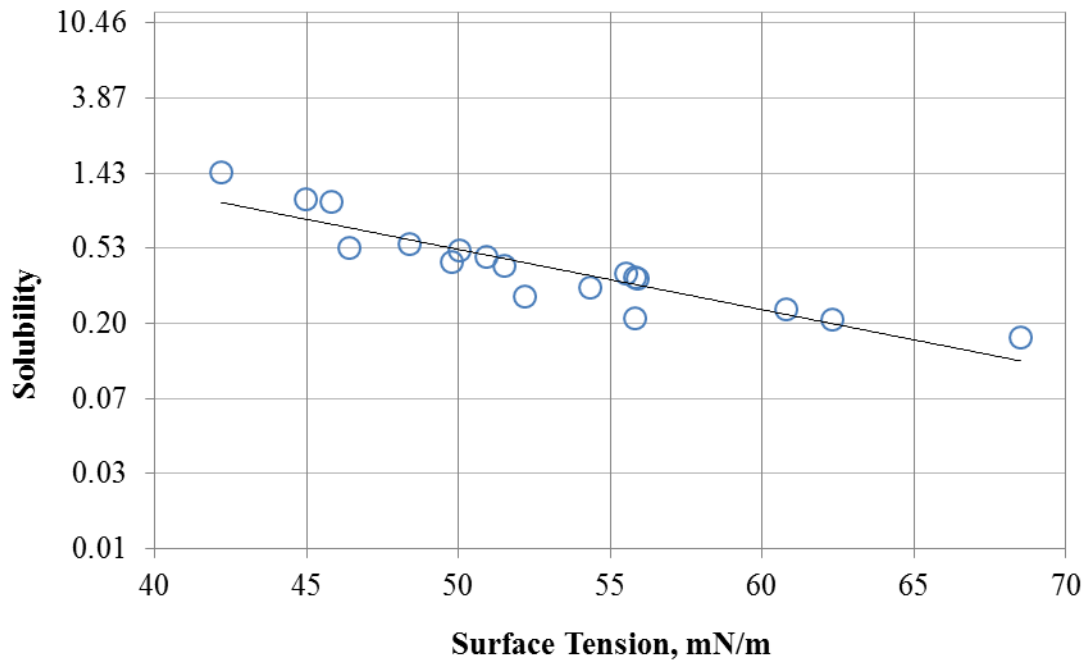


Figure 3.7: Relationship between Solubility and Surface Tension of the Asphalt Binder.

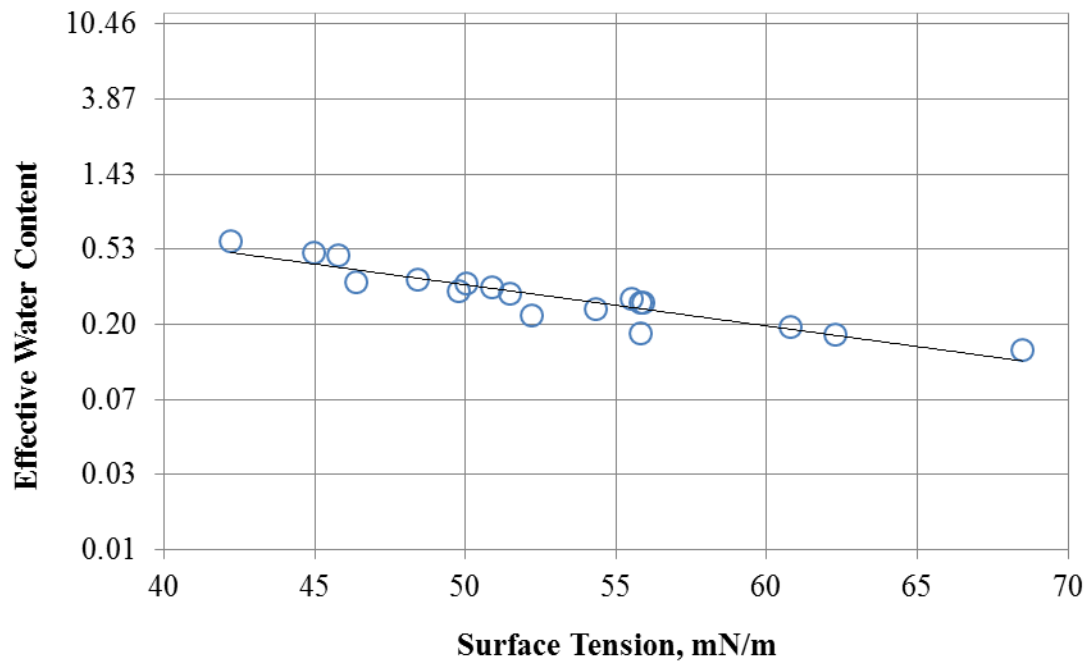


Figure 3.8: Relationship between Effective Water Content and Surface Tension of the Asphalt Binder.

### 3.8. FOAM STABILITY

Foam stability is defined as the rate at which the overall volume of the foam changes with time. Foam stability is a function of stability of individual bubbles. Stability of individual bubbles is in turn influenced by intrinsic asphalt binder properties (such as viscosity and surface tension), initial bubble film thickness and water droplet size. Initial film thickness is a function of  $ER_{max}$ . Foam with higher  $ER_{max}$  (higher gas to liquid ratio by volume) has lower initial film thickness, and vice versa. Water droplet size may be influenced by nozzle design and pressure. All these factors make foam decay a complex process. The main mechanisms of bubble collapse are excessive steam pressure and liquid flow. Excessive steam pressure causes collapse of the unstable bubbles, while liquid flow mainly causes collapse of the semi-stable bubbles. In the case of bubble collapse due to excessive steam pressure, the foam collapse is almost immediate resulting

in a significant reduction of foam volume in the first few seconds. The bubble collapses because of excessive tensile stress on the film that exceeds its tensile strength. The collapse of the semi-stable bubbles due to liquid flow is gradual resulting in a gradual reduction in the overall foam volume with time. Chapter 2 presents additional details on the processes that drive the collapse of foam bubbles. However, it is important to note that binders modified with Additive 1 did not show a sudden collapse in foam volume during the first few seconds. This suggests that the tensile stress of the binder film due to internal steam pressure was less than its tensile strength. It is hypothesized that when the mixing efficiency of asphalt binder with water increases, the potential for larger droplets of water turning into steam and resulting in a sudden bubble collapse decreases. The stability (quantified by k-value) of asphalt binder foams before and after additive modification is presented in Figure 3.9. The data in Figure 3.9 demonstrates that, as before, increasing the water content decreases foam stability. In addition, the data exhibit that liquid additives improved the stability of foams. Figure 3.10 compares the surface tension of binders to k-value. The data suggests that an increase in surface tension of the binders, in general, result in an increase in k-value (a decrease in stability).



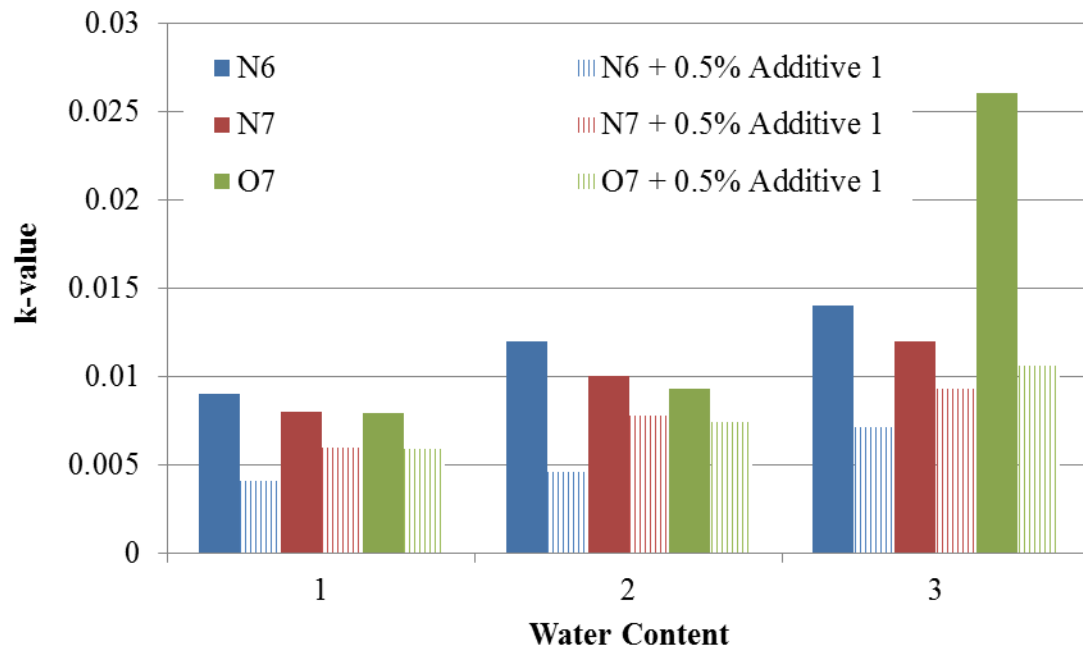


Figure 3.9: Influence of Water Content and Liquid Additive on Stability of Foams.

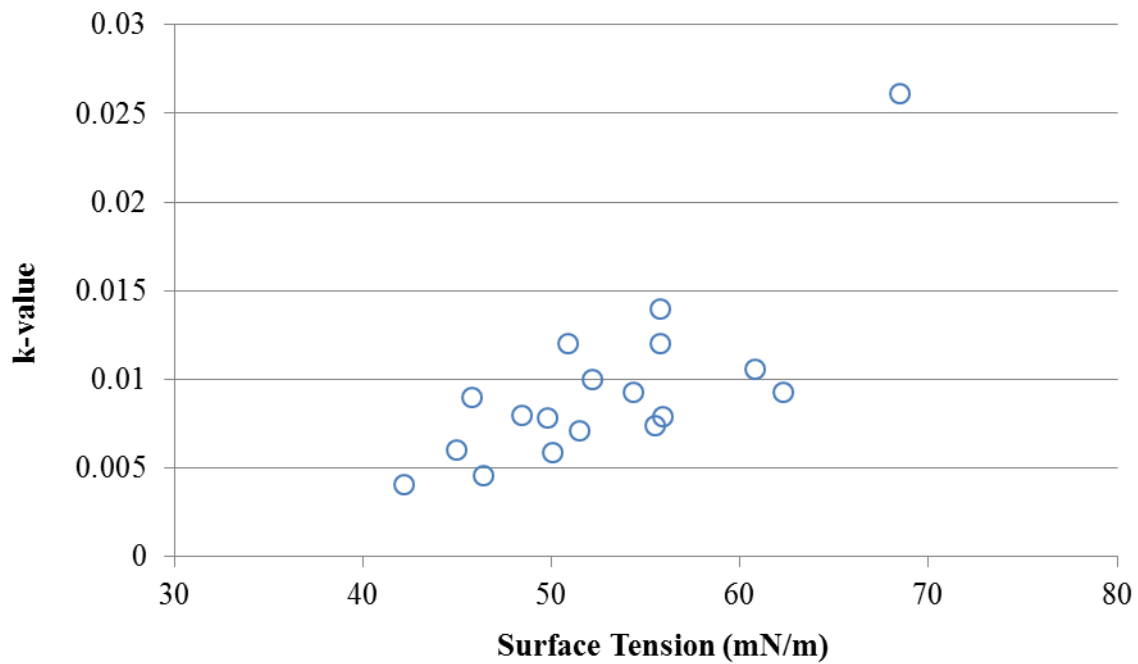


Figure 3.10: Relationship between Surface Tension of Binders and Stability of Foams.

Liquid flow is one of the possible mechanisms that can explain collapse of bubbles. Just after the foam is dispensed into a can, the liquid asphalt starts to flow downwards by gravity along the interconnected network of channels between the bubbles. The rate at which the liquid flows downward is influenced by its viscosity. Hence, the viscosity of asphalt binder impacts rate of bubble collapse. That is, asphalt foam with high liquid viscosity is more stable than that with low viscosity at a specific temperature. To investigate this, a Brookfield rotational viscometer with spindle #27 was used to measure viscosity of binders at a temperature of 135°C. Figure 3.11 shows viscosity of binders with and without Additive 1 modification at 135°C. Results presented in Figure 3.11 demonstrate that Additive 1 decreased viscosity of binders significantly. However, results presented in Chapter 2 exhibited that binders modified with Additive 1 have more expansion and stability compared to the unmodified binders. Therefore, the mechanism that increased in viscosity resulted in an increased stability was ruled out. Instead, based on the previous results it is hypothesized that other factors such as  $ER_{max}$  (which impacts initial bubble film thickness), water droplet size distribution and surface tension of binders dominate rate of decay of asphalt foam.

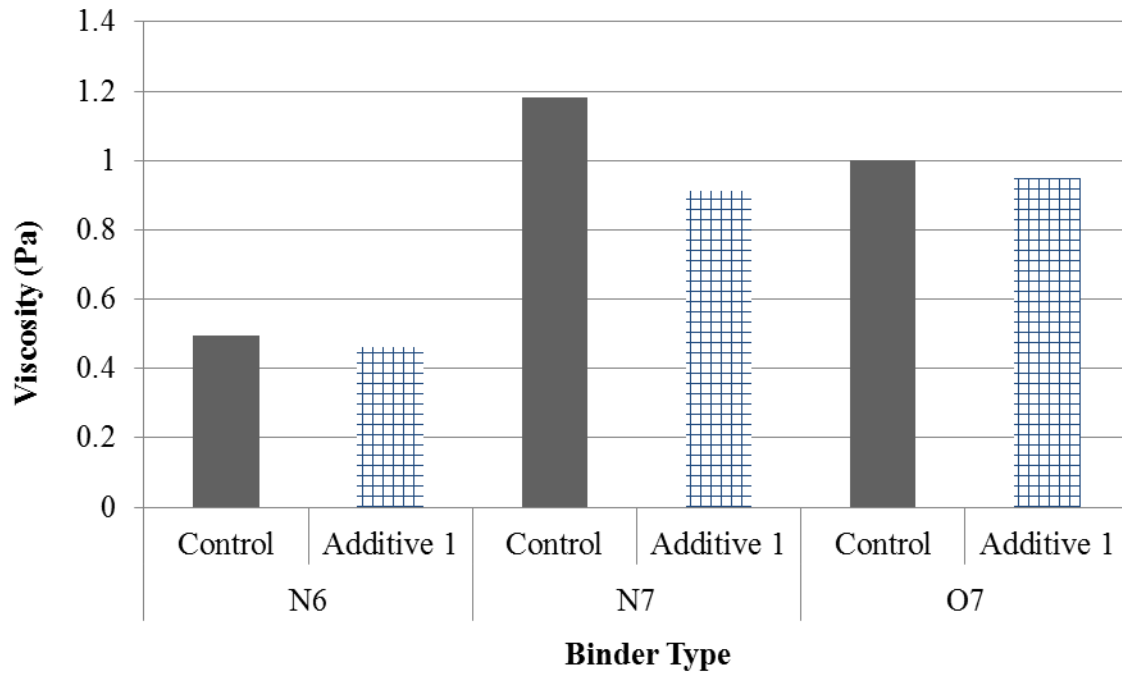


Figure 3.11: Viscosity of Binders at 135°C.

### 3.9. CONCLUSION

The following conclusions were drawn on the basis of the results from the theoretical analysis and experimental data:

1. The surface tension of the binder affects  $ER_{max}$  significantly, not by influencing the internal pressure of bubbles, rather by affecting mixing characteristics of asphalt binder with water.
2. The initial bubble size (or water droplet size) distribution does not affect  $ER_{max}$  of the foam, as long as initial bubble diameter is more than about 100 micro-meters. This corresponds to an initial water droplet size of 0.016 mm or more. Based on experimental results, it is clear that significant expansion is achieved due to bubbles that exceed the above diameter.
3. A comparison of the theoretical to the measured  $ER_{max}$  reveals that only a small fraction of water added to the asphalt binder is effective in foaming. This fraction

of water decreases as the water content increases. The effective water content is an important consideration because it may be possible to optimize the water content used to produce foamed asphalt binder by using less water and thus reducing the risk of a higher humidity environment in the drum mix plant.

4. The physical model presented can be used to assess the effect of water content and binder type on foam quality. More specifically, binders that do not tend to foam with a reasonable expansion ratio can be modified using additives that lower surface tension. This in turn increases the solubility of the water in the binder and the resulting expansion of the foamed binder.

## **Chapter 4: Influence of Foaming on Asphalt Binder and Mixture Properties**

### **4.1. INTRODUCTION**

Despite the promising benefits, successful implementation and use of foaming technology is contingent on the expectation that these mixtures must have the same or better long-term durability and performance as compared to equivalent hot mix asphalt (HMA). The possible impacts of foaming processes on the performance-related properties of asphalt binders and mixtures need to be addressed. Also, the impact of modification processes (liquid additives) used during foaming on asphalt binder and mixture properties should be evaluated.

One other major challenge in the application of foamed binders for warm mix asphalt (WMA) is that there are no established relationships between asphalt binder foam characteristics to mixture workability, coatability, or performance. Most of the research conducted so far has been on binder foam characterization or mixture evaluation. Jenkins (2000) suggested using Foam Index (FI), the area under the ER versus time curve, to determine the optimum foamant water content for base stabilization applications. In this procedure, the optimum water content corresponds to the point where FI is the maximum when FI is plotted against water content. However, other studies found that the FI versus water content did not have a maximum point for some binder foams (Sunarjono 2008). Also, the FI was not compared to mixture workability or coatability. Consequently, the impact of asphalt binder foam characteristics on mixture workability and coatability is unknown.

This chapter presents results from the portion of the study conducted to investigate the influence of foaming process on viscosity, residual moisture, susceptibility to permanent deformation, fracture resistance, and thermal cracking resistance of asphalt

binders. In addition, the significance of foamed asphalt characteristics on coatability and workability of mixtures was evaluated. Presence of residual water entrapped in the binder may alter its rheological properties. Also, presence of water during the foaming and short-term aging processes may promote oxidative aging of asphalt binders. Rheological tests were conducted on foamed binder residues using the dynamic shear rheometer (DSR) and bending beam rheometer (BBR) to verify whether or not these effects exist. Asphalt binder foam parameters obtained using the laser distance measurement (LDM) test were compared with maximum shear stress and coatability index of foamed asphalt mixture to investigate the impact of binder foam characteristics on mixture workability and coatability, respectively.

The specific objectives of this section of the study were to

1. quantify the residual moisture in foamed binders, and evaluate the impact of foaming on viscosity of foamed asphalt binder residues,
2. investigate the effect of foaming process on the short-term and long-term rheological properties of foamed asphalt binder residues,
3. determine whether the asphalt binder interacts with the liquid additive to alter its rheological properties after short-term and long-term aging,
4. relate the foaming characteristics of asphalt binders to mixture coatability and workability.

#### **4.2. MATERIALS AND EXPERIMENTAL PLAN**

A testing plan was developed to accomplish the aforementioned objectives. The possibility of residual water in the foamed binder was evaluated using a PG70-22 (designated as O7) binder at 2% water content. Six PG64-22 binders (N6, O6, T6, H6, M6, and Y6) and two PG70-22 binders (N7 and O7) from different sources were used to

evaluate the foamed binder residue rheological properties. N6, N7 and O7 binders were used to evaluate viscosity of foamed binder residues using the Brookfield viscometer with spindle #27. N6, O6, and Y6 binders were used to compare foamed binder properties to mixture workability and coatability.

To evaluate the high-temperature rheological properties, the control and foamed binder residues (foamed in the Accufoamer) were aged in the RTFO using the ASTM D2872 procedure to simulate short-term aging. In the case of foamed binders, the samples were poured into the rolling thin film oven (RTFO) bottles approximately 15 minutes after foaming. Temperature-frequency sweep testing was conducted using the dynamic shear rheometer (DSR) at a strain of 10% on a 25 mm diameter parallel plate geometry at frequencies between 0.1 and 25 Hz. Testing temperatures were 58, 64, 70, and 76°C for the PG64-22 control and foamed binder residues, and 64, 70, 76, and 82°C for the PG70-22 control and foamed binder residues. For the PG70-22 (O7) binder control and foamed with 2% water content, weight measurements were conducted after 0, 15, 30, 60, and 85 minutes of RTFO-aging at 163°C.

The RTFO residues were further aged in the pressurized aging vessel (PAV) according to the ASTM D6521 procedure to simulate long-term aging. The PAV-aged residues were used to investigate the low- and intermediate-temperature rheological properties. To investigate the intermediate-temperature rheological properties, frequency sweep testing was conducted using the DSR at a strain of 1% on 8 mm diameter parallel plate geometry at frequencies between 0.1 and 25 Hz. The testing temperature was 25°C for the PG64-22 binders and 28°C for the PG70-22 binders. The low-temperature rheological properties were investigated using the bending beam rheometer (BBR) at a temperature of -12°C.

### **4.3. TESTS AND RESULTS**

#### **4.3.1. Residual Moisture in Asphalt Binder**

As discussed previously, one of the mechanisms associated with the collapse of the foamed asphalt binder is when the internal steam pressure causes the bubble diameter to increase to a point where the tensile stresses in the bubble film cause the bubble to collapse and the entrapped steam to escape. However, it is possible that not all the water used for foaming escapes as steam during this process. In fact, results from the Brookfield viscometer shown later in section 4.4.2 suggest the possibility of residual micro-bubbles that influence the viscosity of the asphalt binder. To investigate the possibility of residual water in the foamed binder, the O7 binder at 2% water content was poured into RTFO bottles after foaming and aged in the RTFO at 163°C. Weight measurements were taken for the foamed binder sample as well as the control binder after 0, 15, 30, 60 and 85 minutes of RTFO aging. Two replicates of each test were performed. Figure 4.1 illustrates the weight loss during RTFO aging in the foamed as well as the control binder. Note that the weight loss in a typical binder, as in the case of the control, is associated with the loss of volatiles during short-term aging. Figure 4.1 clearly illustrates that the foamed binder has a greater weight loss compared to the control suggesting that presence of residual water from the foaming process. The error bars in this figure indicate the high and low values for the weight loss. The variability in weight loss for the foamed binder is significantly higher than the control. This is expected because any trapped moisture may not be homogenously distributed. Also, since the total initial water content was 2% by mass of the binder, even a small increase in percent points of weight loss indicates significant fraction of the residual water. It is also observed that the weight loss in the foamed binder slowly approaches that of the control as it aged.



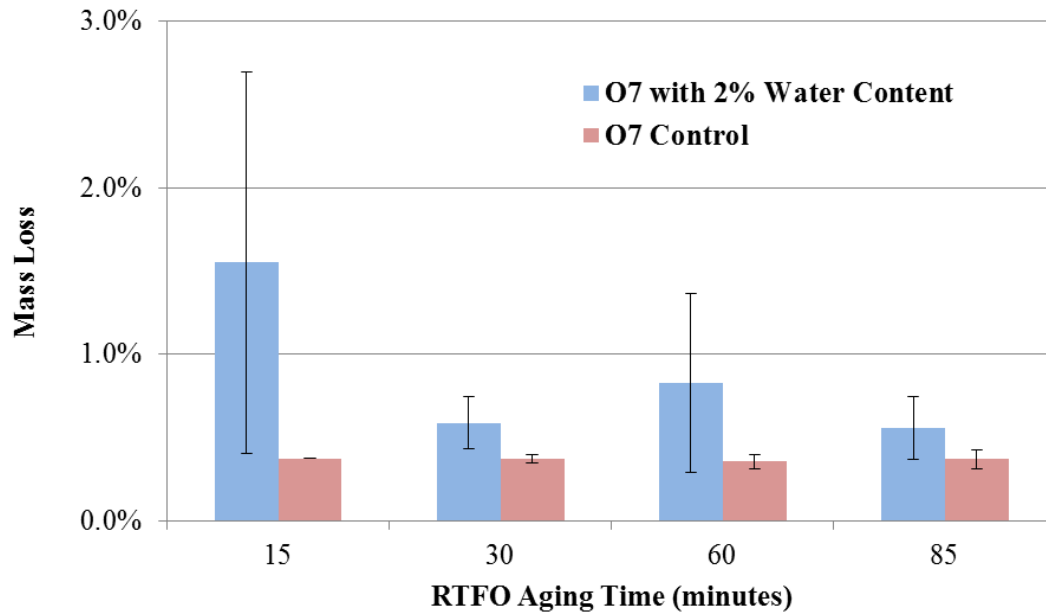


Figure 4.1: Weight Loss in Foamed and Control Binder During RTFO Aging.

#### 4.3.2. Rheological Properties of Foamed Binder Residue

The process of foaming an asphalt binder may alter its rheological properties. For example, the presence of highly polar water molecules during foaming and aging may alter the microstructure and consequently the rheological properties of the asphalt binder. Rheological tests were conducted on foamed binder residues using the dynamic shear rheometer (DSR) and bending shear rheometer (BBR) to verify whether these effects exist.

The high-temperature performance of binders was investigated using the Superpave  $G^*/\sin\delta$  parameter at 10% strain and 10 rad/s frequency, and the high performance grade (PG) temperature of the asphalt binder. The high-temperature grades of the control binders used for foaming were determined after RTFO aging in accordance with AASHTO M320. Similarly, the residues of the foamed binders were RTFO aged and subsequently graded to determine the impact of foaming on the high temperature PG.

Table 4.1 presents the results of the high-temperature PG, and Figure 4.2 shows normalized  $G^*/\sin\delta$  values of binders after foaming with water contents that varied from 1% to 5%. The  $G^*/\sin\delta$  values for the foamed binders were normalized with their respective non-foamed (control) binders. The two lines in Figure 4.2 show the lower and upper single operator precision limits of this test method. The  $G^*/\sin\delta$  values for the foamed binders are considered similar to that of the control binder if the normalized  $G^*/\sin\delta$  values are within the precision limits of the test method. In most cases, foamed binder residues had similar or higher values of resistance to permanent deformation parameter ( $G^*/\sin\delta$ ) when compared with control binders that were subjected to the same short-term aging conditions. There was a slight increase in the high temperature continuous grade of the binders (based on RTFO aged binder). Foaming increased the continuous high temperature grade of O7 and N6 at 1% water content by 2.7°C and 1.2°C, respectively compared to their respective controls. Foaming increased the continuous grade of the other seven binders on average by less than 0.5°C.

Table 4.2 presents the results of the high-temperature PG, and Figure 4.3 shows normalized  $G^*/\sin\delta$  values of foamed binders modified with liquid Additive 1. In this figure, the  $G^*/\sin\delta$  values of foamed binders were normalized with their respective non-foamed, non-modified binder. The results demonstrate that the effect of Additive 1 on the short-term rheological properties of the binders is negligible. It should be noted that these results compare the foamed binder to the control (non-foamed) binder by aging the two different binders under same conditions (163°C for 85 minutes). However, in practice foamed binders will experience reduced short-term aging compared to conventional binders. Hence, reduced short-term aging temperature may (possibly more than) offset the slight increase in the continuous high-temperature grade due to the foaming process.

Binder	Type	High PG Grade	Continuous Grade	Change in continuous PG Grade
N6	Control A	PG64	66.5	-
	1%		67.7	1.2
	3%		67.0	0.5
	5%		67.0	0.5
N7	Control A	PG70	74.2	-
	1%		74.7	0.5
	3%		74.3	0.1
	5%		74.5	0.3
O6	Control A	PG64 (PG70)	69.7	-
	1%		70.1	0.4
	2%		70.2	0.5
	3%		69.3	-0.4
O7	Control A	PG70	72.0	-
	1%		74.7	2.7
	2%		74.8	2.8
	3%		74.7	2.7
T6	Control A	PG64	68.1	-
	2%		69.2	0.6
H6	Control	PG64	69.4	-
	2%		68.6	0.4
M6	Control A	PG64	69.5	-
	2%		69.6	-0.5
Y6	Control A	PG64	67.6	-
	2%		68.3	0.3

Table 4.1: Influence of Foaming on the High-Temperature Grade of Binders.

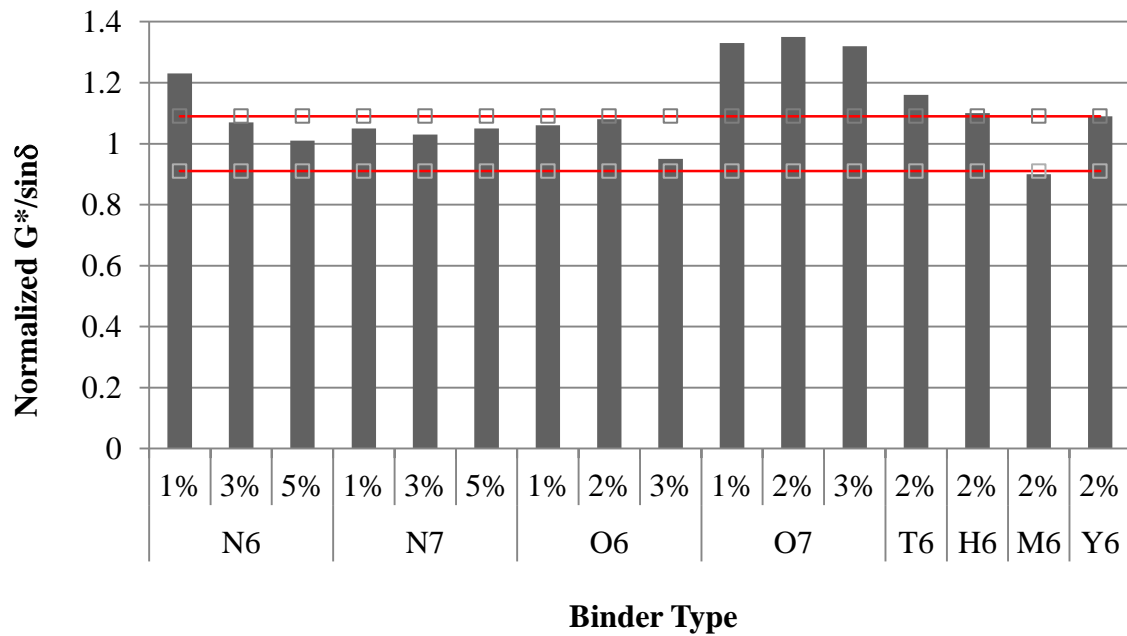


Figure 4.2: Influence of Foaming on Resistance to permanent deformation (the Red Lines Indicate the Lower and Upper Single Operator Precision Limits of the Test Method).

Binder	Water Content	High PG Grade	Continuous Grade	Change in continuous PG Grade
N6 + 0.5% Additive 1	Control B	PG64	66.65	0.15
	1%		66.21	-0.29
	2%		67.33	0.83
	3%		67.26	0.76
N7 + 0.5% Additive 1	Control B	PG70	72.64	-1.57
	1%		74.53	0.32
	2%		74.82	0.61
	3%		73.5	-0.71
O7 + 0.5% Additive 1	Control B	PG70	73.43	1.41
	1%		74.29	2.27
	2%		74.29	2.27
	3%		74.27	2.25

Table 4.2: Influence of Foaming and Liquid Additive on the High-Temperature Grade of Binders.

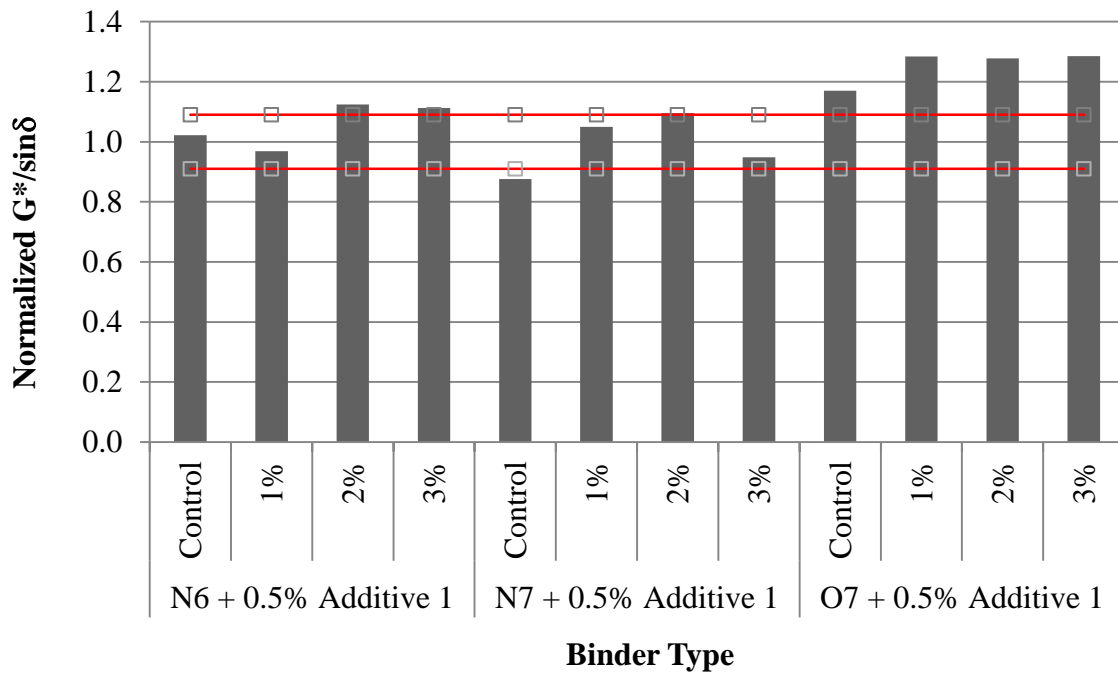


Figure 4.3: Influence of Foaming and Liquid Additive on Resistance to Permanent Deformation (the Red Lines Indicate the Lower and Upper Single Operator Precision Limits of the Test Method).

The intermediate-temperature performance of the PAV-aged foamed binder residues were investigated using the Superpave  $G^*\sin\delta$  parameter at 1% strain and 10 rad/s frequency, measured using the DSR. Figure 4.4 and Figure 4.5 show normalized  $G^*\sin\delta$  values of binders after foaming with and without Additive 1. The  $G^*\sin\delta$  values for the foamed binders were normalized with their respective non-foamed, unmodified binder. Again, the two lines in the figures show the lower and upper single operator precision limits of this test method. The results presented in Figure 4.4 and Figure 4.5 demonstrate that the  $G^*\sin\delta$  values are either similar or slightly greater than that of the control, suggesting that the foaming process has a negligible influence on the intermediate-temperature performance of both the modified and unmodified binders. The slight increase in the  $G^*\sin\delta$  values for some of the foamed binder residues may be

compensated when the foamed binders are subjected to lower short-term aging temperatures.

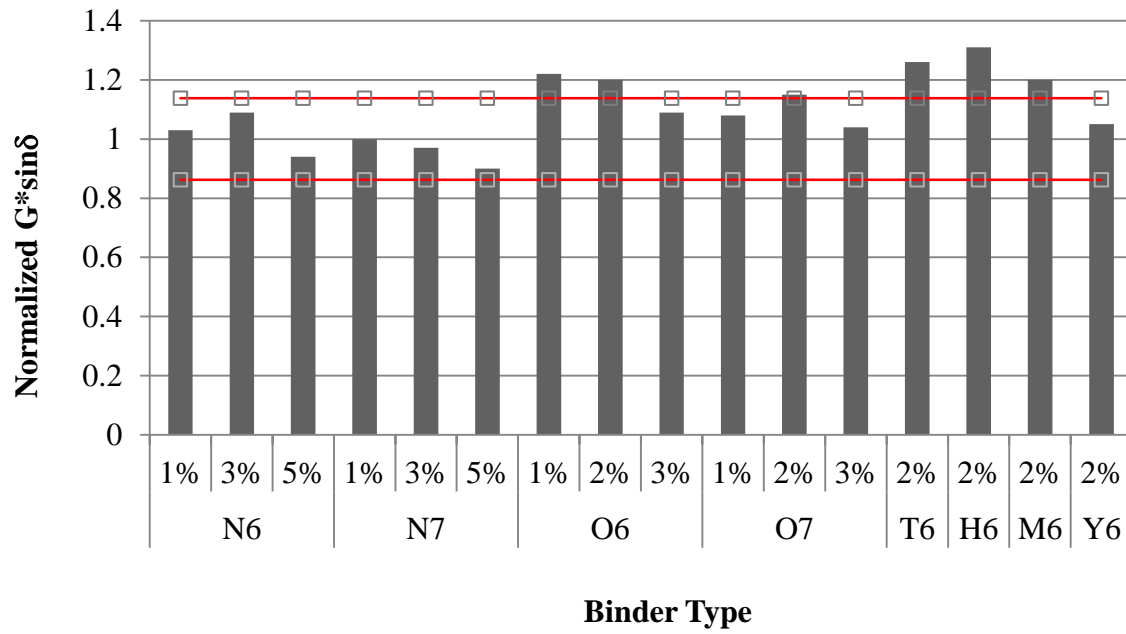


Figure 4.4: Influence of Foaming on Resistance to Fatigue Cracking (the Red Lines Indicate the Lower and Upper Single Operator Precision Limits of the Test Method).

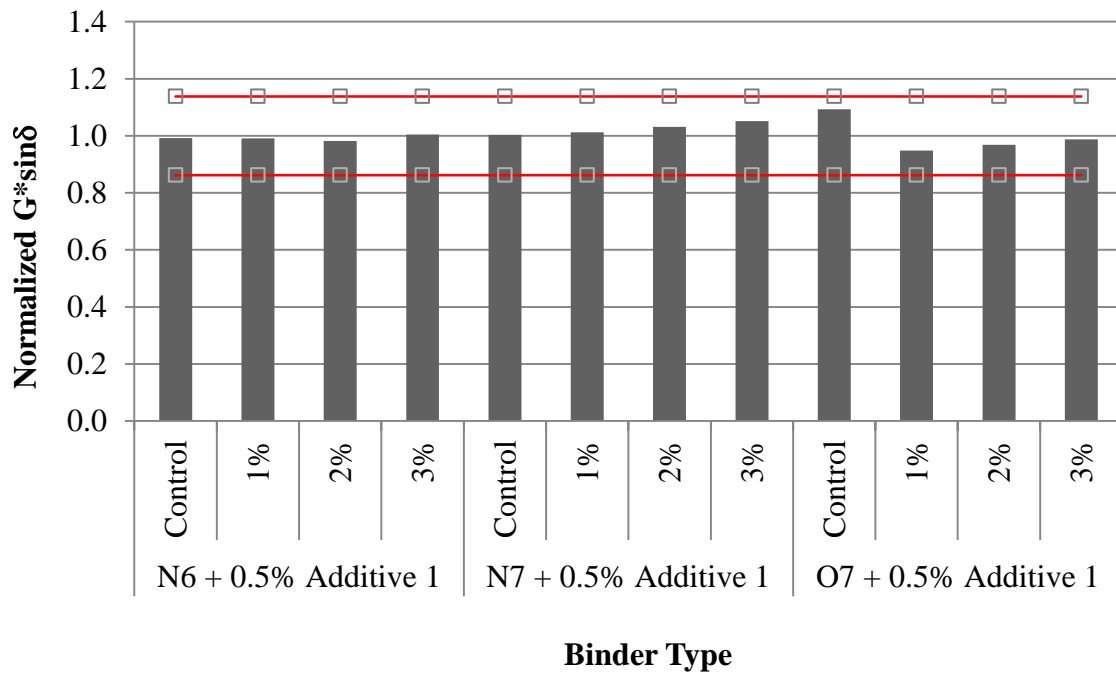


Figure 4.5: Influence of Foaming and Liquid Additive on Resistance to Fatigue Cracking (the Red Lines Indicate the Lower and Upper Single Operator Precision Limits of the Test Method).

The low-temperature performance of foamed binder residues were evaluated after PAV aging using the S and m-value of the BBR parameters. The results presented in Figure 4.6 and Figure 4.7 clearly indicate that the S and m-value at low temperatures were similar to the S and m-value of base binders.

The DSR and BBR results demonstrate that foaming process and liquid additive may not have a significant influence on the short-term and long-term rheological properties of binders.

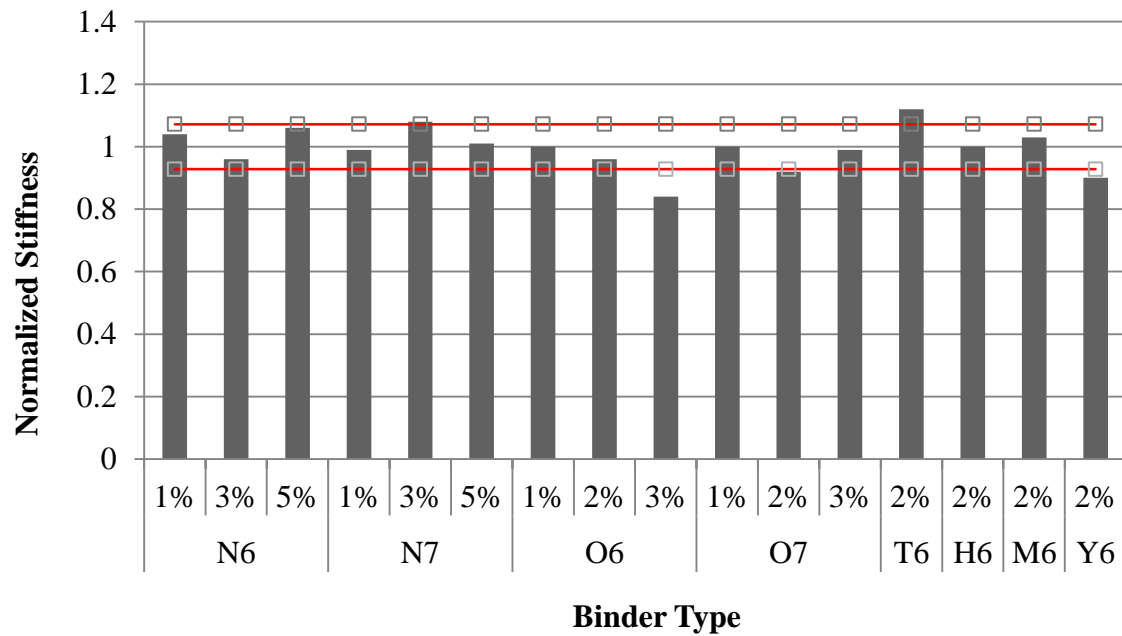


Figure 4.6: Influence of Foaming on Creep Stiffness of Binders at -12°C (the Red Lines Indicate the Lower and Upper Single Operator Precision Limits of the Test Method).

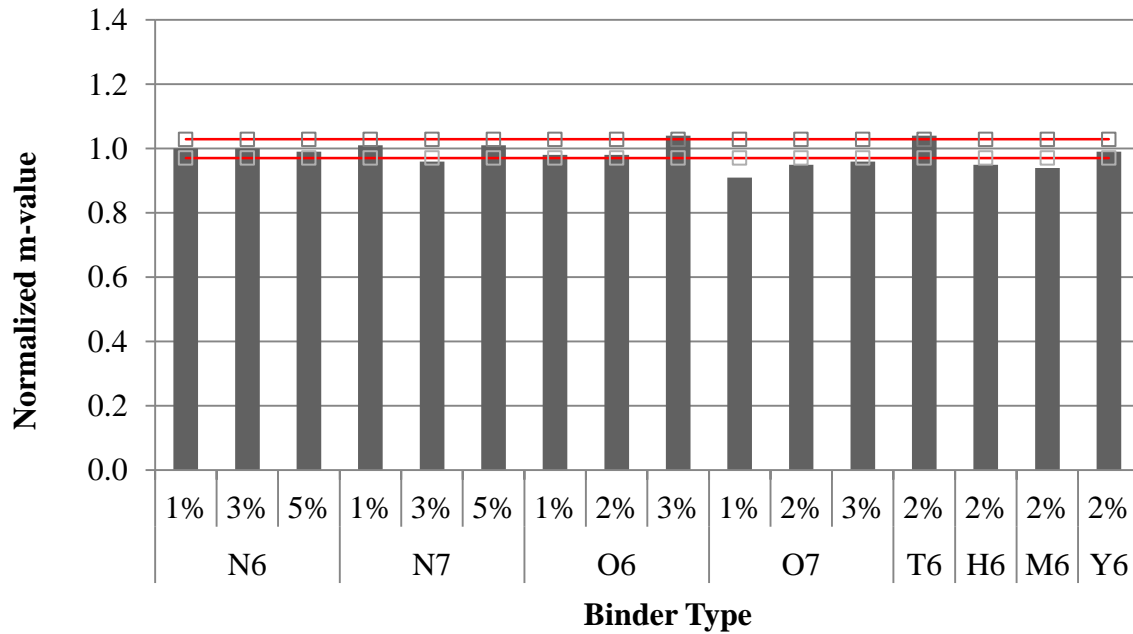


Figure 4.7: Influence of Foaming on the m-value of Binders at -12°C (the Red Lines Indicate the Lower and Upper Single Operator Precision Limits of the Test Method).



#### **4.4. EVALUATING PROPERTIES RELEVANT TO MIXTURE WORKABILITY AND COATABILITY**

The tests in this section are related to evaluating properties relevant to mixture coating and compaction. The viscosity of binder foams was measured, and the foamed binder characteristics were compared with mixture workability and coatability.

##### **4.4.1. Viscosity of Asphalt Binder Foam**

Expansion ratio is an indirect measure of workability (viscosity) of asphalt foams. But, it may sometimes give inconsistent results in terms of viscosity. For example, binders from different sources that have the same maximum expansion ratio may end up having different viscosities. Hence, viscosity measurement of asphalt foams was considered as one approach to quantify the workability of the foamed binder (i.e. its ability to coat aggregate particles and facilitate compaction).

The viscosity of asphalt foam was measured using Brookfield rotational viscometer with a specially fabricated vane spindle (Figure 4.8) at the foaming temperature (160°C) as it collapsed over time. Note that viscosity measurement using a rotational viscometer also subjects the foam to a shearing action between the spindle and the walls of the container. Therefore, viscosity measurements on foamed binders reflect the combined impact of shearing action and foam decay on workability. A heating mantle was used to keep the temperature constant at 160°C. The one-gallon container was removed from the foamer and placed in the heating mantle to measure the viscosity of the foam (typically within 35 seconds from the start time). Due to the delay between moving the container from the foamer to placing it in the heating mantle, the viscosity of the foam in the first 35 seconds was not recorded. Viscosity of N6 control and foamed at 1%, 2%, and 3% water contents is presented in Figure 4.9, as an example. However, data

presented in Figure 4.9 show that the viscosity of A6 was too low at 160°C to detect a significant increase in viscosity as the foam collapses over time. This test method was not sensitive to change in water content and time. This procedure also had a practical challenge. As the final volume of the foam was less than 10 percent of its volume at time zero, the height of the van spindle was limited to the final height of the foam. As a result, it was decided to measure viscosity of binders using the regular Brookfield viscometer with spindle # 27 just after foaming.



Figure 4.8: Asphalt Foam Viscosity Test Setup.

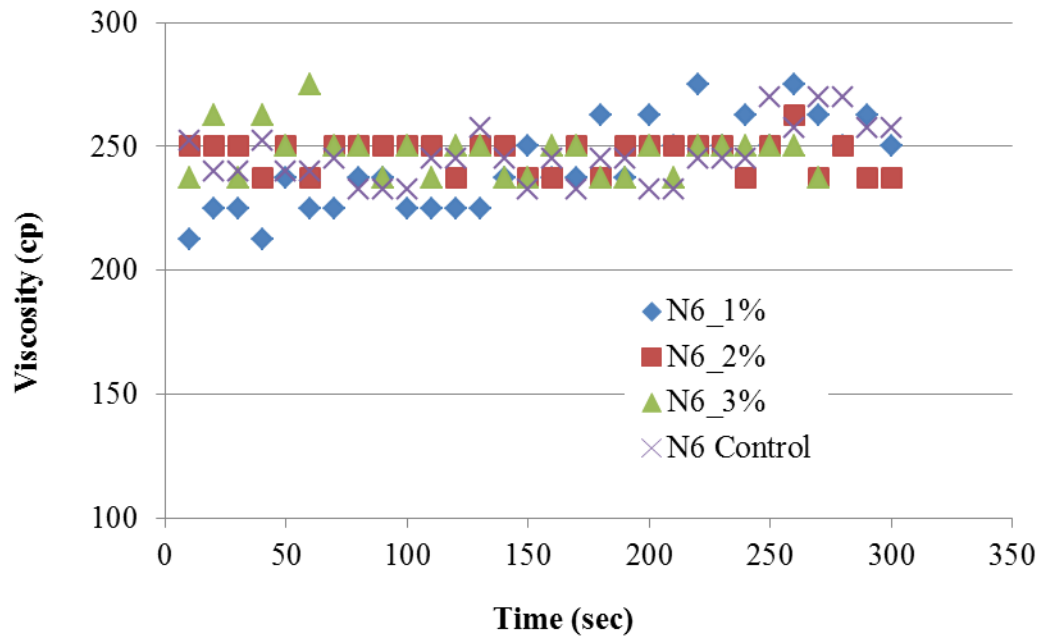


Figure 4.9: Viscosity of N6 foam as it collapse over time at 160°C.

#### 4.4.2. Viscosity of Foamed Binder Residue

As it is discussed in section 4.4.1, direct measurement of asphalt binder foam using a Brookfield rotational viscometer with a specially fabricated vane spindle was not successful. Therefore, measurement of viscosity of the binders just after foaming was undertaken using the regular Brookfield viscometer with spindle # 27. The advantage of this approach is that it will allow for a more sensitive measurement of binder viscosity. However, because of the time it takes to transfer a sample of the foamed binder from the one-gallon collection container into the Brookfield sample holder, and also because of the narrow gap between the spindle and the walls of the container, this method will be only effective to investigate whether or not the presence of any micro-bubbles during the later stages of foaming affect the viscosity (and hence workability of the binder).

The viscosity of asphalt foam was measured using Brookfield rotational viscometer with a #27 spindle immediately after foaming. A sample of the foamed binder

from the one-gallon collection container was poured into the Brookfield sample holder. This process was accomplished within two minutes after dispensing the foam. Viscosity measurements were conducted at 135°C and 20 RPM, and values were recorded after the reading stabilized (15 minutes after the foam was dispensed). The advantage of this approach is that it allows for a more sensitive measurement of binder viscosity. However, because of the time it takes to transfer a sample of the foamed binder from the one-gallon collection container into the Brookfield sample holder, and also because of the narrow gap between the spindle and the walls of the container, this method will be only effective to investigate whether or not the presence of any micro-bubbles during the later stages of foaming affect the viscosity (and hence workability of the binder). Results for the three binders (N6, N7, and O7) at 1%, 2%, and 3% water contents are presented in Figure 4.10. Results show that the foamed binders continue to have viscosities lower than the control even after 15 minutes of foaming; although this effect was more prominent for two of the three binders. Foaming decreased the viscosity of N6, N7, and O7 on average by 7%, 23%, and 16% compared to their respective controls. The decrease was similar for all water contents.

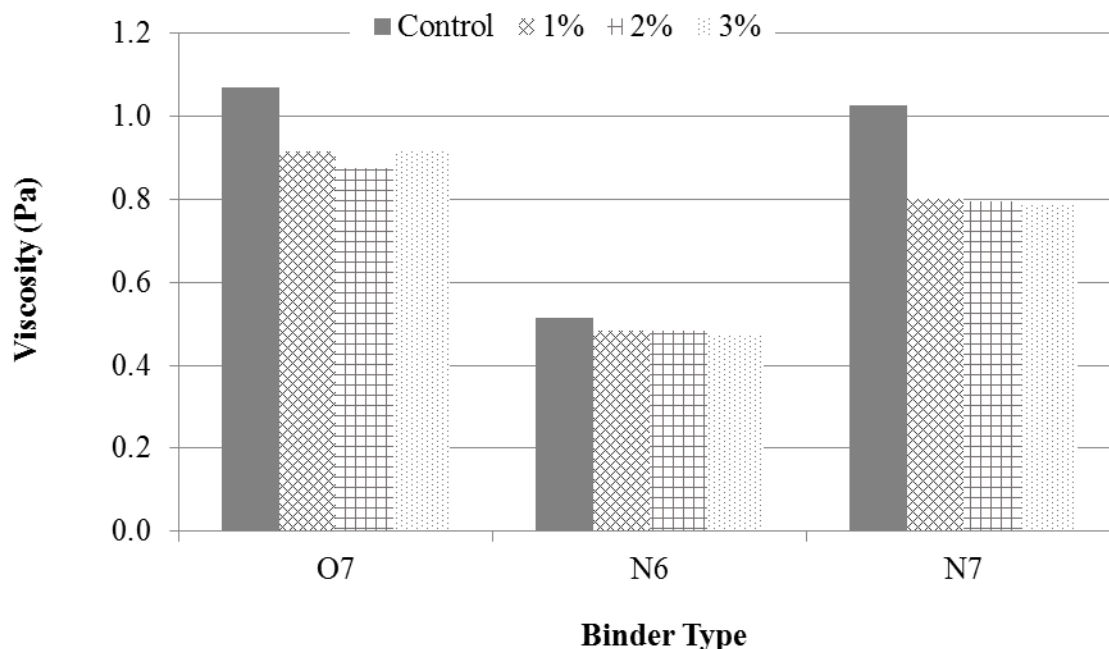


Figure 4.10: Viscosity of Foamed Asphalt Binder Residue.

#### 4.4.3. Comparison of Asphalt Binder Foam Characteristics to Mixture Workability and Coatability

The influence of foamed asphalt binder characteristics on mixture workability and coatability was investigated by comparing foamed binder parameters to workability and coatability of WMA mixtures. Maximum shear stress and coatability index of HMA and WMA mixtures produced in the laboratory using three binders (Y6, N6, and O6) for a NCHRP Project were collected from Texas A & M Transportation Institute (TTI). These data were used to compare asphalt binder foam parameters to mixture workability and coatability.

Workability describes properties of asphalt mixtures related to the ease with which mixtures can be placed, worked by hand, and compacted. Workability impacts movement of mixture through construction equipment, and compaction effort on the roadway. Binder viscosity, aggregate properties, and temperature are the major factors

that impact workability. The concept of mix workability is used to define mixing and compaction temperatures for mix design and field production. In the study conducted by TTI, mixtures were compacted using a Superpave Gyratory Compactor (SGC) at a specified temperature and the compaction data was used to evaluate workability of mixtures. The SGC measures the power required to keep the mold rotating at an angle of  $1.25^\circ$  and calculates the corresponding shear stress as a function of number of gyrations. The maximum shear stress was used as a measure of workability. Mixtures with high maximum shear stress are considered less workable, and vice versa.

Coatability describes the degree of coating of the aggregate surface by the asphalt binder. The aggregates in the mix need to be well-coated for the mixture to be resistant to distresses such as moisture damage. The coatability index determined based on the aggregate absorption method was used as a measure of degree of coatability.

The experimental design for the mixture study consisted of three binders (Y6, N6, and O6) from different sources, and aggregates from a field project in New Mexico. The Wirtgen foamer was used to foam the binders at 1%, 2%, and 3% water contents. The optimum binder content was 5.4% by weight of mix. For the workability evaluation, the HMA mixes were mixed at  $143^\circ\text{C}$ , and compacted at  $135^\circ\text{C}$  following 2hrs of aging at the same temperature. The WMA mixes were mixed at  $135^\circ\text{C}$ , and compacted at  $116^\circ\text{C}$  following 2 hours of aging at the same temperature. For the coatability evaluation, only the coarse aggregate fraction (retained on the 3/8 inch sieve) from the mixture design was used.

Maximum shear stress and coatability index of WMA mixtures were normalized with that of their corresponding HMA values. ER @ 10 sec, and k-value were then compared to the normalized maximum shear stress and coatability index of the mixes. The normalized coatability index and normalized maximum shear stress values for the

mixes produced using N6, O6, and Y6 binders are presented in Figure 4.11 and Figure 4.12. The following observations can be made from these two figures.

- An increase in  $ER_{max}$  (maximum expansion ratio) does not necessarily translate into improvement in mixture workability or aggregate coatability of WMA mixtures.
- Lower water content values showed improvement in both workability and coatability of WMA mixtures compared to HMA mixtures. However, an increase in water content did not appear to have an adverse effect on coatability.
- Workability and coatability typically improved compared to a similar HMA when the water content was between 1% and 2%.

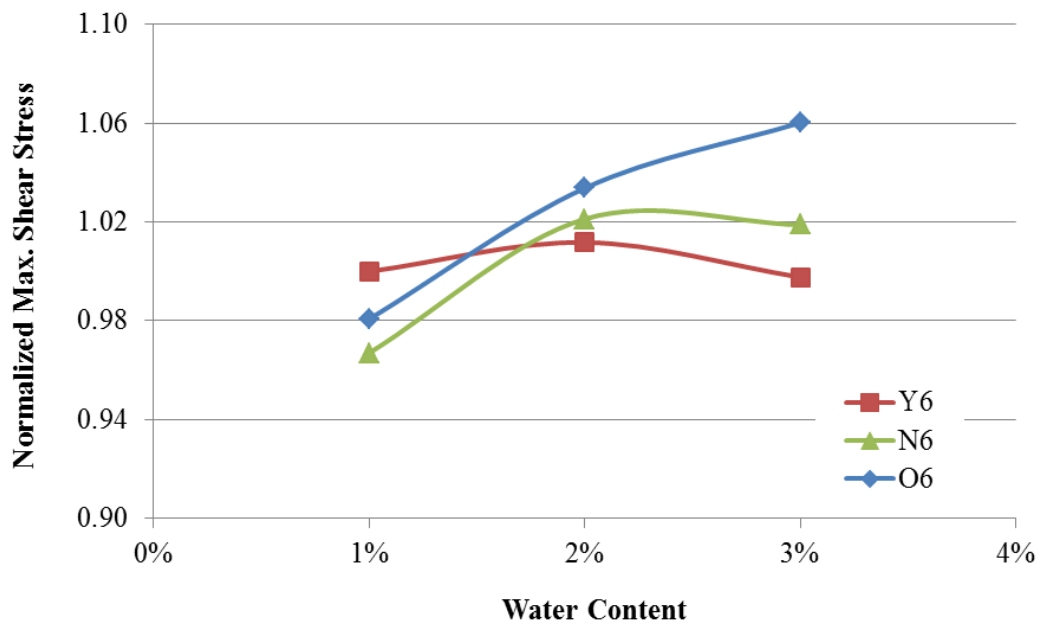


Figure 4.11: Influence of Water Content on Workability of WMA Mixtures (Values Equal to or Lesser than 1.0 Indicate Workability Similar to or Better Than a Similar HMA).

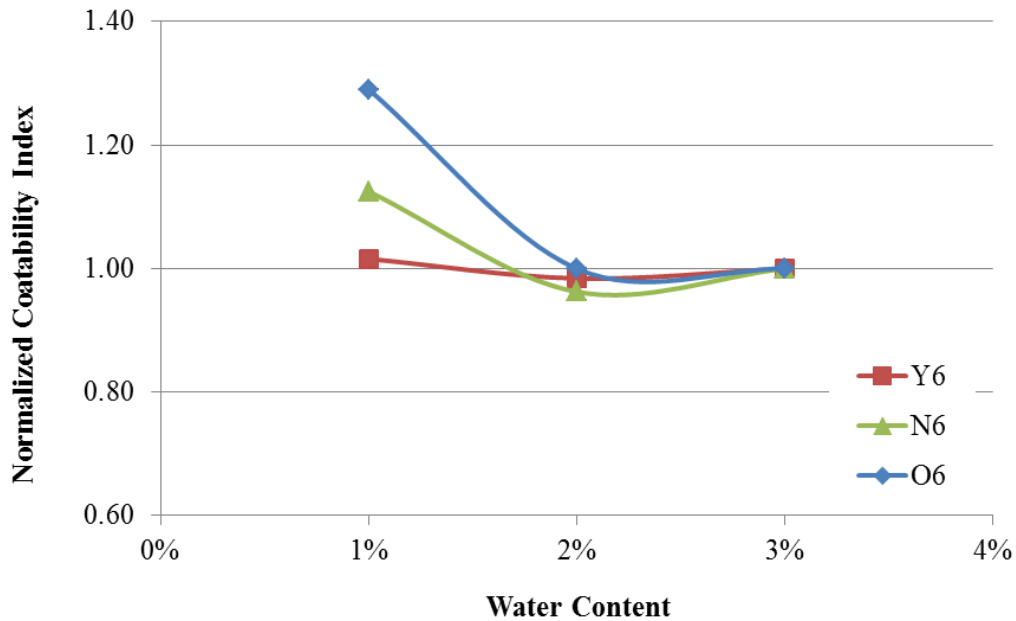


Figure 4.12: Influence of water content on coatability of WMA mixtures (values equal to or greater than 1.0 indicate coatability similar to or better than a similar HMA).

Normalized maximum shear stress and normalized coatability index were compared with ER @ 10 seconds and k-value in Figure 4.13 through Figure 4.16. The results presented in Figure 4.16 for the Y6 binder workability and coatability show less sensitivity to both k-value and ER. Increasing k-value decreased the workability and coatability of mixtures produced using the N6 and O6 binders. However, the coatability of the warm mix asphalt mixtures was as good as the hot mix asphalt mixtures at higher k-values. Better coatability and workability was observed when the ER values of the mixtures were close to 4. Although small in scope, the data collected show that ER value of 4 and k-value of 0.01 deemed a potential surrogate measure for estimating the optimum water content for both the workability and coatability of mixtures.



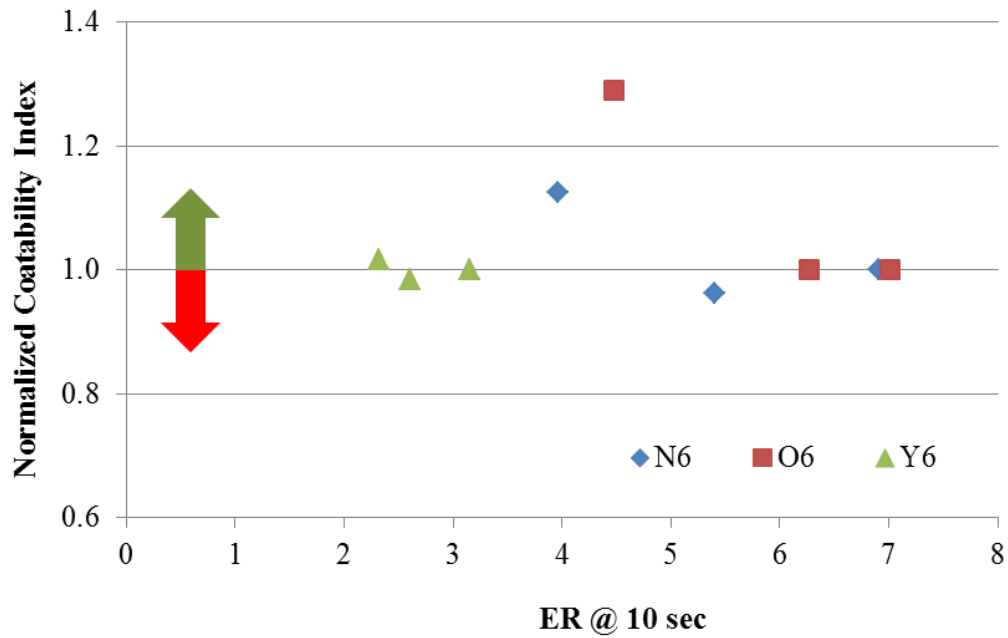


Figure 4.13: Comparison of Asphalt Binder Foam Expansion to Mixture Coatability; the Green Arrow Indicates Desirable Range of Coatability Compared to HMA as a Control.

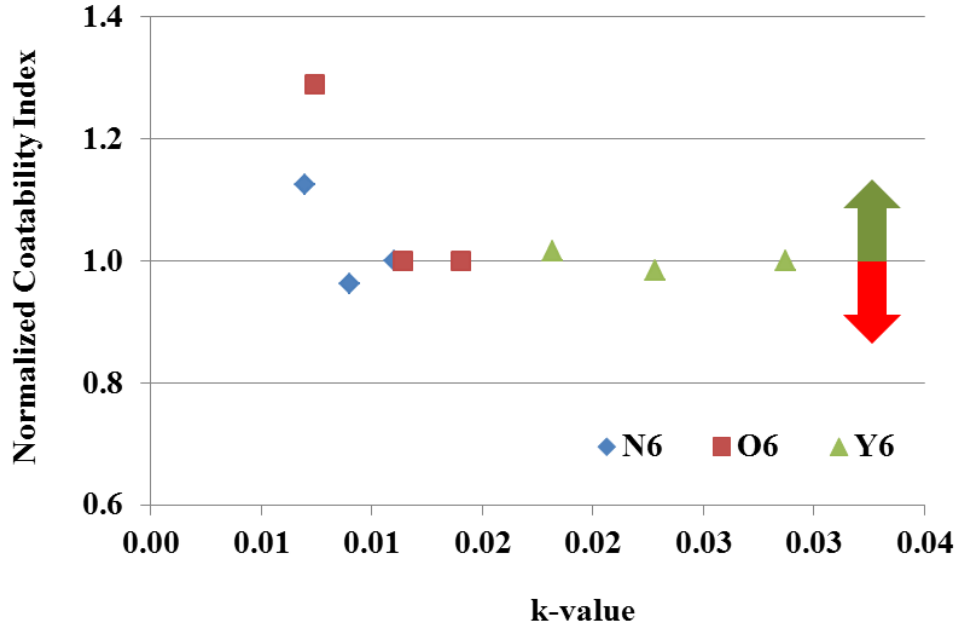


Figure 4.14: Comparison of Asphalt Binder Foam Expansion to Mixture Coatability; the Green Arrow Indicates Desirable Range of Coatability Compared to HMA as a Control.

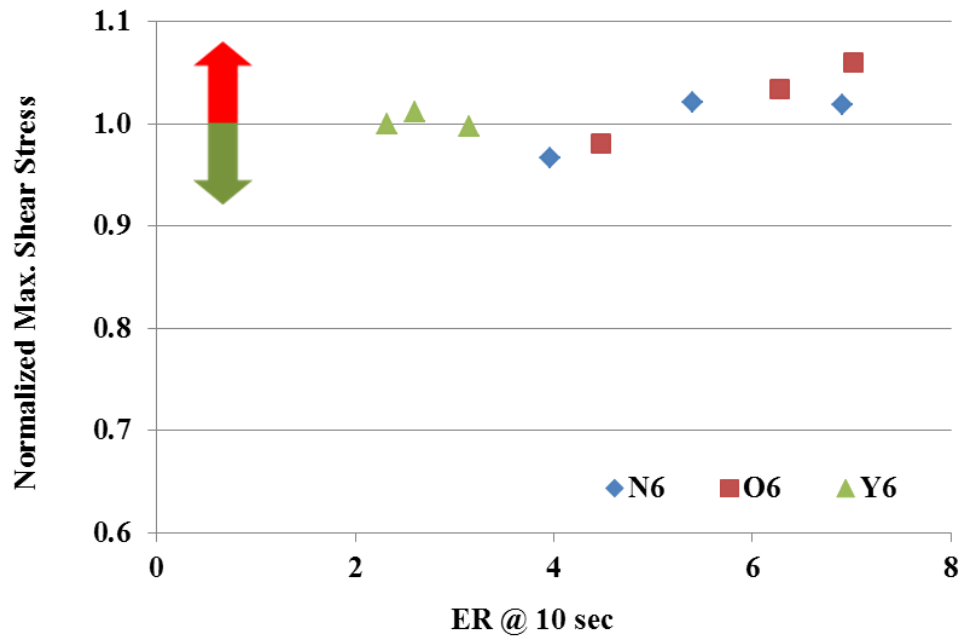


Figure 4.15: Comparison of Asphalt Binder Foam Expansion to Mixture Workability; the Green Arrow Indicates Desirable Range of Shear Stress Compared to HMA as a Control.

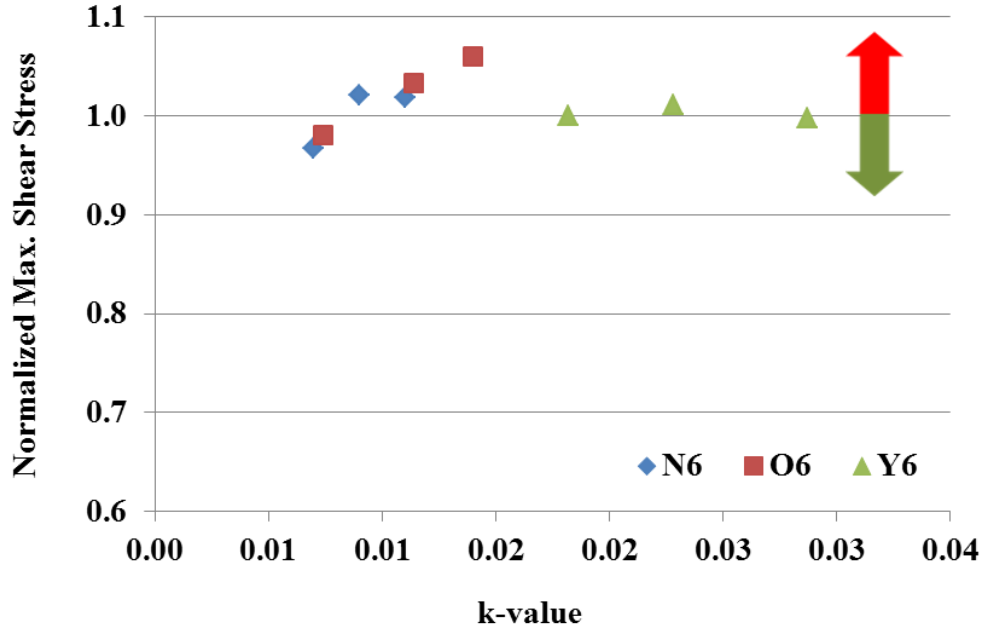


Figure 4.16: Comparison of Asphalt Binder Foam Stability to Mixture Workability; the Green Arrow Indicates Desirable Range of Shear Stress Compared to HMA as a Control.

#### 4.5. CONCLUSION

Measurement of performance-related properties of foamed asphalt residues and mixtures is important for successful implementation of foam-based WMA. In this chapter, the influence of foaming processes and liquid additive on viscosity, residual moisture, and parameters related to the performance grade specifications were evaluated. In addition, the impact of asphalt foam characteristics on mixture workability and coatability were investigated. The following conclusions were drawn based on the results obtained from laboratory testing.

1. During the first 15 minutes of RTFO aging of the foamed binder, the binder continued to lose more mass than the control binder indicating the presence of residual moisture from the foaming process. However, upon the completion of RTFO aging process the mass loss from the foamed binder sample was similar to the mass loss from the control binder. This suggests the presence of trace amounts of water in the asphalt binder even after several minutes and significant collapse of the foam.
2. Viscosity measurements of foamed binder residues were lower than that of the non-foamed binder. The difference, however, was similar regardless of the water content for foaming. These measurements were taken approximately 15 minutes after the foamed binder was produced. These results suggest the presence of micro-bubbles that possibly reduce the viscosity of the foamed binder compared to the control binder.
3. In most cases, the high-temperature continuous grade of foamed binders was similar or slightly higher than the control binders. The magnitude of this increase varied with the type of binder and was most significant for one of the PG 70-22 binders. However, in practice foamed binders will experience reduced short-term

aging compared to conventional binders. Hence, reduced short-term aging temperature may (possibly more than) offset the slight increase in the continuous high-temperature grade due to the foaming process.

4. The intermediate- and low-temperature properties of the foamed binder residue after PAV aging showed no significant change for the S and m-value BBR parameters, and for the  $G^*\sin\delta$  DSR parameter as compared to the control binder.
5. An increase in the maximum expansion ratio of asphalt binder foam does not necessarily translate into improvement in mixture workability or aggregate coatability of WMA mixture. Results from limited mixture tests show that workability and coatability of WMA typically improved compared to a similar HMA when the water content was between 1% and 2%. Although very limited in scope, the data collected also show that ER value of 4 measured at 10 seconds and a k-value of 0.01 served as a surrogate indicator for optimum workability and coatability of mixtures. This aspect of the study must be investigated further in the future with a comprehensive experimental design that consists of binders and aggregates from different sources, different foaming devices and liquid additives as well as field trials.

## **Chapter 5: Summary of Findings and Recommendations**

Warm mix asphalt is an asphalt mixture production technology that promises to reduce production costs and greenhouse gas emissions. Foamed asphalt binder is increasingly being used to produce WMA; the use of WMA increased by 67% from 2010 to 2011, and by over 300% since 2009 (by volume). In 2011, 19% of pavements in the US were constructed using WMA, and plant foaming was responsible for 95% of the total WMA production. This dissertation addresses several issues related to the use of foamed asphalt binder for WMA applications. It is envisioned that the findings from this study will be used to compare additional laboratory foaming devices and field samples in future research. The major findings from this study are the following:

1. A laser distance measurement (LDM) method was proposed to measure properties of foamed asphalt binders. It was demonstrated that the method is promising in terms of its ability to provide a detailed history of the behavior of foamed asphalt binder as the foam collapses. It was also shown that the method is repeatable and sensitive to differentiate between foaming characteristics of different binders, water contents, liquid additives as well as foaming devices. This procedure can be used as a surrogate test method to relate the foaming characteristics of asphalt binders to the workability and coatability of full asphalt mixtures. It was also shown that the graduated dipstick method currently being used is inappropriate to characterize foamed asphalt binders.
2. The foaming characteristics of different asphalt binders (expansion and time-stability) varied with the source and type of the asphalt binder in addition to external factors such as water content, foaming device and liquid additive. For any given asphalt binder, the  $ER_{max}$  increased with an increase in the water

content and the relationship appears to be linear. However, an increase in the water content also resulted in an increase in k-value of the foam. Previous studies have suggested that the collapse of foam over time follows an exponential decay form. Data collected in this study using a more precise and faster method to measure expansion indicates that the asphalt foam (except additive modified foam) does collapse following an exponential decay form, but only few seconds after foaming. During the first few seconds (typically 1 to 4 seconds), the ER of the foam diminishes significantly at a much faster rate. This observation was consistent for the foam evaluated using both laboratory foaming units for all combinations of water contents and binder types. LDM results of binders modified with an additive demonstrated that asphalt binder foam characteristics (both expansion ratio and stability) can be significantly improved using carefully selected liquid additives. However, results with another additive did not result in any substantial change in the foaming characteristics of the binder. In the context of the ability of foamed binders to effectively coat the aggregate particles, the maximum expansion ratio may be relatively less important compared to other factors such as rate of collapse of the semi-stable foam.

3. The surface tension of the binder affects  $ER_{max}$  significantly, not by influencing the internal pressure of bubbles, rather by affecting solubility of asphalt binder with water. A physical model is developed for expansion of asphalt binder foam based on foam physics and fluid mechanics of micro-droplets. The model relates foamant water and asphalt binder mixing efficiency with the surface tension of the asphalt binder. The model can be used to predict which binder can be effectively foamed and used, and whether any chemical modification to the binder is necessary to achieve the same. Results indicate that only a small percentage of

- water is effective in foaming the asphalt binder. More specifically, binders that do not tend to foam with a reasonable expansion ratio can be modified using additives that lower its surface tension. This in turn increases the solubility of the water in the binder and the resulting expansion of the foamed binder.
4. Measurement of performance-related properties of foamed asphalt residue is important for successful implementation of foam-based WMA. Rheological tests conducted on foamed binder residues indicated that foaming process or liquid additive does not have a significant influence on the short-term or long-term rheological properties of binders.
  5. Based on a very limited number of mixture tests it was also observed that an increase in the maximum expansion ratio of asphalt binder foam does not necessarily translate into improvement in mixture workability or aggregate coatability of WMA mixture. Results from limited tests conducted on mixtures show that workability and coatability of WMA typically improved compared to a similar HMA when the water content was between 1% and 2%. It is possible to use ER and k-value as indicators for foaming characteristics that will result in adequate coating and workability of the mixture. This approach must be further investigated in future research studies.

## **Appendix 1: Determining Asphalt Binder Expansion and Collapse by Using the Laser Distance Measurement (LDM) test**

This Appendix shows the AASHTO draft procedure developed to determine the asphalt binder foam expansion and collapse by using the laser distance measurement test.

### **A1.1. SCOPE**

This test method is for the measurement of expansion and collapse of foamed asphalt binder dispensed by a laboratory foaming unit or sampled at a hot-mix plant using a laser distance measurement device. While working with or handling foamed asphalt binder, lab personnel may be exposed to extreme heat and pressure, hazardous materials, and dangerous equipment operations. This standard does not address procedures and practices needed to ensure a safe and hazard free working environment in the laboratory or at a hot-mix plant. Hence, it is the responsibility of the user of this standard to ensure safety. The values stated in SI units are to be regarded as the standard.

### **A1.2. SIGNIFICANCE AND USE**

This standard is used to measure the change in height and corresponding volume of the foamed asphalt binder in real time. The laser-based sensor comprises an emitter and detector to measure the distance from the sensor to a reflecting surface based on the phase-shift principle. The laser sensor measures the height of the surface by reflecting light of different wavelengths over a very small circular spot of about 1 mm in diameter. The laser sensor collects data at frequently of 1 Hz.

This standard is used to determine the expansion and decaying characteristics of asphalt binders. The results from these procedures can be used to

- determine the maximum expansion ration,  $ER_{max}$  at different conditions (i.e. temperature, water content, binder type, foaming device, and/or pressure),



- characterize the decaying rate of the foam at different conditions (i.e. temperature, water content, binder type, foaming device, and/or pressure),
- use the data obtained from this test into a foam decaying model to determine asphalt foam characteristics as a function of time, and
- investigate the influence of binder type, water content, foaming device, temperature, and pressure on foam expansion and decay properties.

### **A1.3. APPARATUS**

The following pieces of equipment are required to conduct the test:

1. Laboratory foaming unit that dispenses a specified amount of foamed bitumen or sampling port in a hot-mix plant that can be controlled to dispense a specified amount of foamed bitumen.
2. Laser distance meter (LDM) or measurement device that uses phase-shift principle to measure distances with a resolution of 0.1 mm or better and repeatability of +/- 0.3 mm or better and a data collection rate of 1 data point per second or better. The device must also acquire the time at which the measurement was made with a resolution of 100 milliseconds or better.
3. A tripod or other suitable means to mount the laser distance meter.
4. Clean one-gallon cylindrical metal cans for each measurement.
5. A heating mantle to accommodate one gallon metal can, if the measurements are to be made under a constant temperature.
6. Personal protective equipment and other safety gear as needed.
7. Computer to collect data acquired by the laser distance meter.

#### **A1.4. PROCEDURE**

The following are brief description of procedures followed to measure foam characteristics of asphalt binders in the laboratory or field.

1. Ensure that the foaming equipment is calibrated according to the manufacturer's recommendation. Calibration may vary from one binder type to another.
2. Calibrate the height of the binder in the one-gallon can with respect to the weight of the binder in the can. Although the metal may be cylindrical, the bottom of the can may be grooved in order to strengthen it. For small amounts of binder dispensed during foaming, the groove can accommodate a significant mass fraction of the binder (Figure A1.1). In order to avoid errors in volumetric measurement it is important to calibrate the weight of binder to height of binder in the one-gallon can. For this calibration, mount the laser distance meter (LDM) on a tripod at a suitable location. The tripod and the LDM should be stable and not susceptible to vibrations. Weigh the empty one-gallon can and place it under the LDM. Point the LDM to the bottom of the empty can (Figure A1.2). The laser should point at a flat portion of the can, preferably in the center. The distance to the bottom of the can should be recorded and the exact location of the can should be marked. Pour about 50 g of hot asphalt in the can so that a smooth and flat binder surface is created. Measure the exact mass of the place the can in the previous position and measure the distance from the LDM to the surface of the binder. Subtract the last two measurements to obtain the height of the binder in the can. Repeat the procedure at least twice after adding more binder to the can and weighing it each time. The weight versus height of binder will be used for future calculations.



Figure A1.1: Illustration of the bottom of the one-gallon; the grooves can accommodate a significant mass fraction of the binder especially when the mass dispend is small.



Figure A1.2: Illustration of the LDM pointing into an empty can for calibration.

3. Prepare the LDM to make measurements for the foamed asphalt binder. Mount the LDM on the tripod at a suitable location that is not susceptible to movement or vibration. Weigh the empty one-gallon can and place it under the LDM. Point

- the laser from the LDM to the bottom of an empty one-gallon can. The laser should point as close to the center of the can as possible. Start data acquisition to get at least 5 points that correspond to the distance between the LDM and the bottom of the can.
4. Dispense the specified amount of foamed binder into the one-gallon can. Depending on the foaming equipment (or location in case of a field test), it may or may not be possible to dispense the foamed binder while the LDM is pointing into the can. In situations where the can must be moved away from the LDM to collect the foamed binder sample, ensure that the location of the can is marked and that the can is placed under the LDM as soon as possible after collecting the sample. Also, in this case the time at which the sample was dispensed must be recorded using the LDM.
  5. Record the distance between the top of the foamed asphalt and the LDM using the LDM over time. Record the data for at least five minutes or until the change in the height of the binder sample is less than 0.1 mm whichever comes later. Note that if the measurements are conducted with the can placed at room temperature, the binder sample may cool before all the bubbles can escape. In this case, the volume of the binder may not reach the minimum volume without the foam.
  6. Weigh the can to obtain the actual mass of the binder dispensed. Use the measured weight of the binder sample dispensed to verify the calibration of the foaming unit and also to obtain minimum height of the non-foamed binder using the binder weight-height calibration from before,  $h_{\text{final}}$ . If a heating mantle is used and it is ensured that the change in volume has stabilized, then the final height can also be directly obtained by subtracting the distance measured by the LDM after

foam collapse to the distance measured by the LDM to the bottom of the can before dispensing the binder.

#### A1.5. REPORT

1. Obtain the distance between the top of the foamed asphalt and the LDM as a function of time from the computer and report it to the nearest 0.1 mm. Convert the distance measured by the LDM to height of the foamed binder at any time  $t$ ,  $h_t$ , by subtracting it from the distance measured to the bottom of the container.
2. Determine the final height of the foam,  $h_{final}$ , from the weight to height relationship established in the previous section.
3. Calculate the expansion ratio of the binder at any time  $t$ ,  $ER_t$  as  $(h_t - h_{final}) / h_{final}$ . For the maximum expansion ratio, the maximum

height of the binder measured from the marking left behind by the collapsing foam on the inside of the can is used. Note that the start time is the time when the binder sample was dispensed into the one-gallon can.

4. Plot the expansion ratio versus time. The data from the LDM can be smoothened using the following function:

$$ER_t = 1 + (ae^{-bt}) + (ER_{max} - a - 1)(e^{-ct}).$$

where,  $ER_t$  is the expansion ratio at any time  $t$ ,  $a$ ,  $b$ , and  $c$  are constants, and  $ER_{max}$  is the maximum expansion ratio that was directly measured during the foaming process.

5. Use the ER data after 10 seconds of foaming to determine the rate of collapse of the semi-stable foam (k-value). The rate of collapse of the semi-

stable foam is determined as the parameter  $k$  obtained by fitting the ER versus time to an exponential curve:  $ER_t = 1 + ce^{-kt}$ .

## References

- Abel, F. (1978). *Foamed Asphalt Base Stabilization*. State of Colorado, Division of Highways.
- Abel, F., and Hines, C. R. (1979). *Base Stabilization with Foamed Asphalt*. Interim Report, Colorado Department of Transportation, Denver, CO.
- Berthier, J. (2008). *Microdrops and digital microfluidics*. William Andrew Pub., Norwich NY.
- Bhasin, A., Howson, J. E., Masad, E., Little, D. N., and Lytton, R. L. (2007). "Effect of Modification Processes on Bond Energy of Asphalt Binders." *Transportation Research Record: Journal of the Transportation Research Board*, 1998, 29–37.
- Brennen, M., Tia, M., Altschaeffl, A. G., and Wood, L. E. (1983). "Laboratory Investigation of the Use of Foamed Asphalt for Recycled Bituminous Pavements." *Transportation Research Record*, (911).
- D'Angelo, J., Harm, E., Bartoszek, J., Baumgardner, G. L., Corrigan, M., Cowser, J., Harman, T., Jamshidi, M., Jones, W., Newcomb, D., Prowell, B., Sines, R., and Yeaton, B. (2008). *Warm-Mix Asphalt: European Practice*. Federal Highway Administration.
- Engelbrecht, D. C. (1999). "Manufacturing Foam Bitumen in a Standard Drum Mixing Asphalt Plant." *7th Conference on Asphalt Pavements for Southern Africa*, South Africa.
- FHWA. (2013). *Every Day Counts: Warm Mix Asphalt*. Federal Highway Administration, Washington, D.C.
- Fu, P., Jones, D., and Harvey, J. T. (2011). "The effects of asphalt binder and granular material characteristics on foamed asphalt mix strength." *Construction and Building Materials*, 25(2), 1093–1101.

- Hansen, K. R., and Copeland, A. (2013). *Asphalt Pavement Mix Production Survey on Reclaimed Asphalt Pavement, Reclaimed Asphalt Shingles, and Warm-Mix Asphalt Usage: 2009-2011*. Federal Highway Administration, Washington, DC.
- He, G., and Wong, W. (2006). "Decay properties of the foamed bitumens." *Construction and Building Materials*, 20(10), 866–877.
- Huang, X. L., Catignani, G. L., and Swaisgood, H. E. (1997). "Micro-scale Method for Determining Foaming Properties of Protein." *Journal of Food Science*, 62(5), 1028–1060.
- Hurley, G. C., and Prowell, B. (2005). *Evaluation of Aspha-Min Zeolite for Use in Warm Mix Asphalt*. National Center for Asphalt Technology, Auburn, AL.
- Jenkins, K. J. (2000). "Mix Design Considerations for Cold and half-Warm Bituminous Mixes with Emphasis on Foamed Bitumen." Ph.D. thesis, University of Stellenbosch, Stellenbosch, South Africa.
- Kutay, M. E., and Ozturk, H. I. (2012). "Investigation of Moisture Dissipation in Foam-Based Warm Mix Asphalt Using Synchrotron-Based X-Ray Microtomography." *Journal of Materials in Civil Engineering*, 24(6), 674–683.
- Leibson, I., Holcomb, E. G., Cacosso, A. G., and Jacmic, J. J. (1956). "Rate of flow and mechanics of bubble formation from single submerged orifices. II. Mechanics of bubble formation." *AIChE Journal*, 2(3), 300–306.
- Namutebi, M. (2011). "Some Aspects of Foamed Bitumen Technology." dissertation, KTH.
- NAPA. (2011). *Asphalt Pavement Overview*. National Asphalt Pavement Association.



- Osmari, P., Arega, Z., and Bhasin, A. (2013). *Wetting Characteristics of Asphalt Binders at Elevated Temperatures*. Final Report, Center for Transportation Research, The University of Texas at Austin, Austin, TX, 48.
- Pellicer, J., García-Morales, V., and Hernández, M. J. (2000). “On the demonstration of the Young-Laplace equation in introductory physics courses.” *Physics Education*, 35(2), 126.
- Phillips, L. G., Haque, Z., and Kinsella, J. E. (1987). “A Method for the Measurement of Foam Formation and Stability.” *Journal of Food Science*, 52(4), 1074–1077.
- Saye, R. I., and Sethian, J. A. (2013). “Multiscale Modeling of Membrane Rearrangement, Drainage, and Rupture in Evolving Foams.” *Science*, 340(6133), 720–724.
- Schick, C. (2004). “A mathematical analysis of foam films.” Doctoral Dissertation, Kaiserslautern University of Technology, Kaiserslautern, Germany.
- Schramm, L. L. (Ed.). (1994). *Foams: Fundamentals and Applications in the Petroleum Industry*. American Chemical Society.
- Sunarjono, S. (2008). “The influence of Foamed Bitumen Characteristics on Cold-Mix Asphalt Properties.” Doctoral Dissertation, The University of Nottingham, United Kingdom.
- Uhlig, H. H. (1937). “The Solubilities of Gases and Surface Tension.” *The Journal of Physical Chemistry*, 41(9), 1215–1226.
- Wilde, P. J. (1996). “Foam Measurement by the Microconductivity Technique: An Assessment of Its Sensitivity to Interfacial and Environmental Factors.” *Journal of Colloid and Interface Science*, 178(2), 733–739.
- Xu, J. (2011). *Microcellular Injection Molding*. John Wiley & Sons.